TUTORIAL

Theory and practice of Materials Analysis for Microelectronics with a nuclear microprobe

Ettore Vittone

Physics Department

University of Torino, Italy

IBIC for the functional characterization of semiconductor materials and devices

Measurement of the their electronic properties and performances

Main physical observable: current
Current = F(carrier density; carrier transport)

Free carriers (electron/hole) transport
Two mechanisms: Drift and Diffusion

Drift: by the electrical force $v=\mu \cdot E$
Diffusion: by a concentration gradient

Recombination/trapping

Carrier lifetime τ

Principles of radiation detection techniques

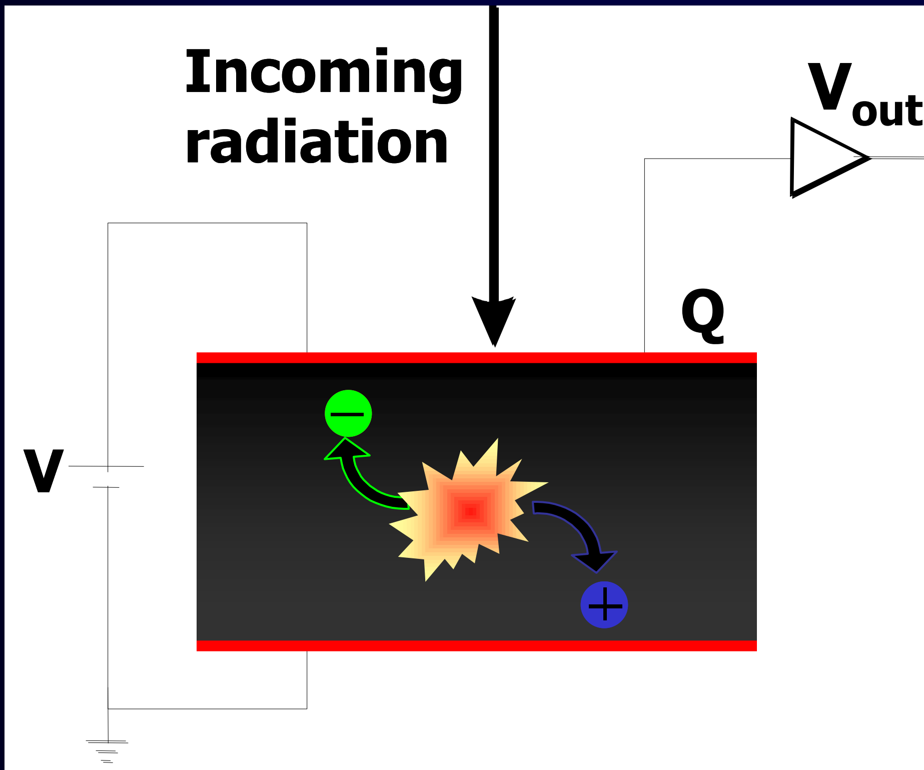

Deposited Energy

↓

Moving charge q

↓

Induced charge Q

↓

Output Signal V_{out}

$$V_{out} = F(\text{Deposited Energy, Free Carrier Transport})$$

Nuclear spectroscopy

Material characterisation

Using MeV ions to probe the electronic features of semiconductors

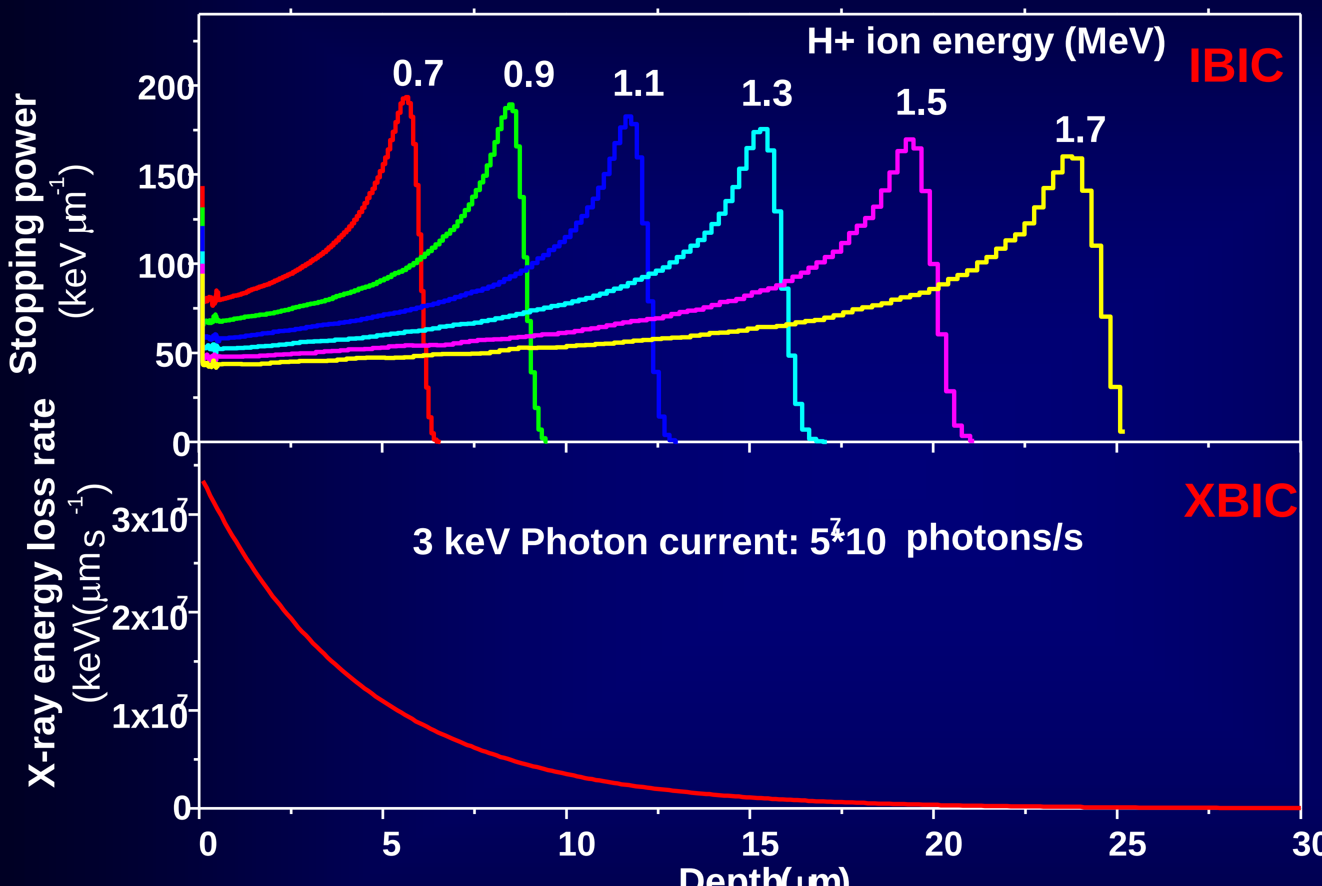

SRIM (Stopping and Range of Ion in Matter)

Electrode energy loss very small (≅ 1%)

- ➢long range
- ➢low lateral scattering
- ➢a wide choice of ion range and electronic energy losses

- ✓**analysis through thick surface layers**
- ✓**charge pulses height spectra almost independent on topography .**
- ✓**profiling**

Electron/Hole pair generation

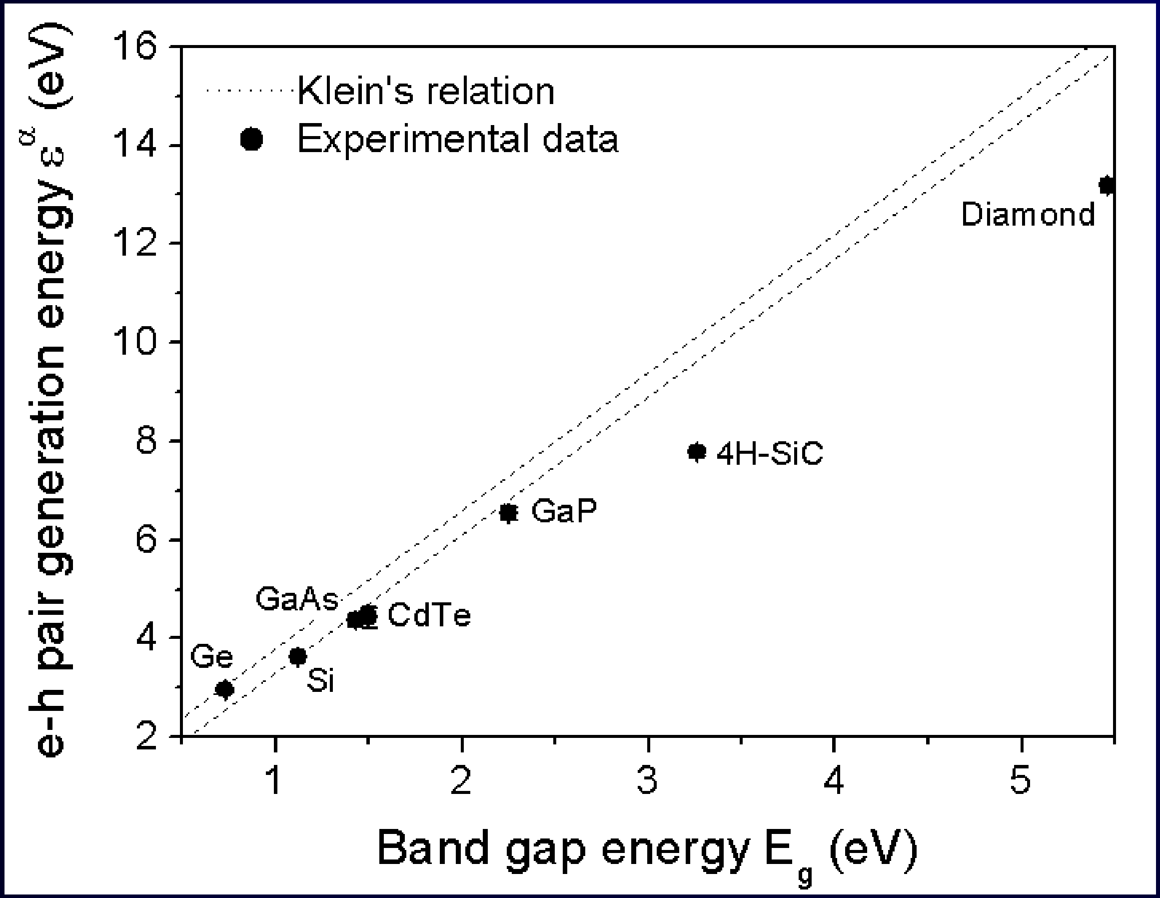

$$N_{eh} = \frac{E_{ion}}{\varepsilon_{eh}}$$

1 MeV in diamond generates about 77000 e/h pairs

Each high energy ion creates large numbers of charge carriers to be measured above the noise level.

A. Lo Giudice et al. Applied Physics Letters 87, 22210 (2005)

Physical Observable: Induced current/charge

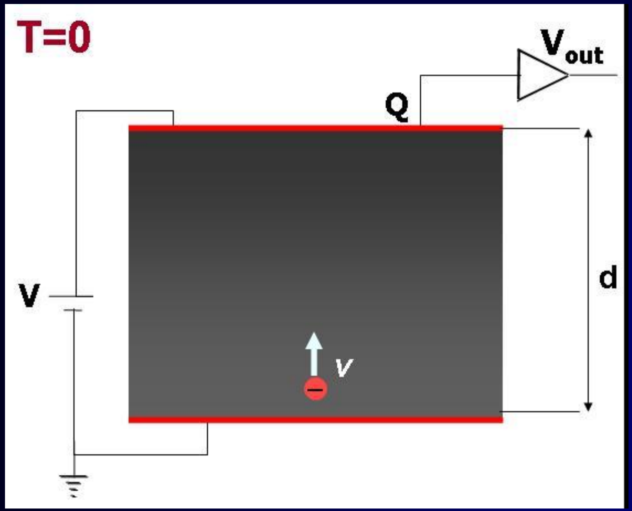

Shockley-Ramo Theorem

$$v = \mu \cdot E$$

The current is induced by the motion of charges in presence of an electric field

Induced current

$$I(t) = q \cdot \frac{v}{d}$$

Physical Observable: Induced current/charge

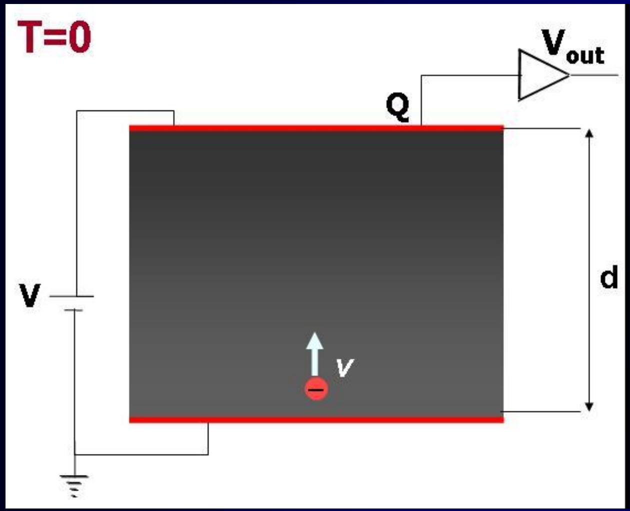

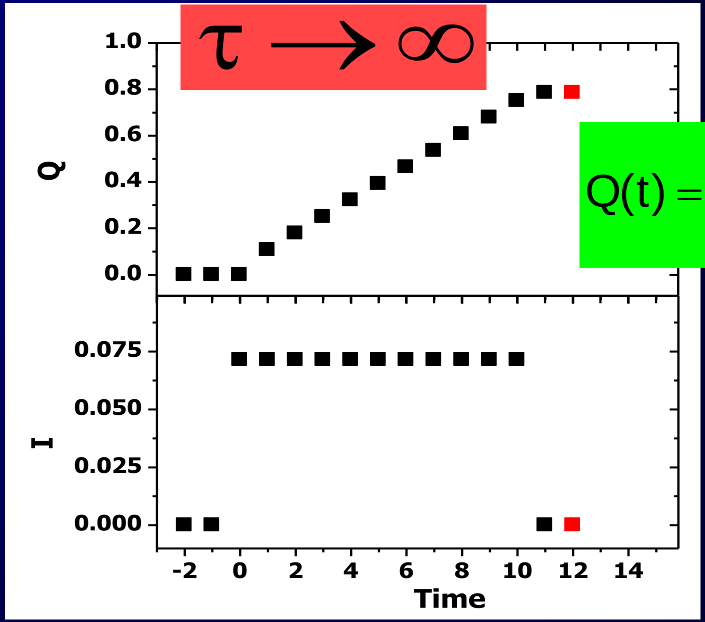

$$\tau \longrightarrow \infty$$

$$Q(t) = \int_0^T I(t)dt$$

$$I(t) = q \cdot \frac{v}{d}$$

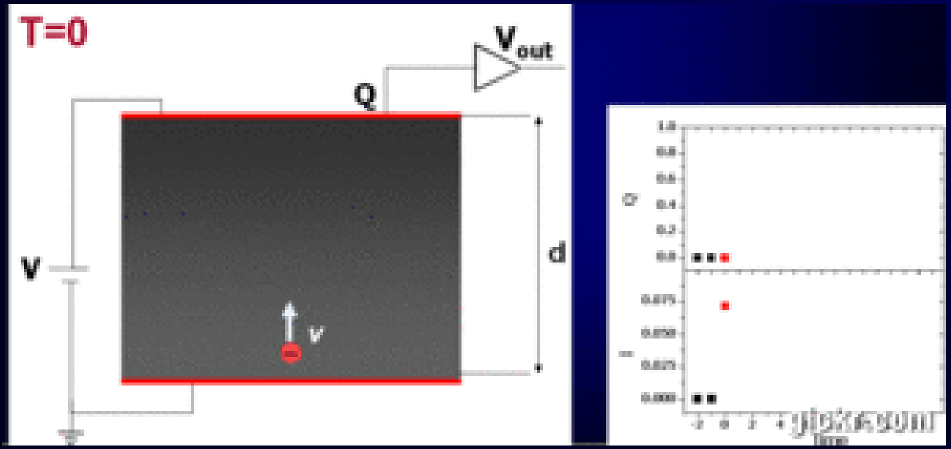

W. Shockley, J. Appl. Phys. 9 (1938) 635.

S. Ramo, Proc. I.R.E. 27 (1939) 584.

CARRIER LIFETIME τ

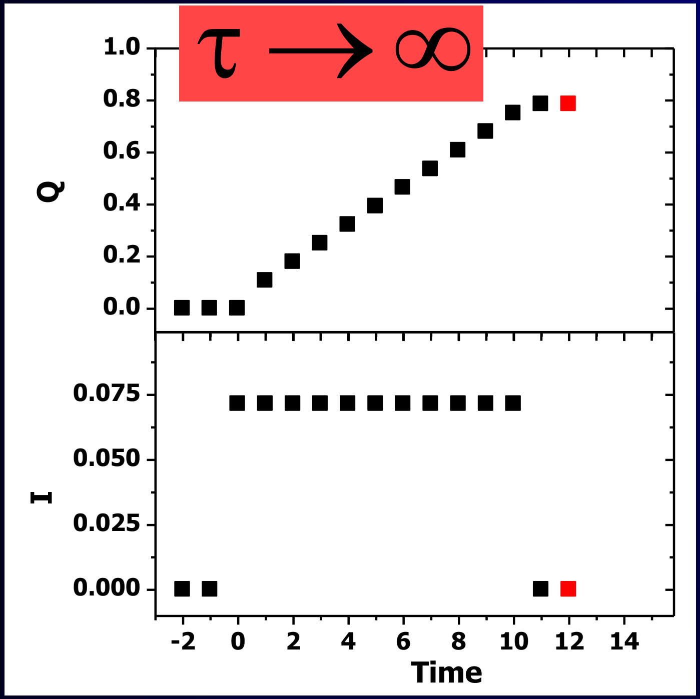

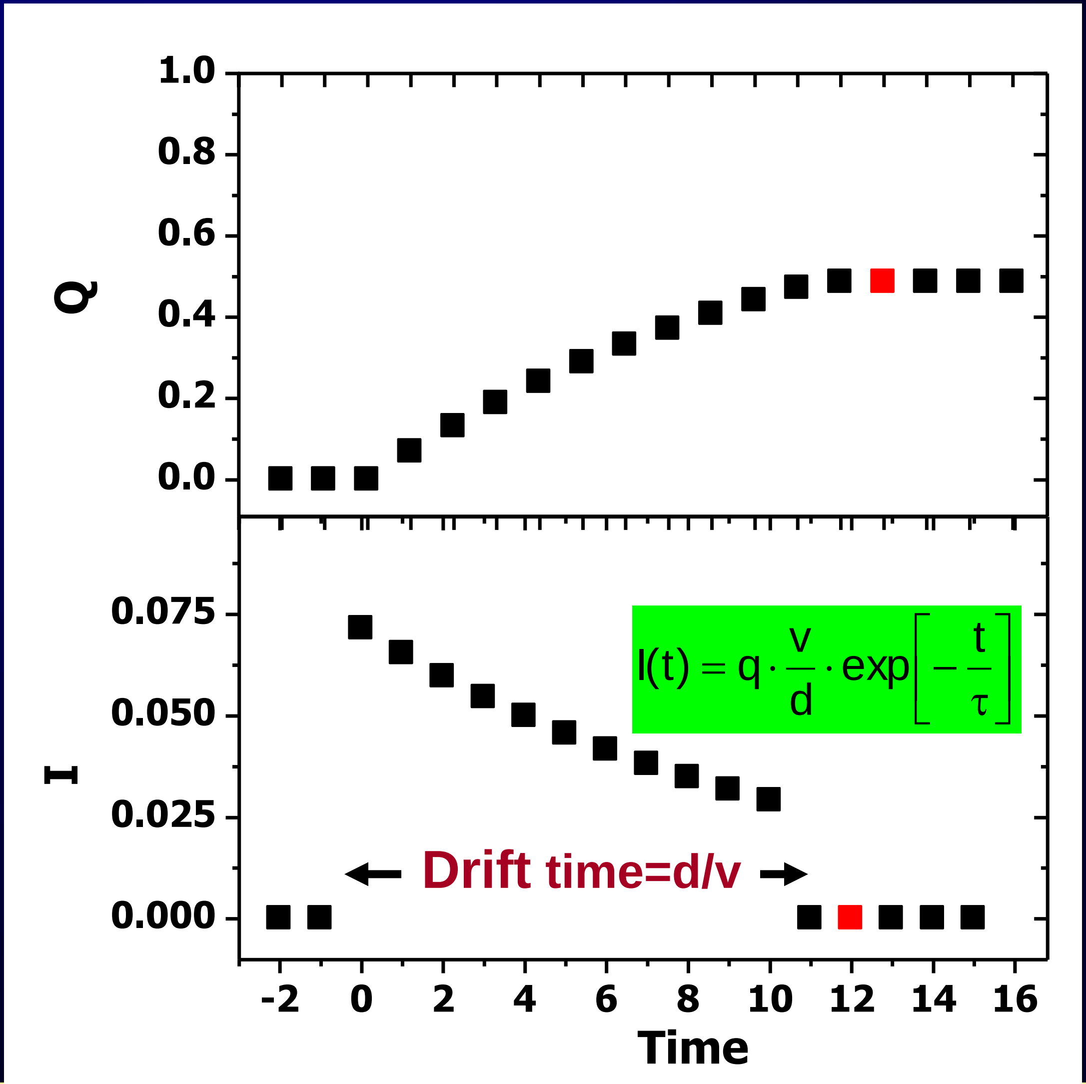

Induced current

IIa diamond; resistivity about 10^{15} Ω·cm; dielectric constant =0.5 pF/cm; Dielectric relaxation time = 500 s.

Charge neutrality not maintained

400 μm thick natural diamond,

biased at 40 V @ RT

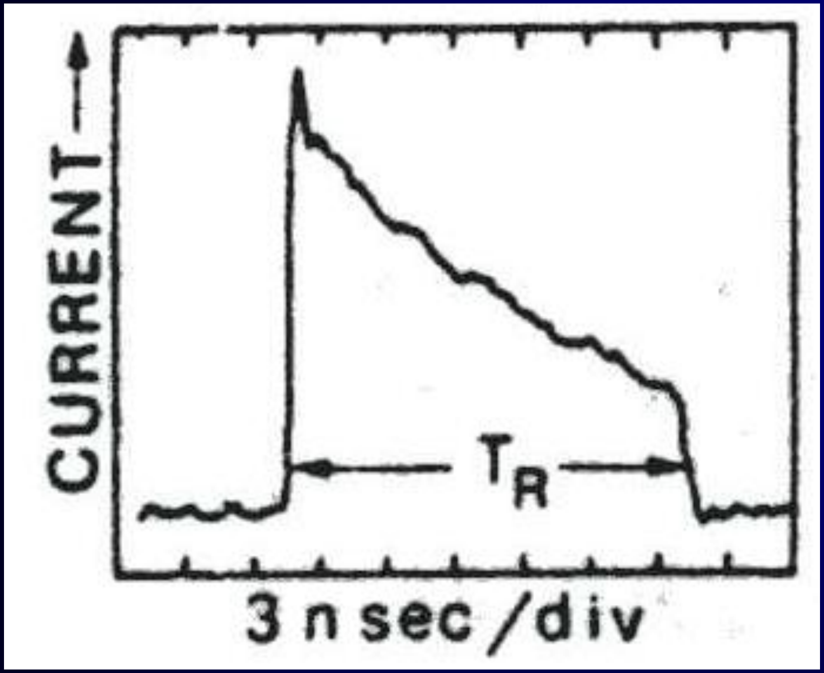

C. Canali, E. Gatti, S.F. Koslov, P.F. Manfredi, C. Manfredotti, F. Nava, A. Quirini
Nucl. Instr. Meth. 160 (1979) 73-77

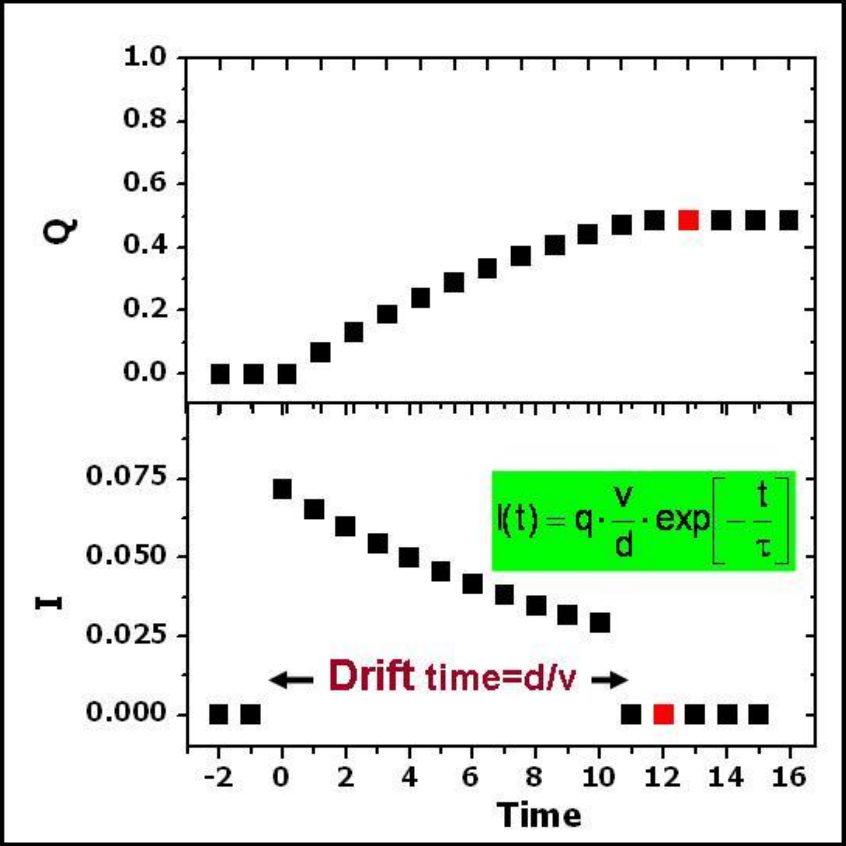

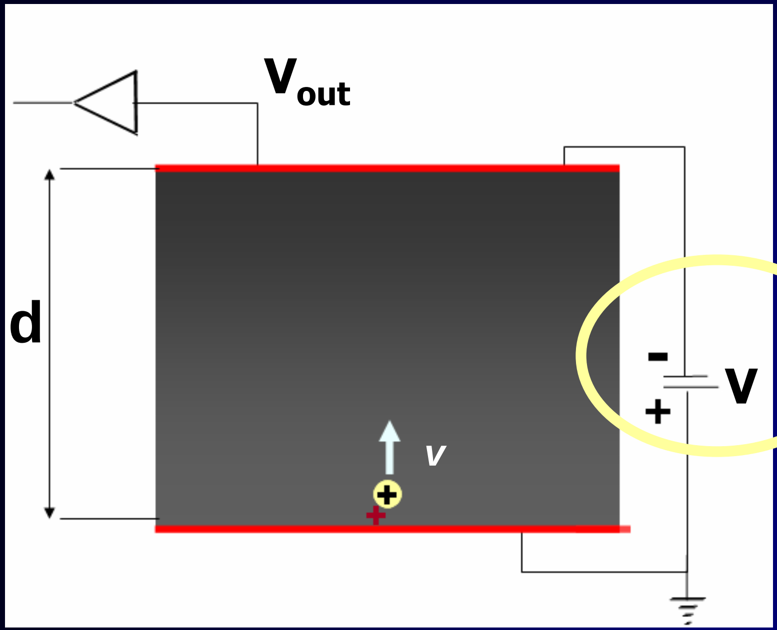

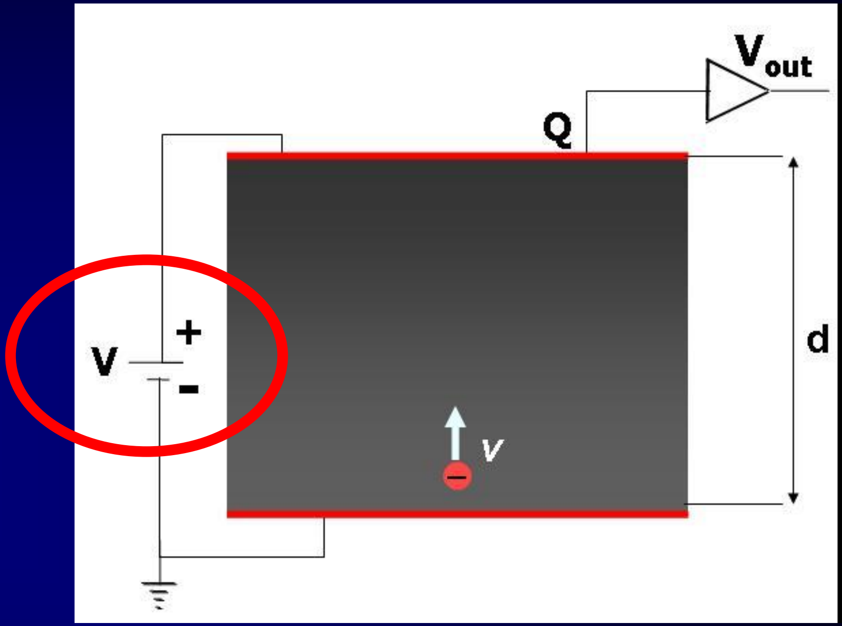

Generation at the anode -> Hole collection

Generation at the cathode -> Electron collection

$$CCE \approx \frac{\mu\tau_e E}{d}\left(1 - \exp\left(\frac{-d}{\mu\tau_e E}\right)\right)$$

K. Hecht, Z. Physik 77, (1932) 23

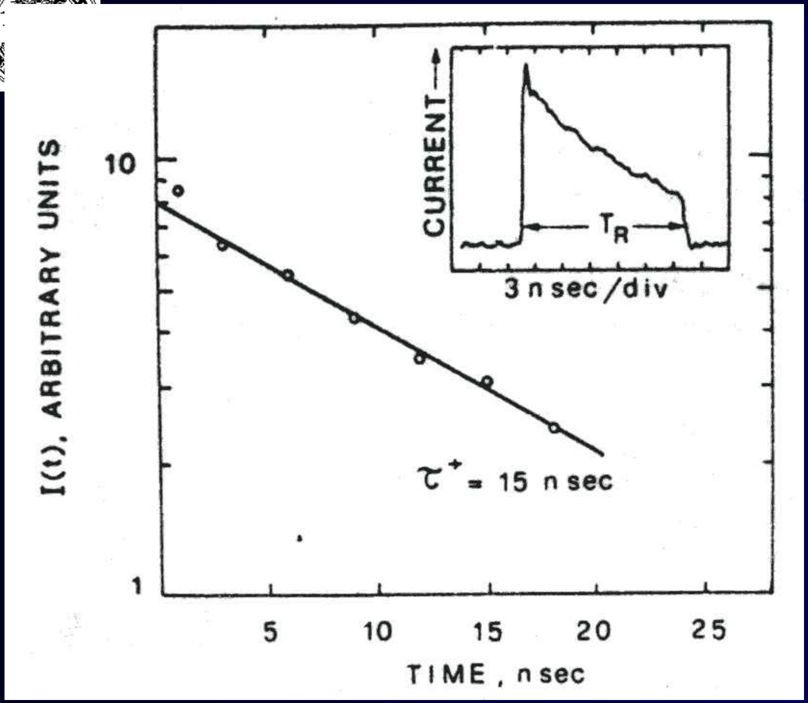

C. Canali, E. Gatti, S.F. Koslov, P.F. Manfredi, C. Manfredotti, F. Nava, A. Quirini
Nucl. Instr. Meth. 160 (1979) 73-77

400 μm thick natural diamond,

biased at 40 V @ RT

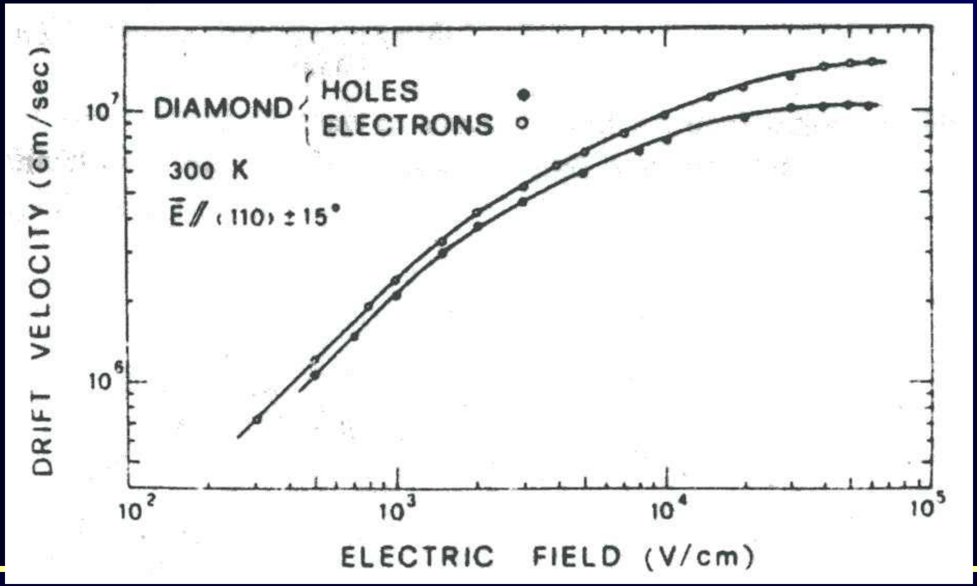

Drift velocity; $v = \mu E = d/T_R$

Mobility; $\mu = d^2/(T_R * V_{Bias})$

$$v = \mu \cdot E$$

The current is induced by the motion of charges in presence of an electric field

Induced current

$$I(t) = q \cdot \frac{v}{d}$$

Schottky electrode

50 μm thick N-type epitaxial 4H-SiC layer

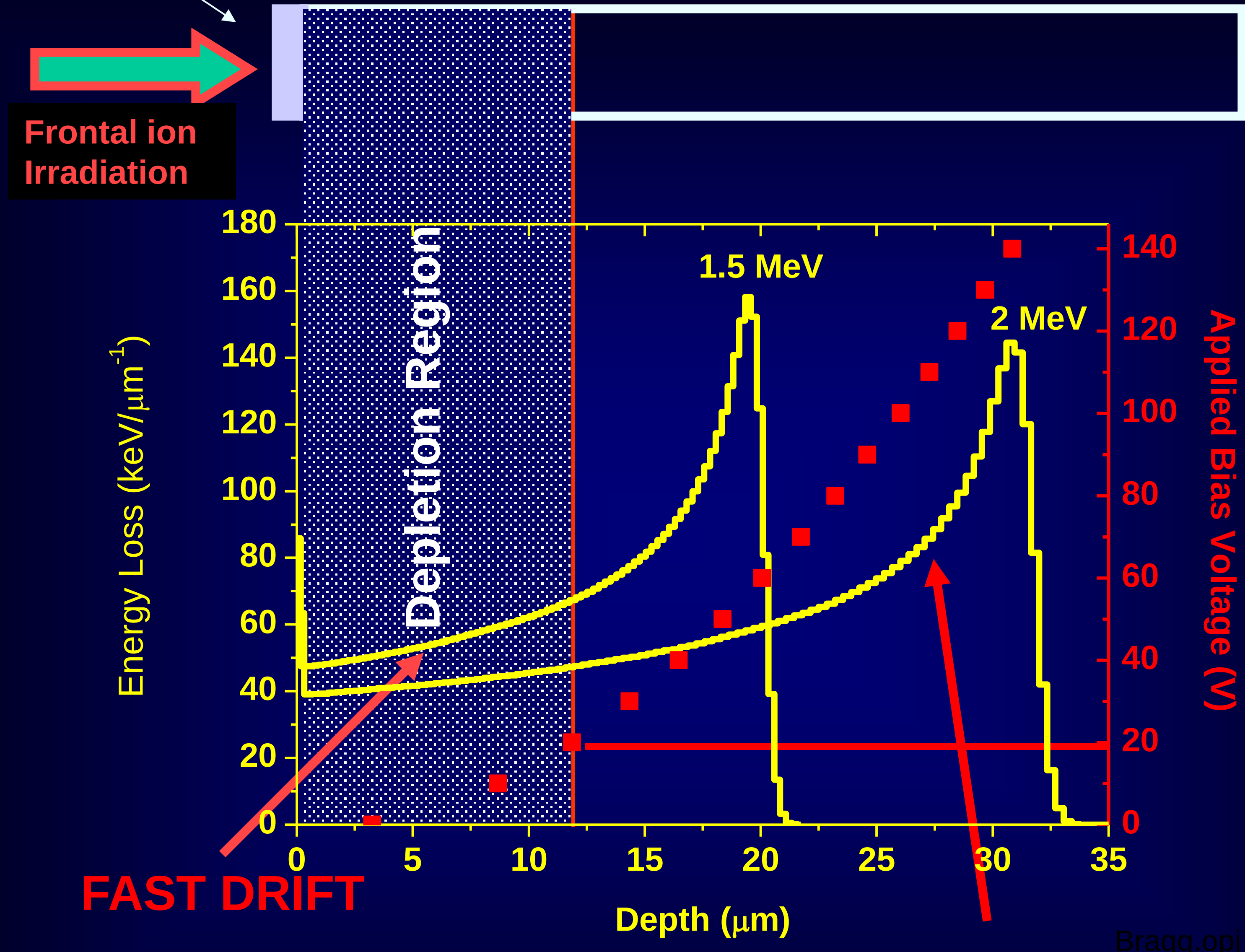

COMPLETE COLLECTION

DIFFUSION

Contribution from the neutral region

Contribution from the depletion layer

$$Q = Q_{Depl} + Q_{Neutr} \propto \left[\int_0^W \left(\frac{dE}{dx}\right)\cdot dx\right] + \left[\int_W^d \left(\frac{dE}{dx}\right)\cdot \exp\left[-\frac{x-W}{L_p}\right]\cdot dx\right]$$

Frontal ion Irradiation

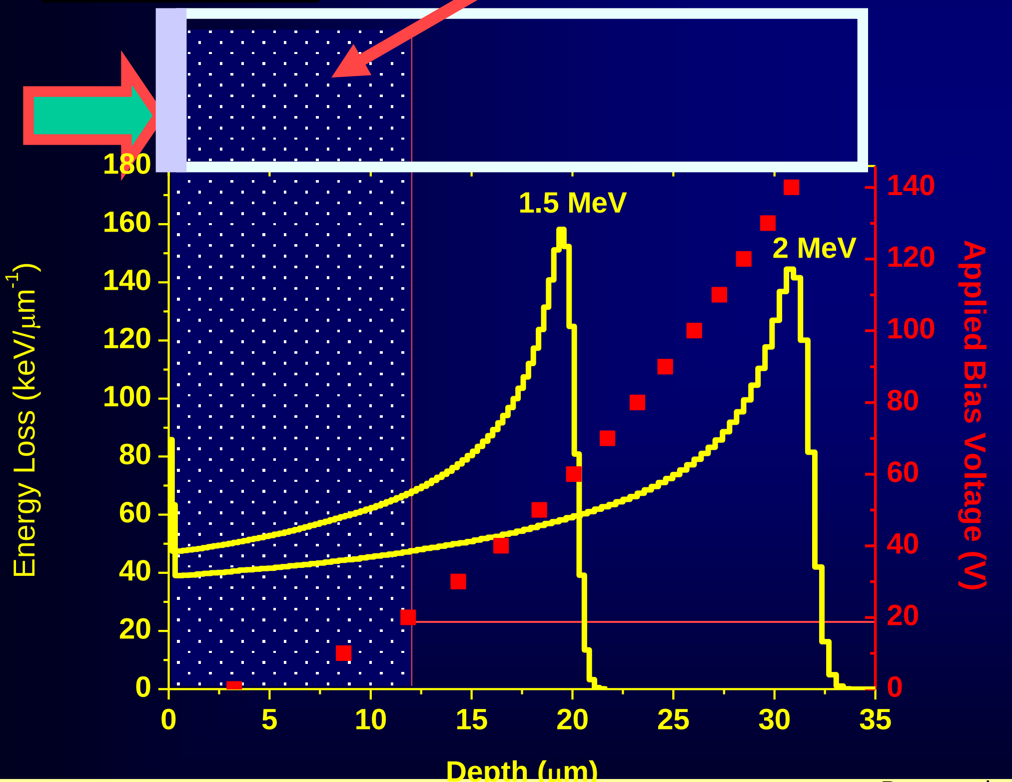

4H-SiC Schottky diode

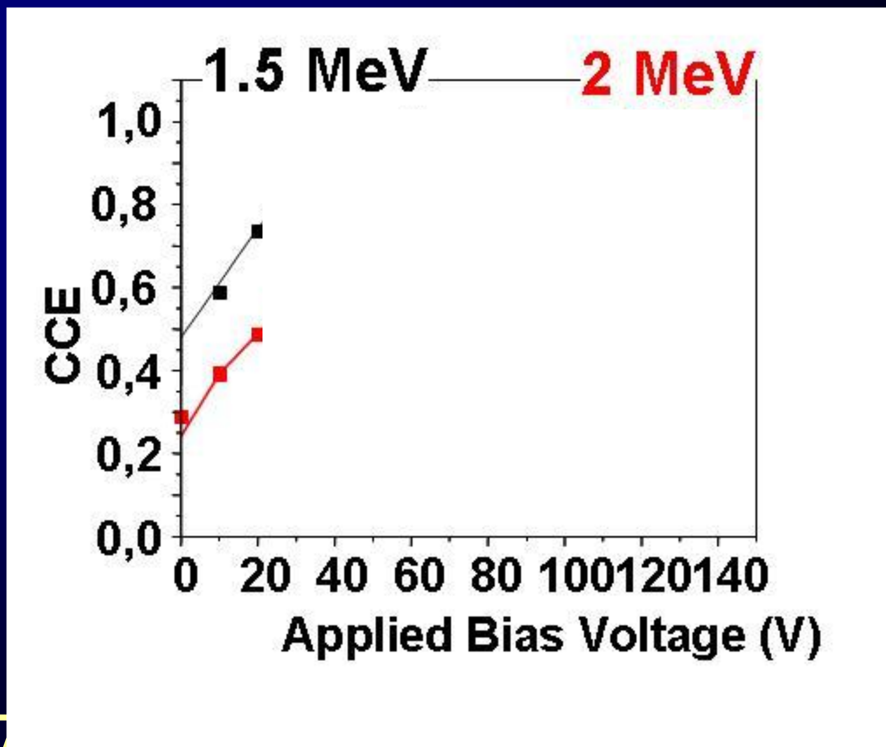

Contribution from the neutral region

Contribution from the depletion layer

$$Q = Q_{Depl} + Q_{Neutr} \propto \left[\int_0^W \left(\frac{dE}{dx}\right) \cdot dx\right] + \left[\int_W^d \left(\frac{dE}{dx}\right) \cdot \exp\left[-\frac{x-W}{L_p}\right] \cdot dx\right]$$

Frontal ion Irradiation

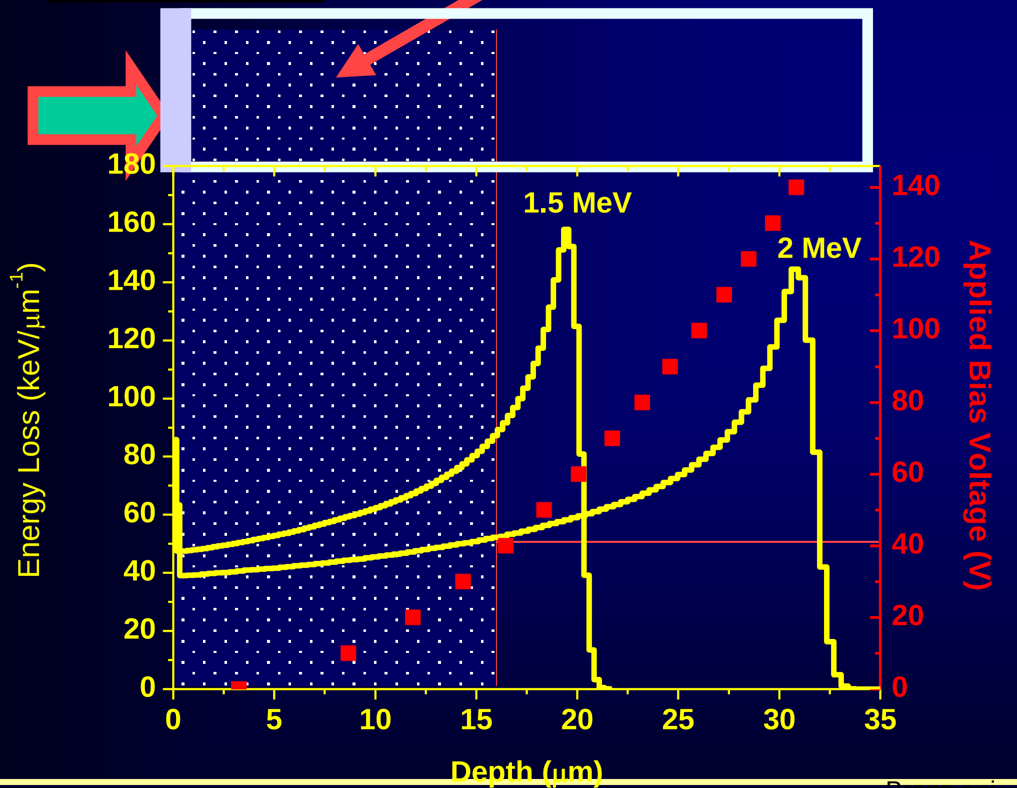

4H-SiC Schottky diode

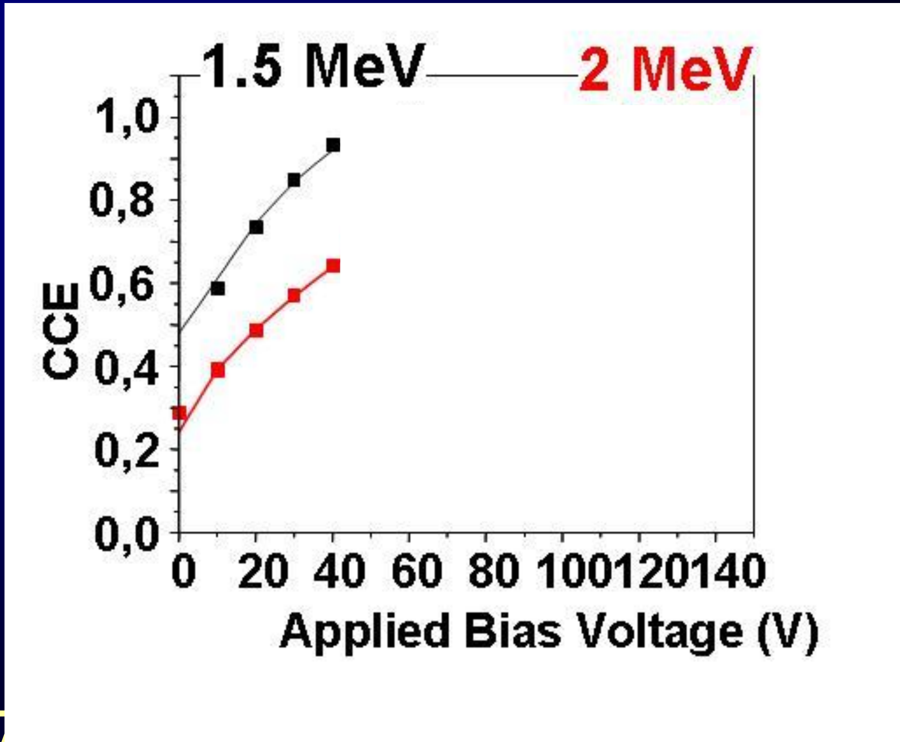

Contribution from the neutral region

Contribution from the depletion layer

$$Q = Q_{Depl} + Q_{Neutr} \propto \left[\int_0^W \left(\frac{dE}{dx}\right) \cdot dx\right] + \left[\int_W^d \left(\frac{dE}{dx}\right) \cdot \exp\left[-\frac{x-W}{L_p}\right] \cdot dx\right]$$

Frontal ion Irradiation

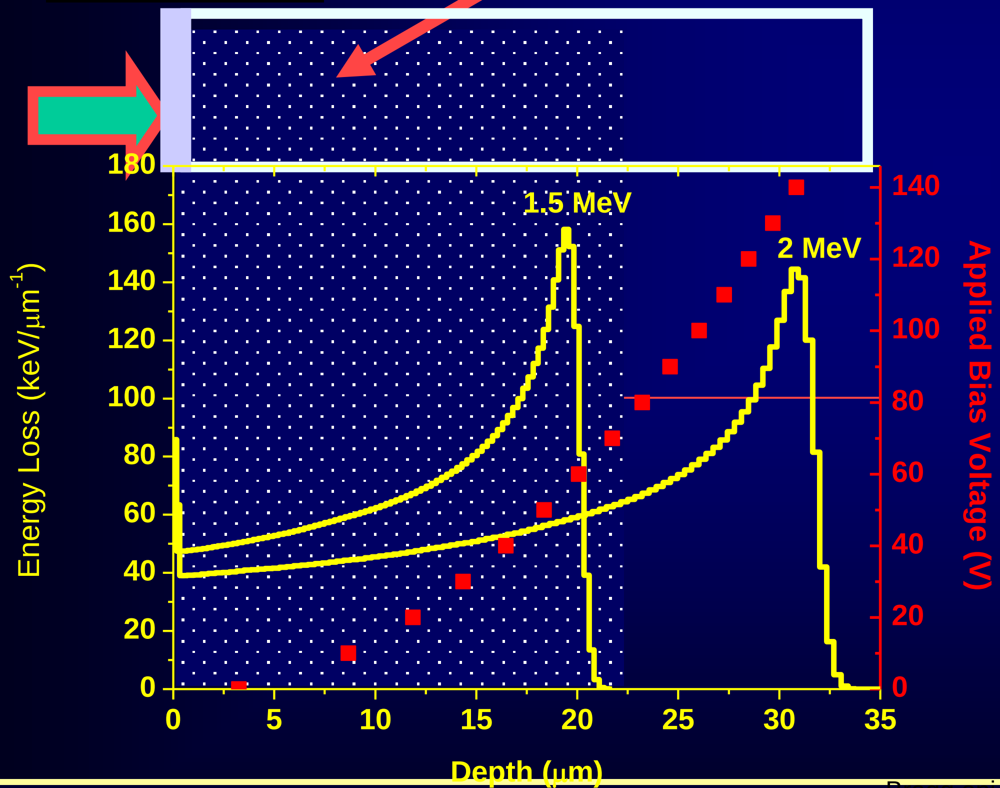

4H-SiC Schottky diode

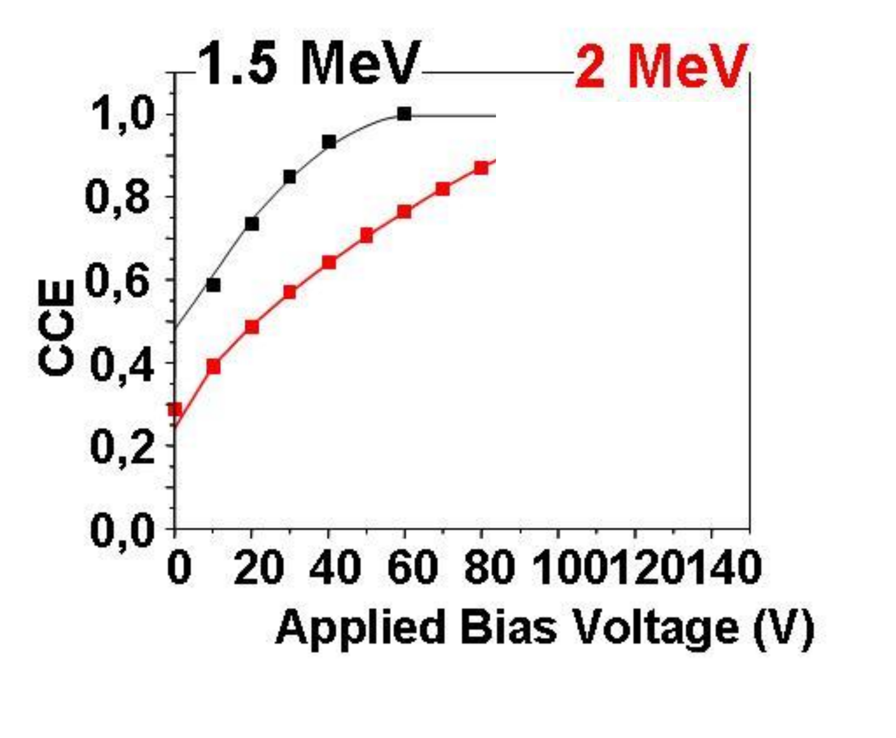

Contribution from the neutral region

Contribution from the depletion layer

$$Q = Q_{Depl} + Q_{Neutr} \propto \left[\int_0^W \left(\frac{dE}{dx}\right)\cdot dx\right] + \left[\int_W^d \left(\frac{dE}{dx}\right)\cdot \exp\left[-\frac{x-W}{L_p}\right]\cdot dx\right]$$

Frontal ion Irradiation

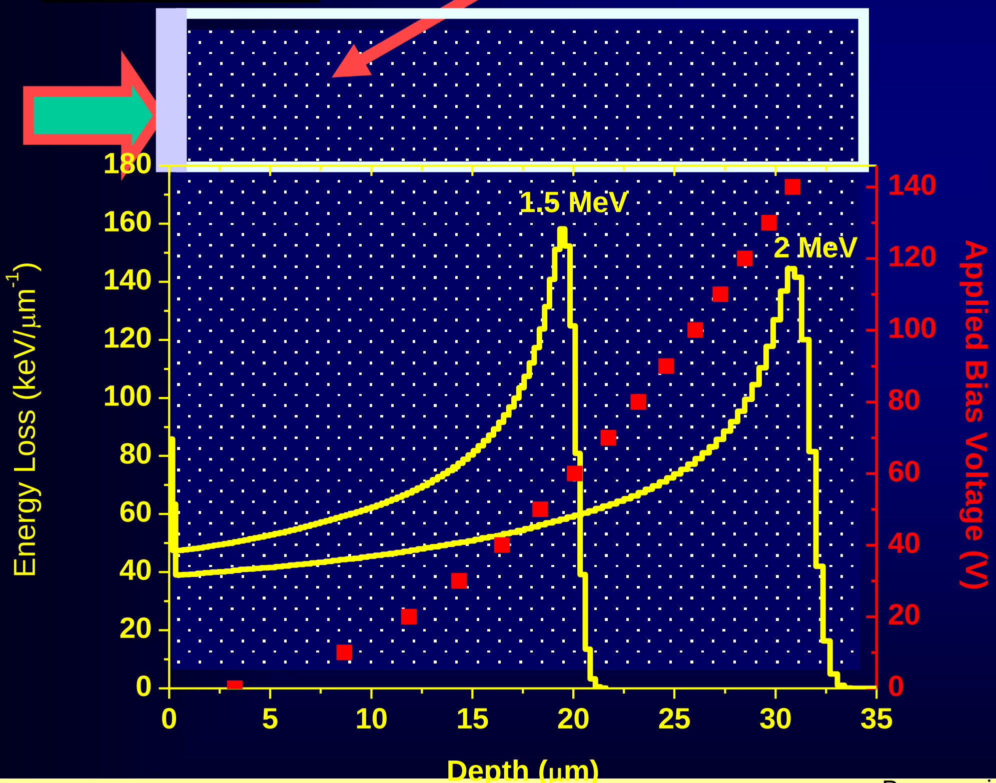

4H-SiC Schottky diode

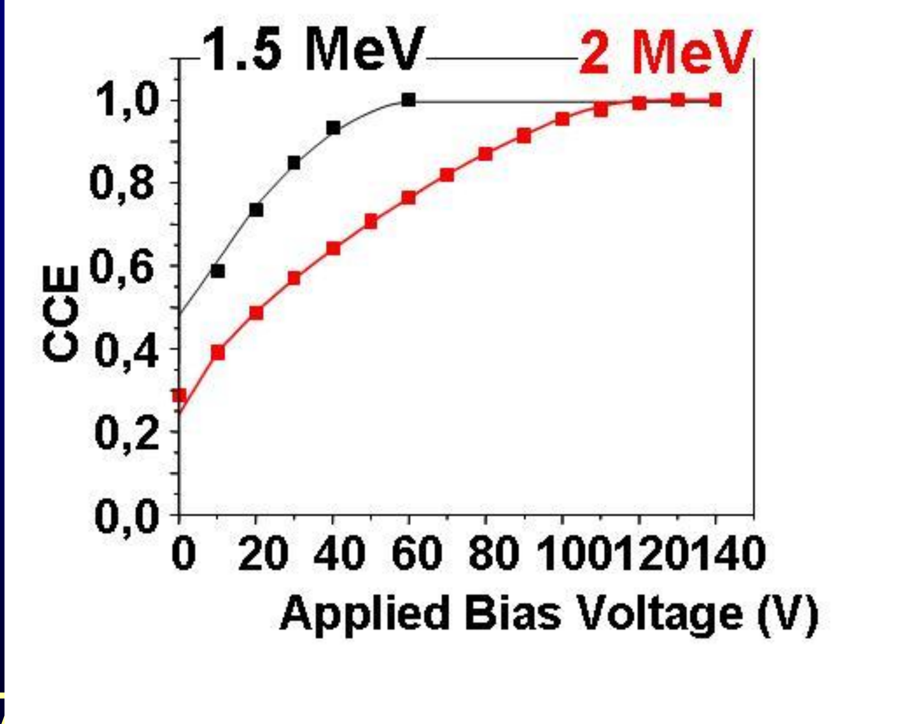

Contribution from the neutral region

Contribution from the depletion layer

$$Q = Q_{Depl} + Q_{Neutr} \propto \left[\int_0^w \left(\frac{dE}{dx}\right)\cdot dx\right] + \left[\int_w^d \left(\frac{dE}{dx}\right)\cdot \exp\left[-\frac{x-W}{L_p}\right]\cdot dx\right]$$

Active region width

minority carrier diffusion length

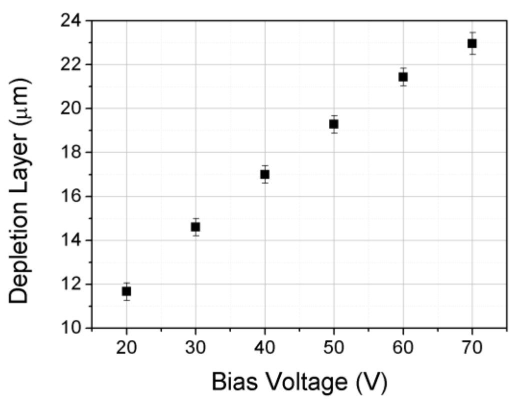

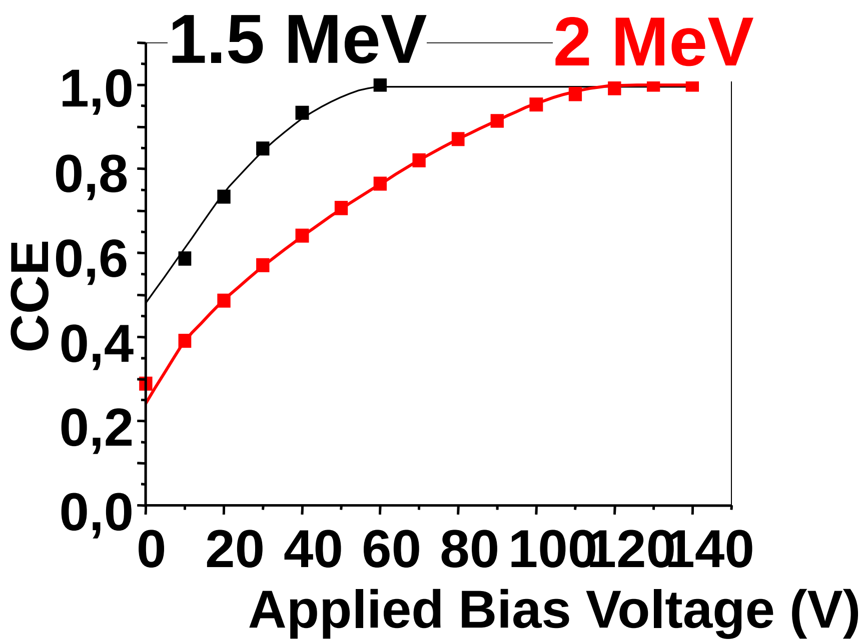

L_p=(9.0 0.3) µm

D_p = 3 cm^2/s

τ_p = 270 ns

4H-SiC Schottky diode

Temperature dependent IBIC (TIBIC)

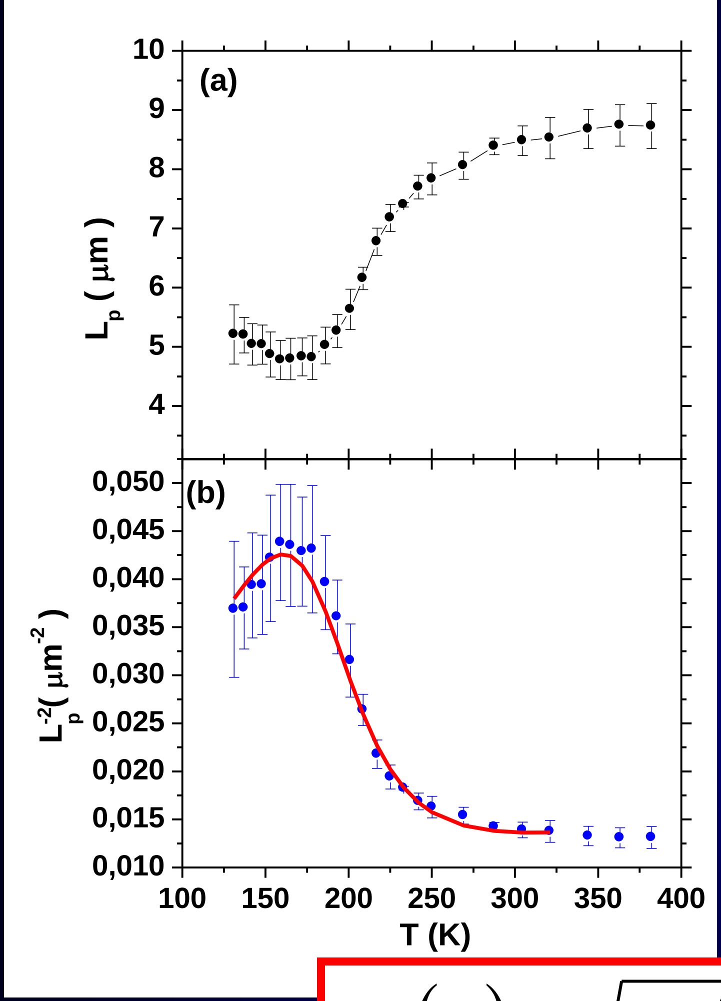

$$L_p(T) = \sqrt{D_p(T)\cdot\tau_p(T)}$$

Two trapping levels

$$\frac{1}{L_p^2} = \frac{1}{D_p\cdot\tau} = \frac{1}{D_p}\cdot\left(\frac{1}{\tau(T)} + \frac{1}{\tau_B}\right) = A\cdot\frac{1}{T^{-0.5}}\cdot\left[\frac{1}{T^{-0.5} + \frac{B}{N_D}\cdot T\cdot\exp\left(-\frac{E_t}{k_B T}\right)} + \frac{1}{\tau_B}\right]$$

The fitting procedure provides a trapping level of about 0.163 eV which is close to the value found in similar 4H SiC Schottky diodes by DLTS technique (S1 level).

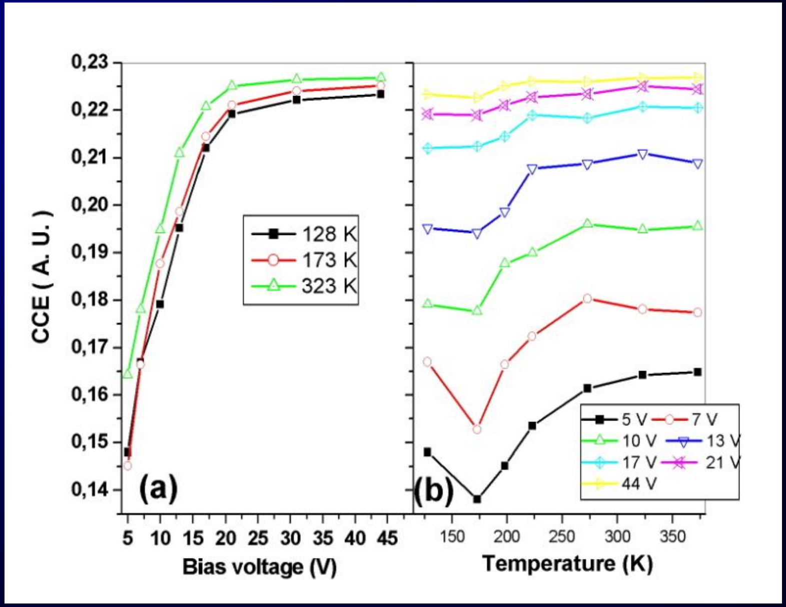

From Spectroscopy to micro-spectroscopy

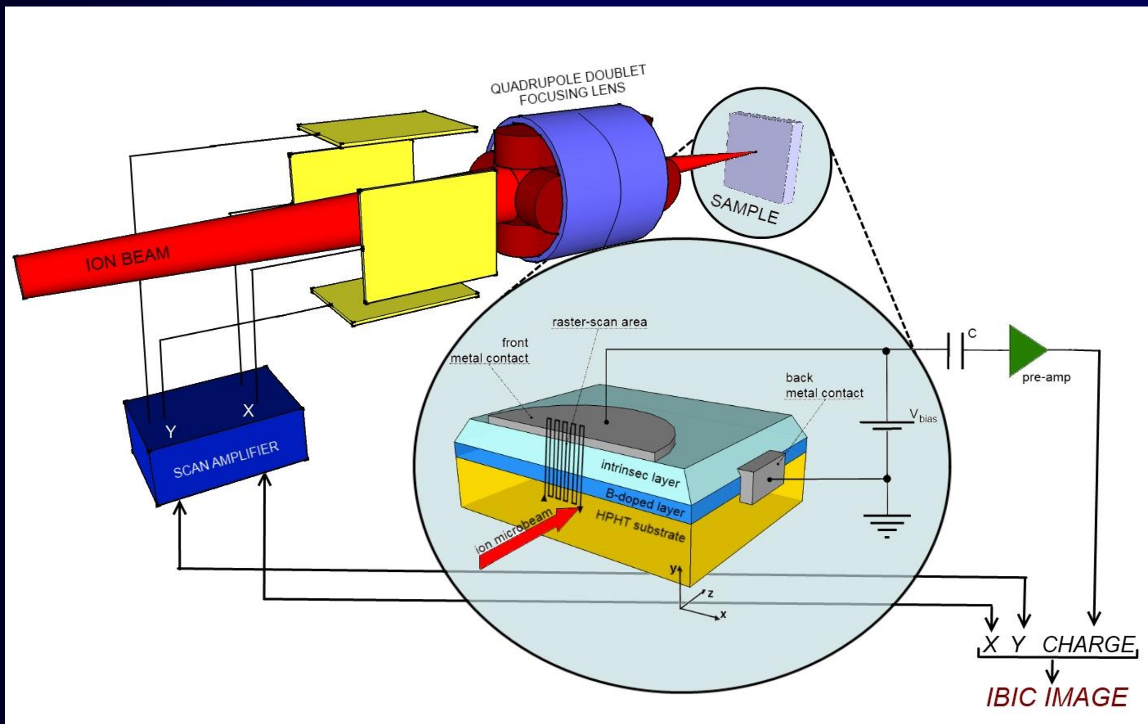

Use of focused ion beams

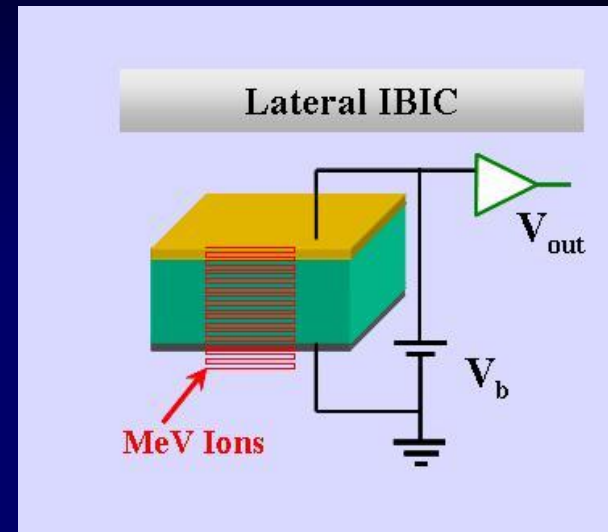

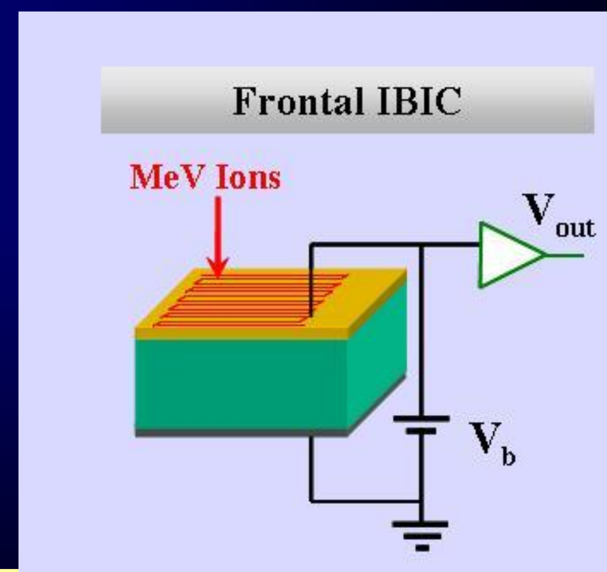

Trajectories

One advantage of IBIC over other forms of charge collection microscopy is that it provides high spatial resolution analysis in thick layers since the focused MeV ion beam tends to stay 'focused' through many micrometers of material.

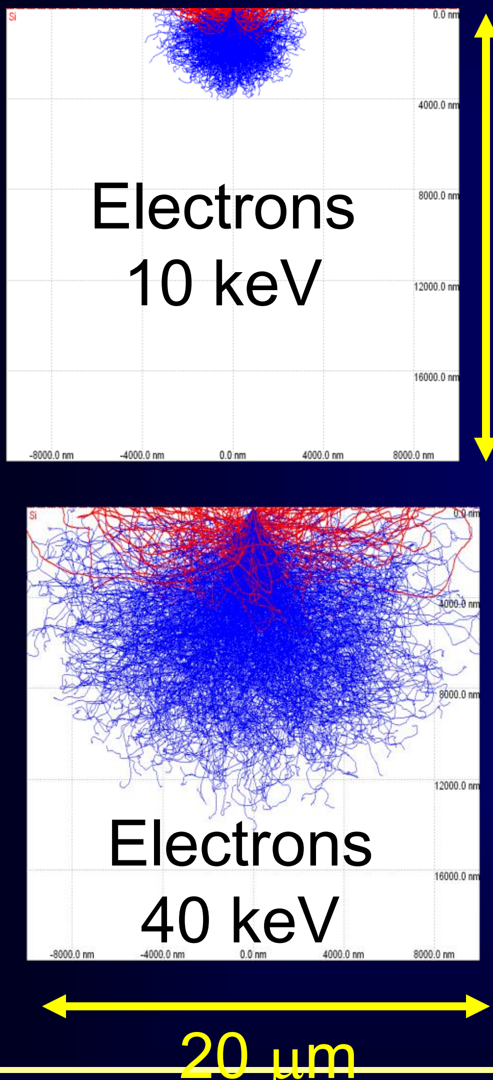

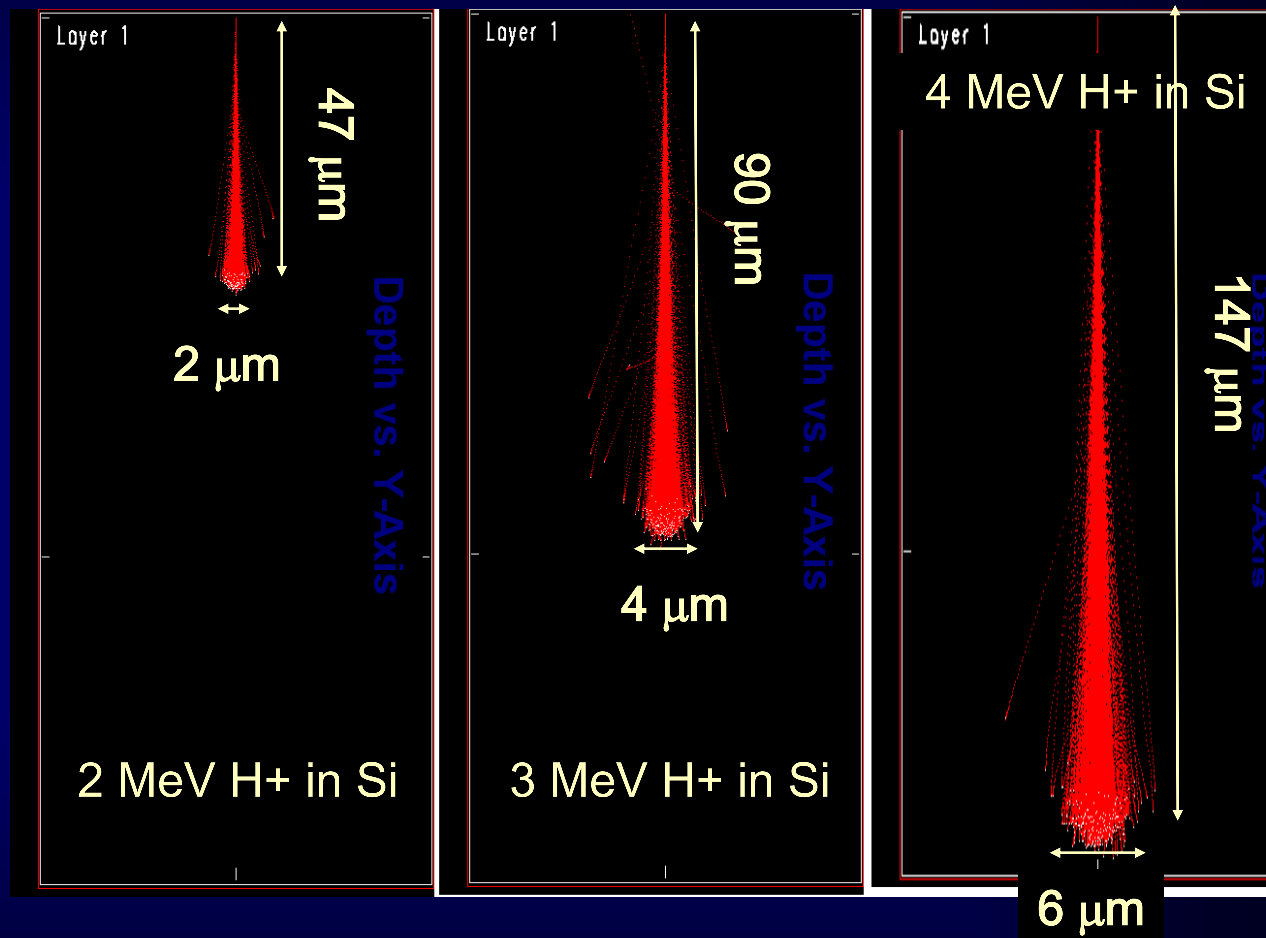

Abs#151-F. Watt: nuclear microprobe, towards nanometer spost sizes

Frontal IBIC

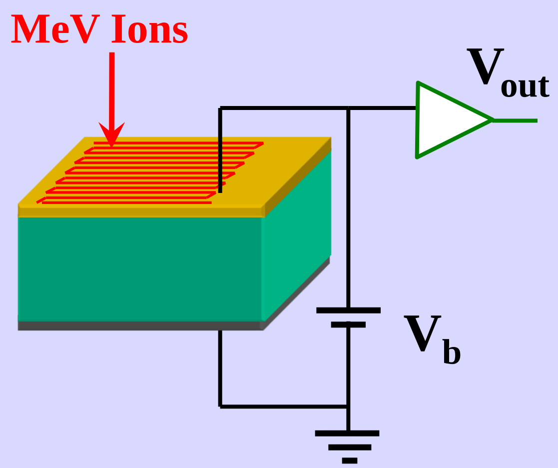

Nuclear Instruments and Methods in Physics Research B 100 (1995) 133–140

IBIC investigations on CVD diamond

C. Manfredotti [a,b,*], F. Fizzotti [a,b], E. Vittone [a,b], M. Boero [a,b], P. Polesello [a,b], S. Galassini [c,d], M. Jaksic [e], S. Fazinic [e], I. Bogdanovic [e]

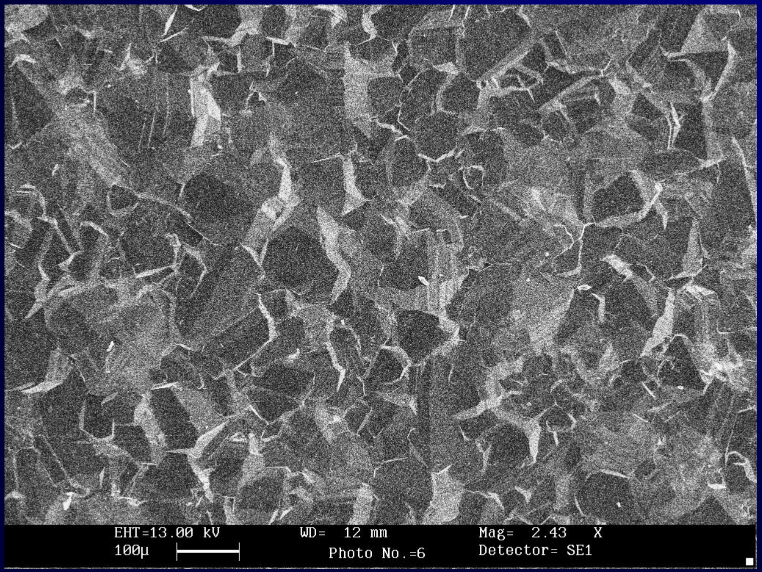

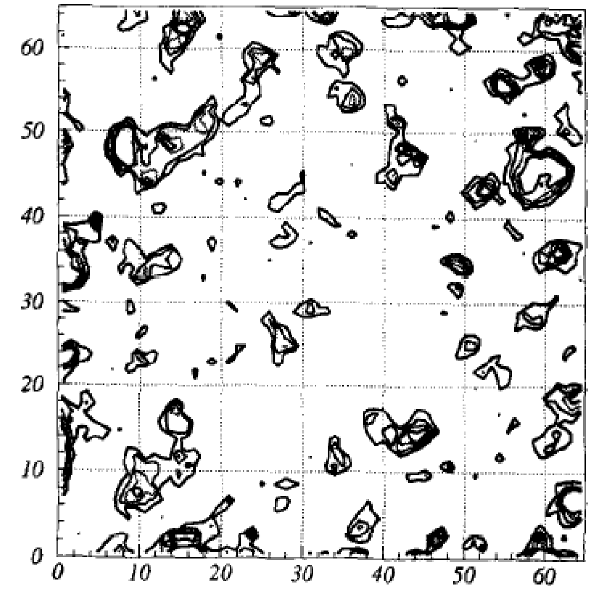

Fig. 2. Contour plot of the spectrum reported in Fig. 1. Iso-counting contours are displayed. The region contains 128×128 pixels, but it has been visualized in a 64×64 representation.

Frontal IBIC

APPLIED PHYSICS LETTERS VOLUME 84, NUMBER 22 31 MAY 2004

Temperature-dependent emptying of grain-boundary charge traps in chemical vapor deposited diamond

S. M. Hearne, D. N. Jamieson,[a)] E. Trajkov, and S. Prawer
School of Physics, University of Melbourne, Victoria, 3010, Australia
J. E. Butler
Naval Research Laboratory, Washington, DC 20375

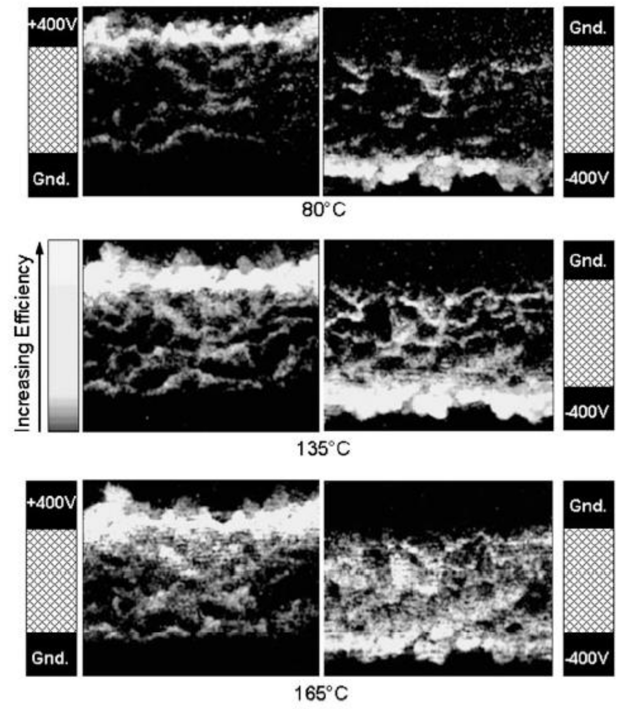

FIG. 1. Ion beam induced charge (IBIC) maps using a scanned 2 MeV He$^+$ microprobe of the charge collection in CVD diamond at various temperatures. The location of the electrodes is shown. Note that the charge collection efficiency is always highest near to the anode.

IBIC imaging with 2 MeV protons

IBIC maps of polycrystalline diamond inter-digitated detectors show 'hot spots' at electrode tips due to concentration of the electric field

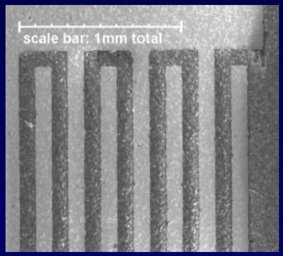

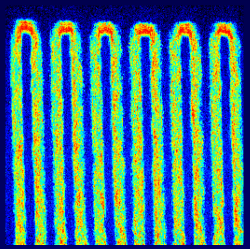

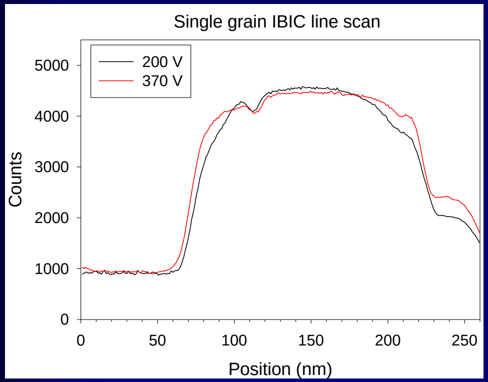

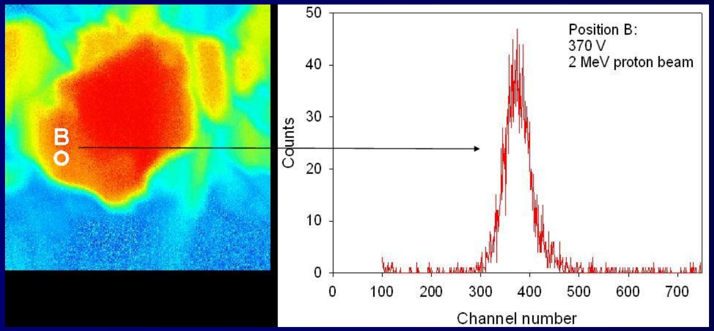

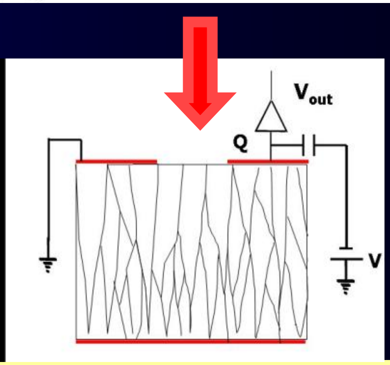

Intra-crystallite charge transport

M.B.H.Breese et al. NIM-B 181 (2001), 219-224; P.Sellin et al. NIM-B 260 (2007), 293-294

Poster Session I (23/07/2012) h. 17.30-18.40

Poster #75

Aleksandr Ponomarev

Investigation of Cd1-xMnxTe Polycrystalline Thin Films

Using Nuclear Microprobe Techniques

LATERAL IBIC-TRIBIC

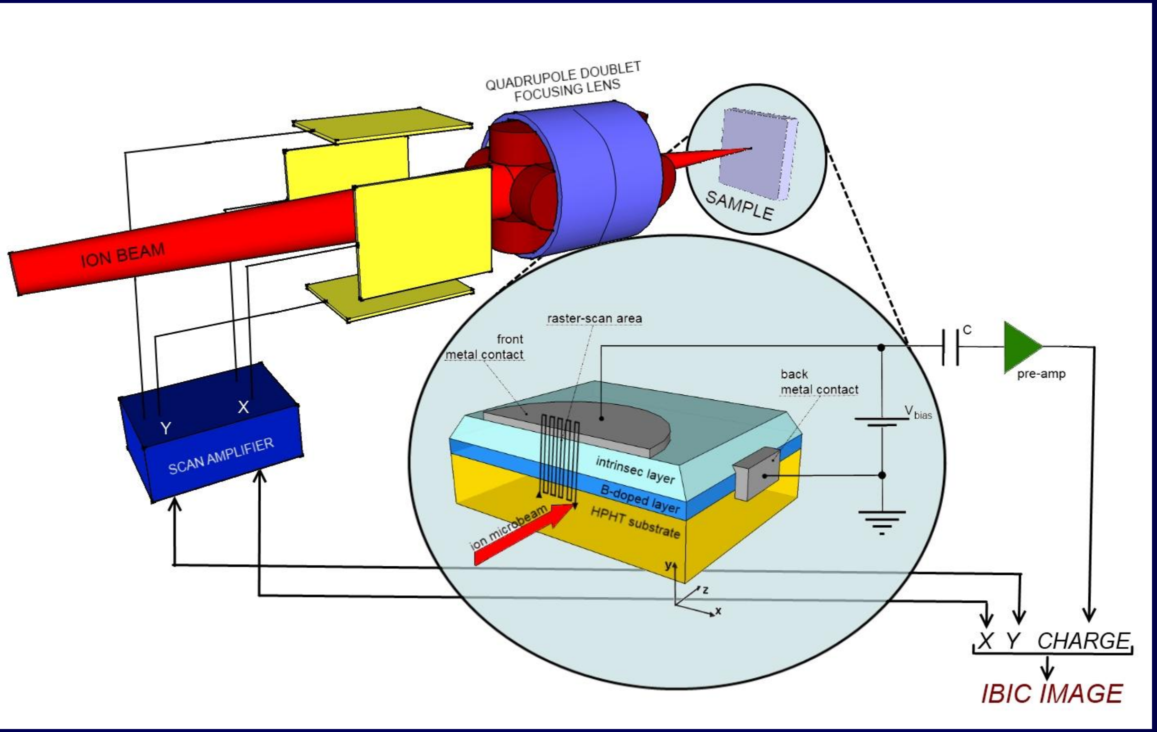

Monocrystalline Diamond Schottky diode

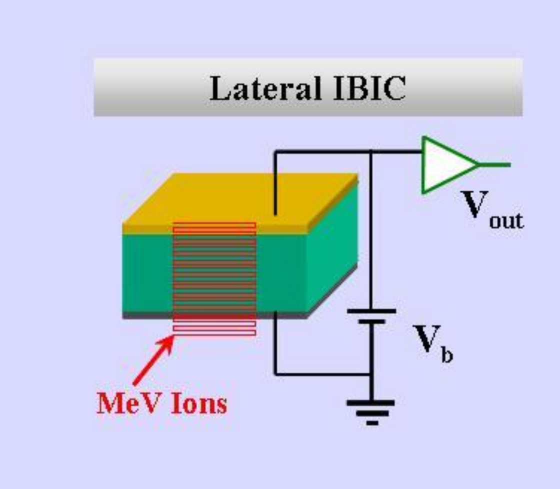

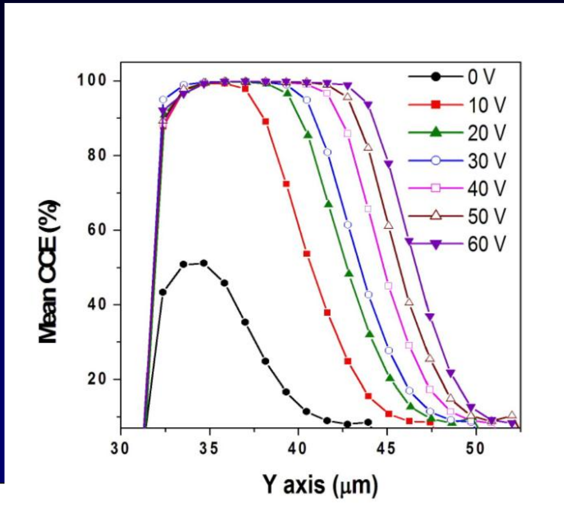

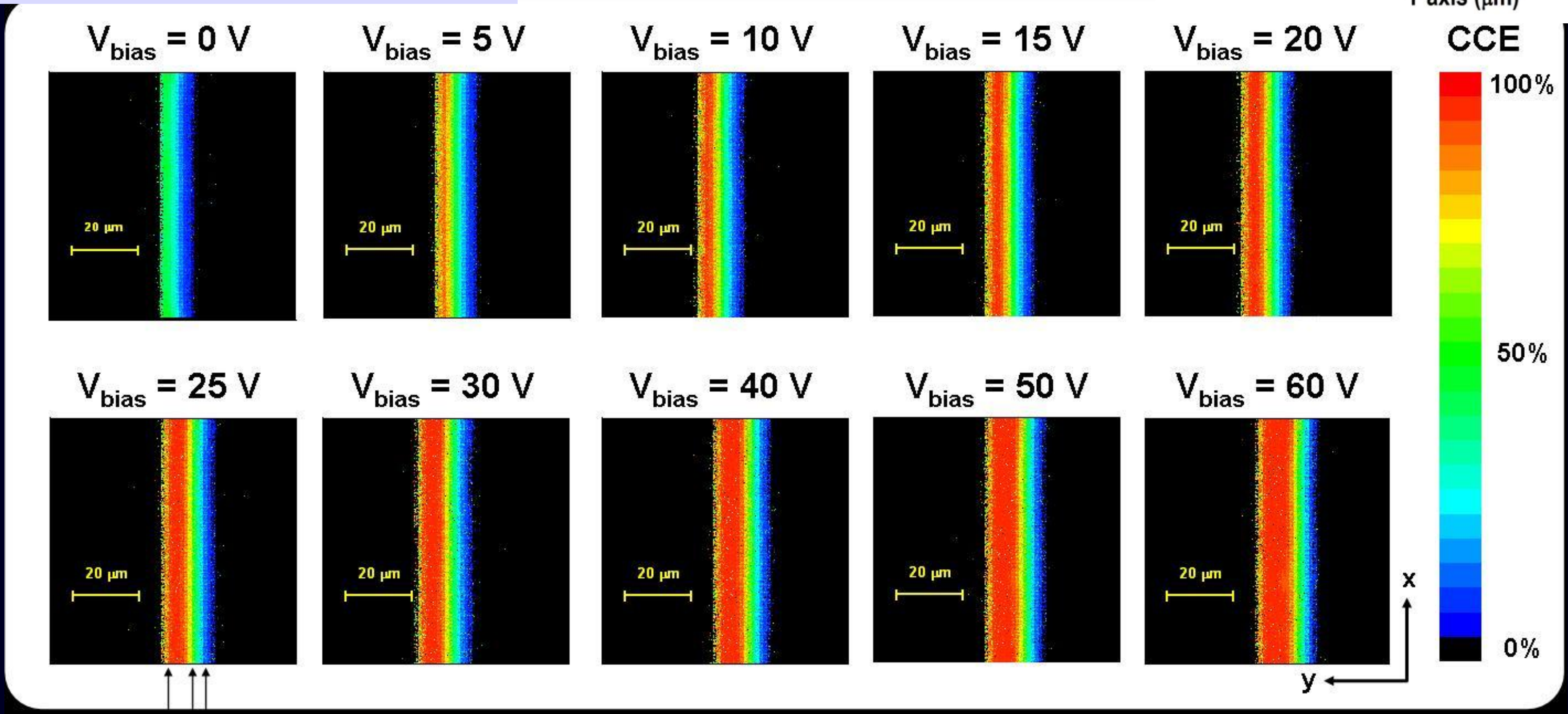

Plateaux: Depletion region (active region) Vs. Bias voltage

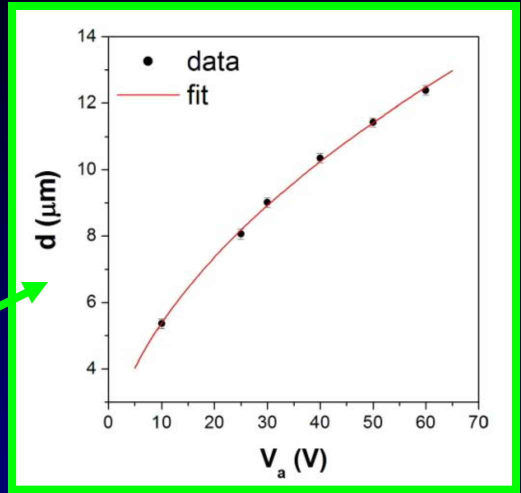

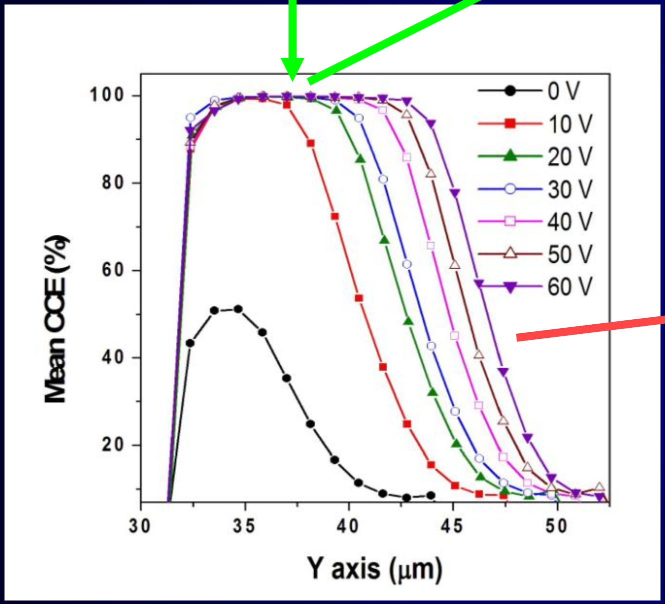

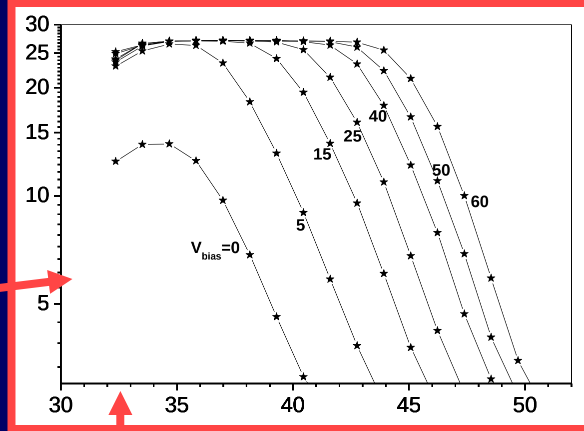

Exponential-like decay outside the highly efficient depletion region

$$\text{Electron diffusion length}: L_e = \sqrt{D_e \cdot \tau_e} = (2.57 \pm 0.17)\mu m$$

$$\text{Mobility} \cdot \text{lifetime} : \mu_e \cdot \tau_e = (2.57 \pm 0.3) V/cm^2$$

A high-speed imaging system for Time Resolved digital IBIC at Surrey

Lateral TRIBIC

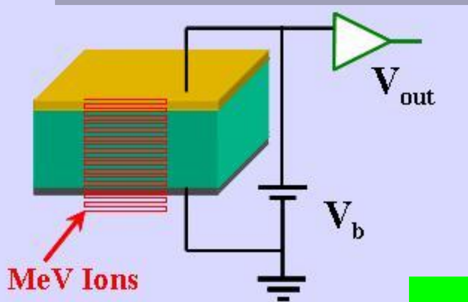

CdZnTe

radiation detector

$$v = \mu \cdot E$$

Induced current

$$I(t) = q \cdot \frac{v}{d}$$

P.J. Sellin et al. / Nuclear Instruments and Methods in Physics Research A 521 (2004) 600–607

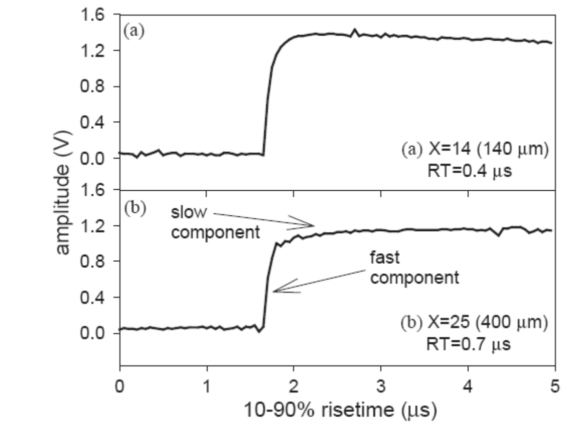

Fig. 3. Typical single pulse shapes obtained from CZT, with no averaging applied. The indicated distances are measured from the cathode.

606 *P.J. Sellin et al. / Nuclear Instruments and M*

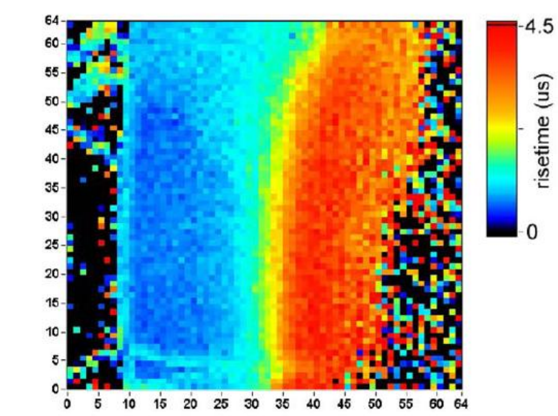

Fig. 6. Digital IBIC image of pulse risetime in CdZnTe, extracted from the same data set used to generate Fig. 4.

Poster Session III (26/07/2012) h. 16.15-18.00

Poster #171

Natko Skukan

CVD diamond as a position sensitive detector

using charge carrier transition time

Pulse shapes calculation

Shockley-Ramo theorem

Currents to Conductors Induced by a Moving Point Charge

W. Shockley
Bell Telephone Laboratories, Inc., New York, N. Y.
(Received May 14, 1938)

Currents Induced by Electron Motion*
SIMON RAMO†, ASSOCIATE MEMBER, I.R.E.

$$I = -q \cdot \mathbf{v} \cdot \frac{1}{d}$$

Gunn's theorem

Solid-State Electronics Pergamon Press 1964. Vol. 7, pp. 739–742. Printed in Great Britain

A GENERAL EXPRESSION FOR ELECTROSTATIC INDUCTION AND ITS APPLICATION TO SEMICONDUCTOR DEVICES

J. B. GUNN
IBM Watson Research Center, Yorktown Heights, New York

(*Received* 2 *March* 1964; *in revised form* 26 *March* 1964)

Abstract—A new formula is deduced, under rather general conditions, for the charges induced upon a system of conductors by the motion of a small charge nearby. The conditions are found under which this result can be simplified to yield various previously derived formulas applicable to the problem of collector transit time in semiconductor devices.

$$I = -q \cdot \mathbf{v} \cdot \frac{\partial \mathbf{E}}{\partial V}$$

Weighting field

Induced current into the sensing electrode

$$I = -q \cdot \mathbf{v} \cdot \frac{\partial \mathbf{E}}{\partial V} = -q \cdot \mathbf{v} \cdot \mathbf{E}_w$$

Weighting field

Weighting potential:

$$\nabla \psi_w = -\mathbf{E}_w = -\nabla \frac{\partial \psi}{\partial V} \Rightarrow \psi_w = \frac{\partial \psi}{\partial V}$$

Equation of motion: $\mathbf{v} = \frac{d\mathbf{r}}{dt}$

$$Q = \int_{t_A}^{t_B} I dt = -q \int_{t_A}^{t_B} \mathbf{v} \cdot E_w dt = -q \int_{\mathbf{r}_A}^{\mathbf{r}_B} E_w d\mathbf{r} =$$

$$= q \cdot \left(\psi_w(\mathbf{r}_B) - \psi_w(\mathbf{r}_A) \right) = q \cdot \left(\left. \frac{\partial \psi}{\partial V} \right|_{\mathbf{r}_B} - \left. \frac{\partial \psi}{\partial V} \right|_{\mathbf{r}_A} \right)$$

The induced charge Q into the sensing electrode

is given by the difference in the weighting potentials between any two positions (r_A and r_B) of the moving charge

To evaluate the total induced charge

Magnetic effects are negligible;

Electric field propagates instantaneously

Free carrier velocities much smaller than the light speed

Excess charge does not significantly perturb the electric field

Evaluate the actual potential ψ by solving the Poisson's equation

↓

Evaluate the Gunn's weighting potential $\frac{\partial\psi}{\partial V}$

V is the bias potential at the sensitive electrode

→

Solve the transport (continuity) equations

↓

$$Q = q\cdot\left(\left.\frac{\partial\psi}{\partial V}\right|_{r_B} - \left.\frac{\partial\psi}{\partial V}\right|_{r_A}\right)$$

The induced charge Q into the sensing electrode is given by the difference in the weighting potentials between any two positions (r_A and r_B) of the moving charge

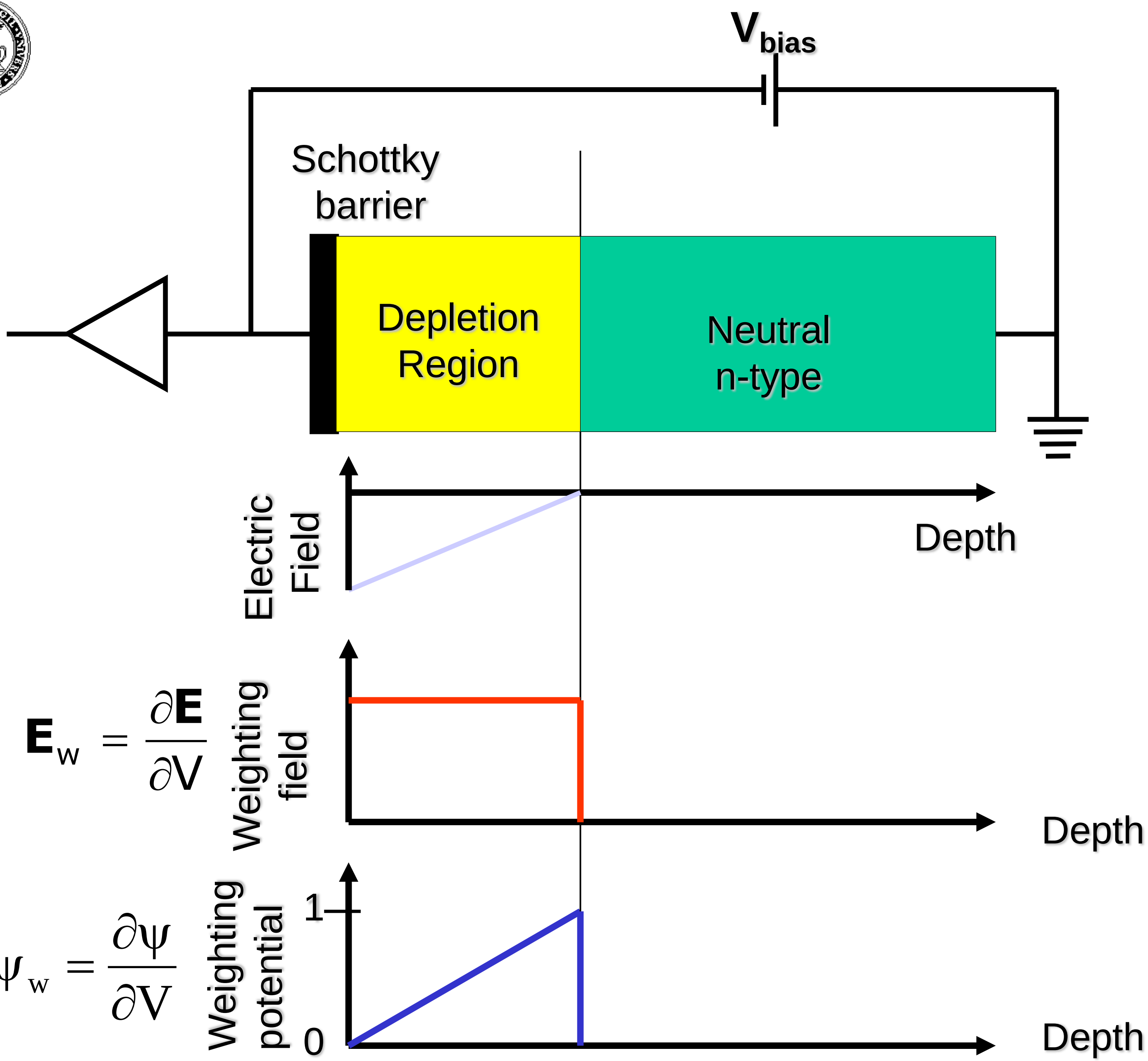

$$\mathbf{E}_w = \frac{\partial \mathbf{E}}{\partial V}$$

$$\psi_w = \frac{\partial \psi}{\partial V}$$

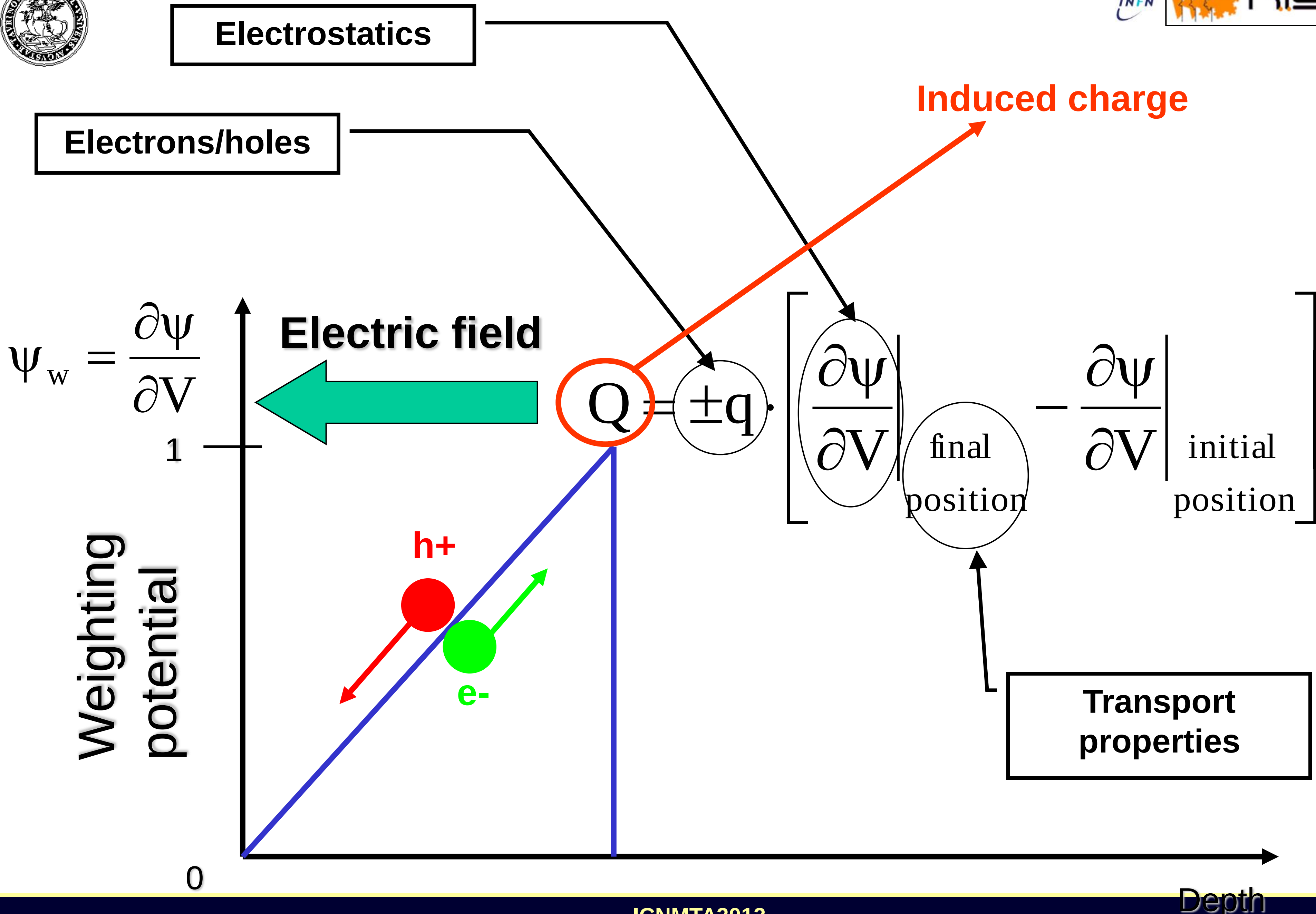

Electrostatics
Electrons/holes
Induced charge
Electric field
$\Psi_w = \frac{\partial \psi}{\partial V}$
$Q = \pm q \cdot \left[\left.\frac{\partial \psi}{\partial V}\right|_{\text{final position}} - \left.\frac{\partial \psi}{\partial V}\right|_{\text{initial position}} \right]$
1
0
Weighting potential
h+
e-
Transport properties
Depth

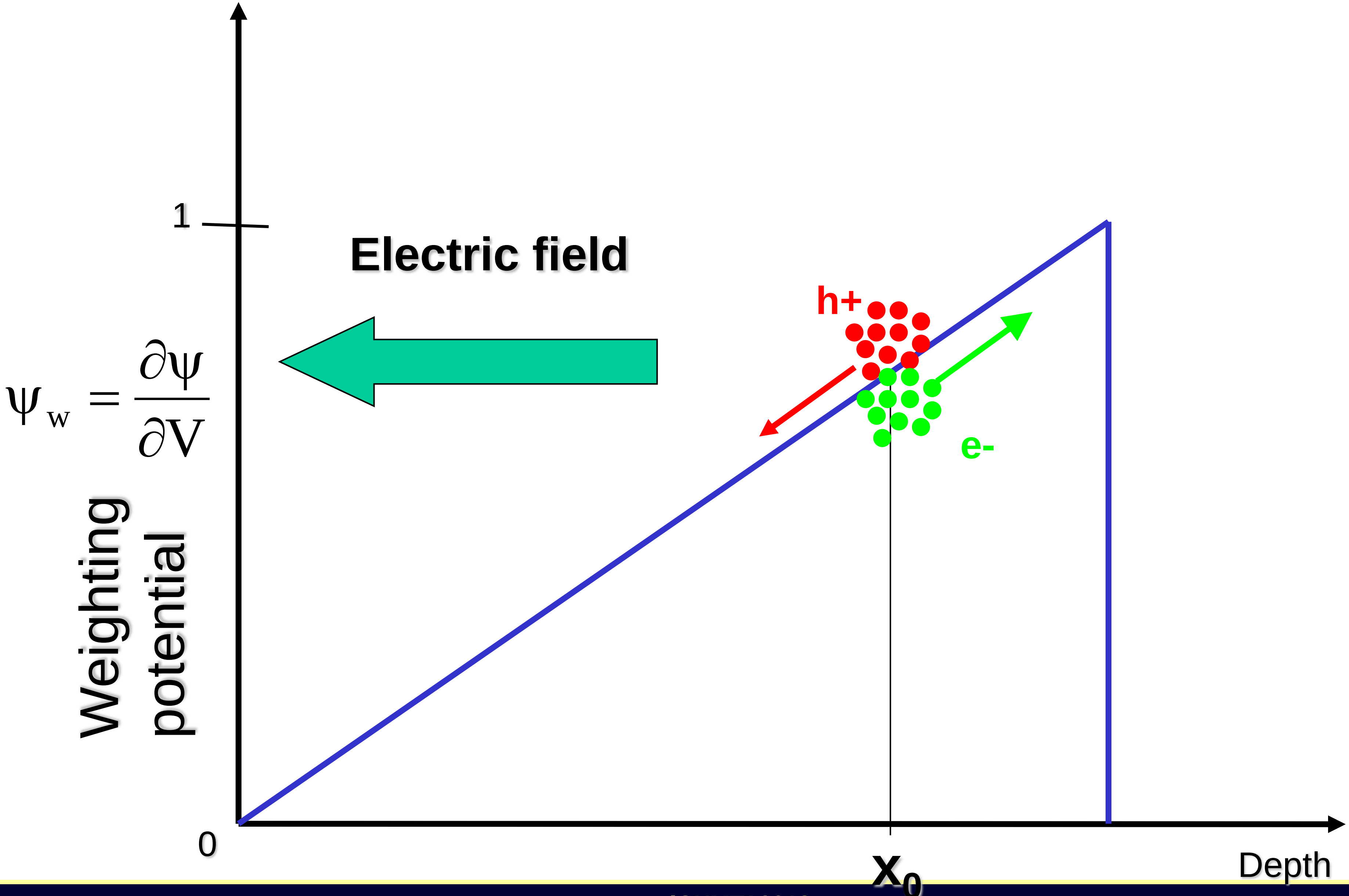

1
Electric field
h+
e-
$\psi_w = \frac{\partial \psi}{\partial V}$
Weighting potential
0
x_0
Depth

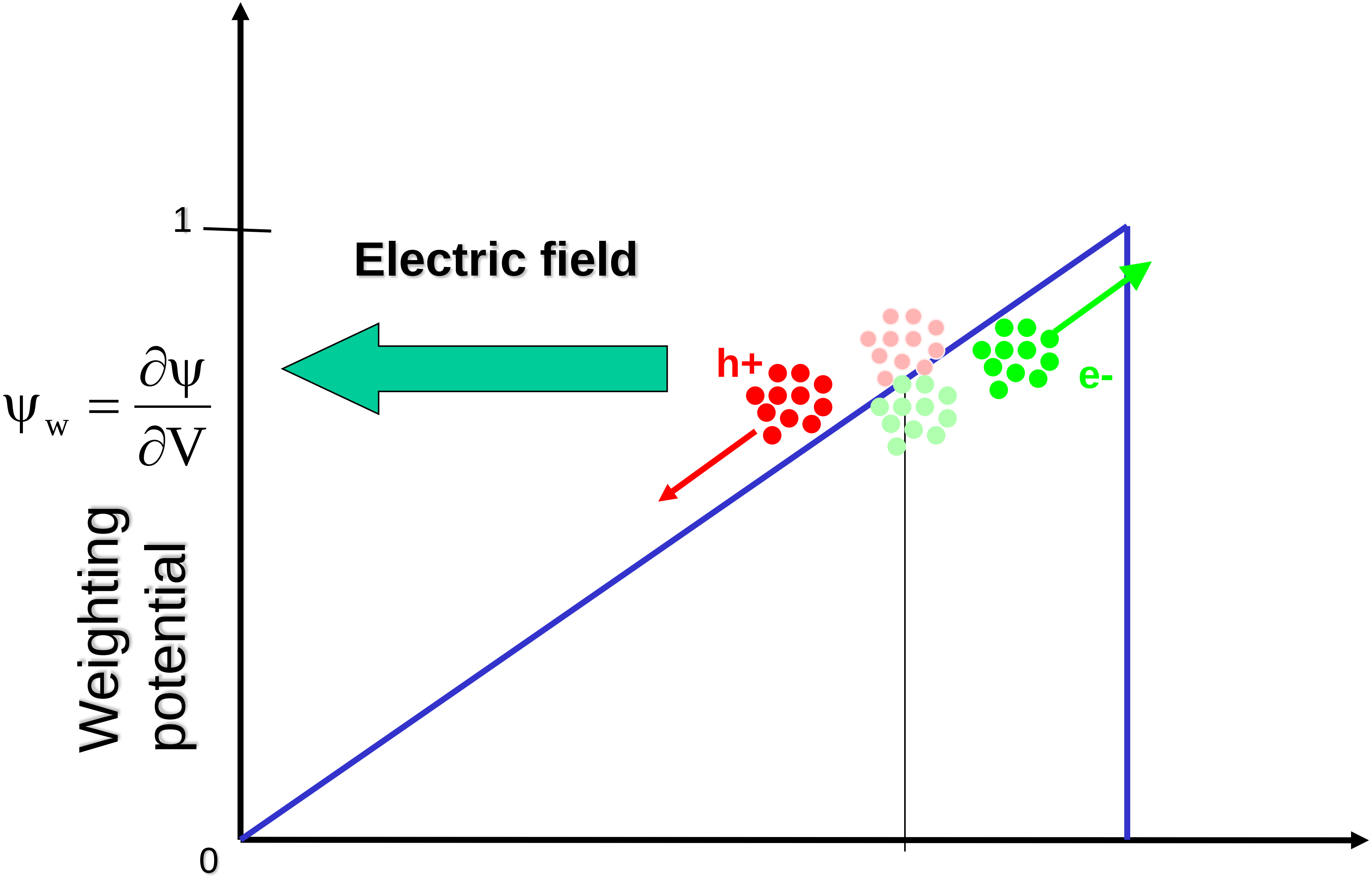

1
0
Electric field
h+
e-
$\psi_w = \frac{\partial \psi}{\partial V}$
Weighting potential

$$CCE = \frac{Q_{collected}}{Q_{Generated}} = \frac{q \cdot \sum_{electrons} \left[\left. \frac{\partial \psi}{\partial V} \right|_{\substack{final \\ position}} - \left. \frac{\partial \psi}{\partial V} \right|_{\substack{initial \\ position}} \right]}{q \cdot [\text{Total Number of electrons}]} = 1 - \frac{x_0}{w}$$

$$\psi_w = \frac{\partial \psi}{\partial V}$$

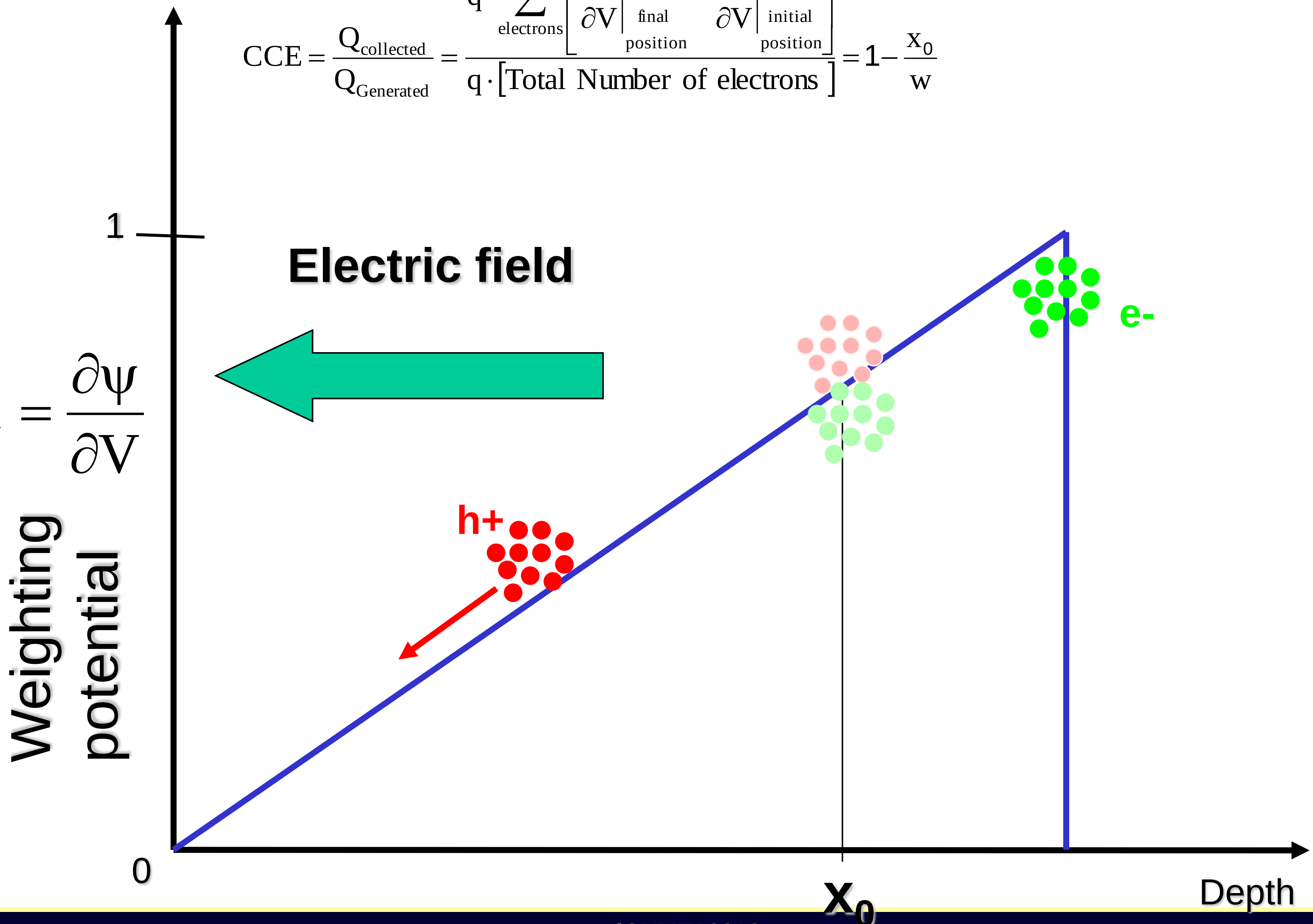

$$\psi_w = \frac{\partial \psi}{\partial V}$$

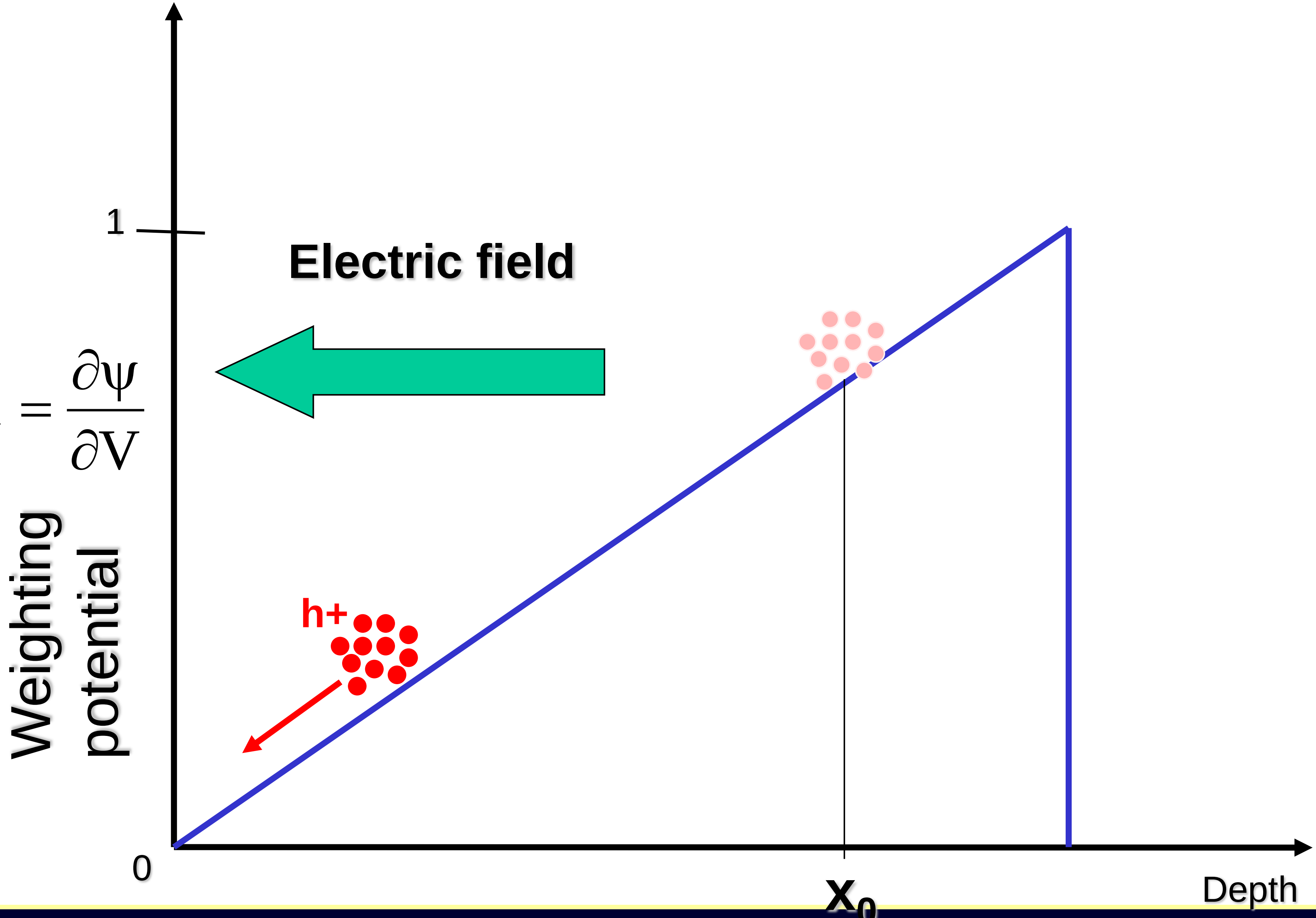

$$CCE = \frac{Q_{collected}}{Q_{Generated}} = \frac{q \cdot \sum_{holes} \left[\left. \frac{\partial \psi}{\partial V} \right|_{\substack{final \\ position}} - \left. \frac{\partial \psi}{\partial V} \right|_{\substack{initial \\ position}} \right]}{q \cdot [\text{Total Number of holes}]} = \frac{x_0}{w}$$

$$CCE_{ToT} = \frac{\text{electrons}_{\ collected}}{\text{electrons}_{\ Generated}} + \frac{\text{holes}_{\ collected}}{\text{holes}_{\ Generated}} = \left(1 - \frac{x_0}{w}\right) + \frac{x_0}{w} = 1$$

$$\psi_w = \frac{\partial \psi}{\partial V}$$

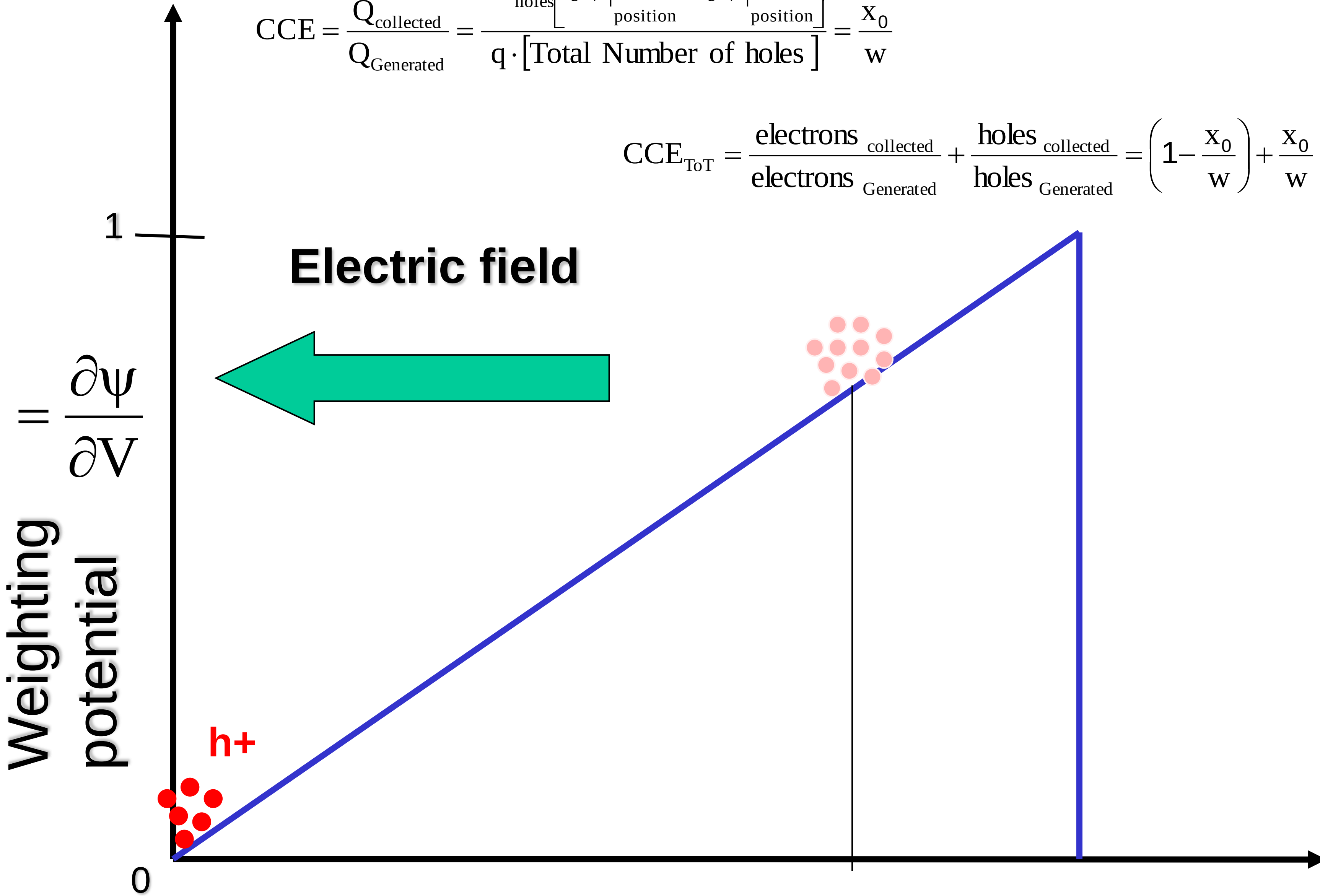

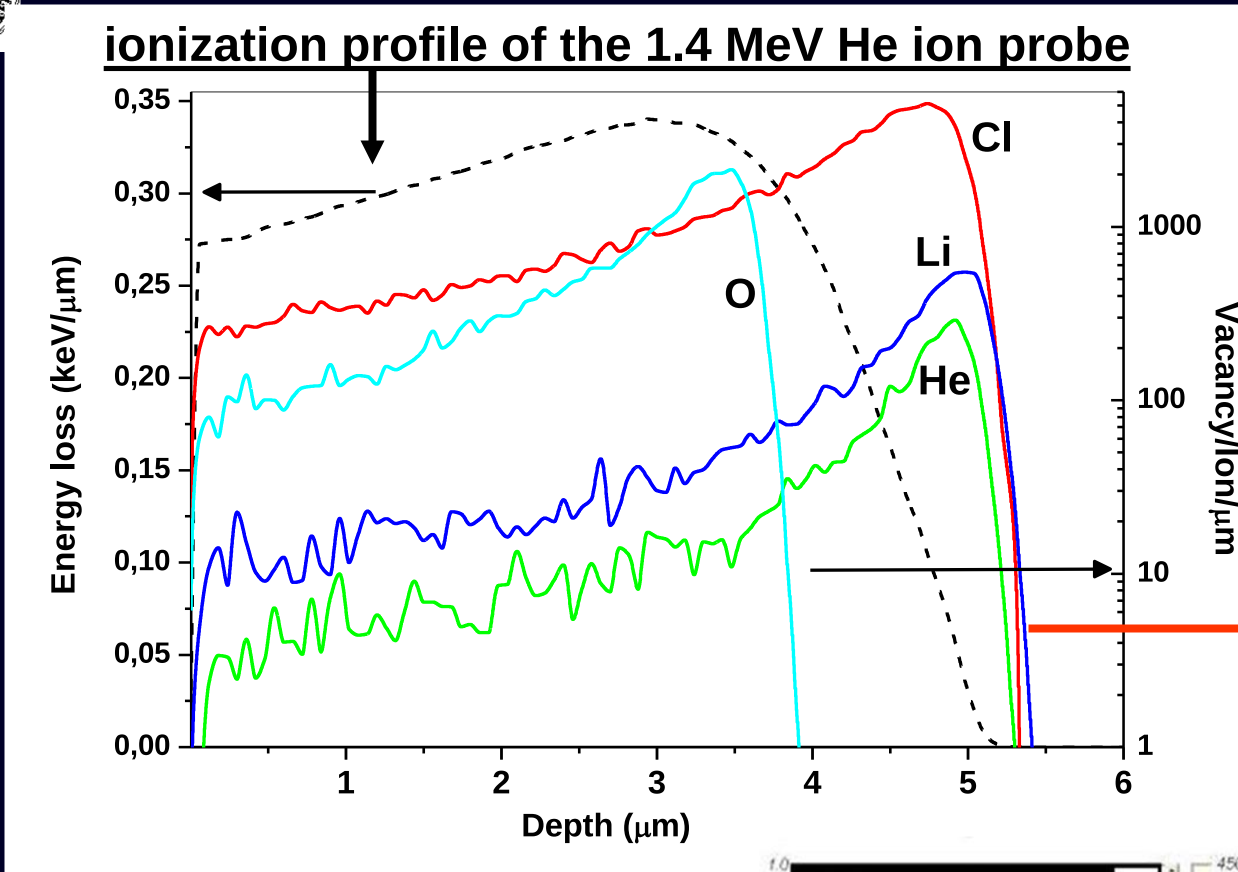

Vacancy profiles generated by
11 MeV Cl,
4 MeV O,
2.15 MeV Li
1.4 MeV He

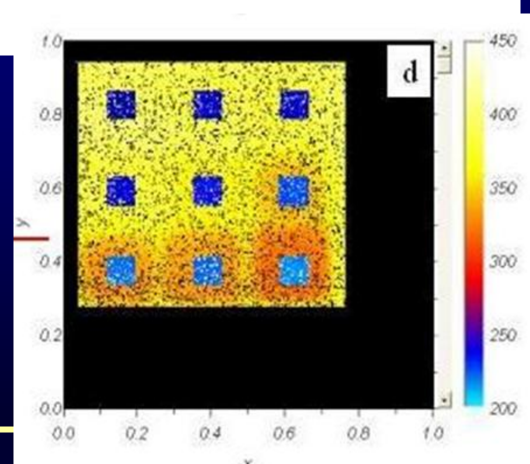

Effects of localized recombination centres

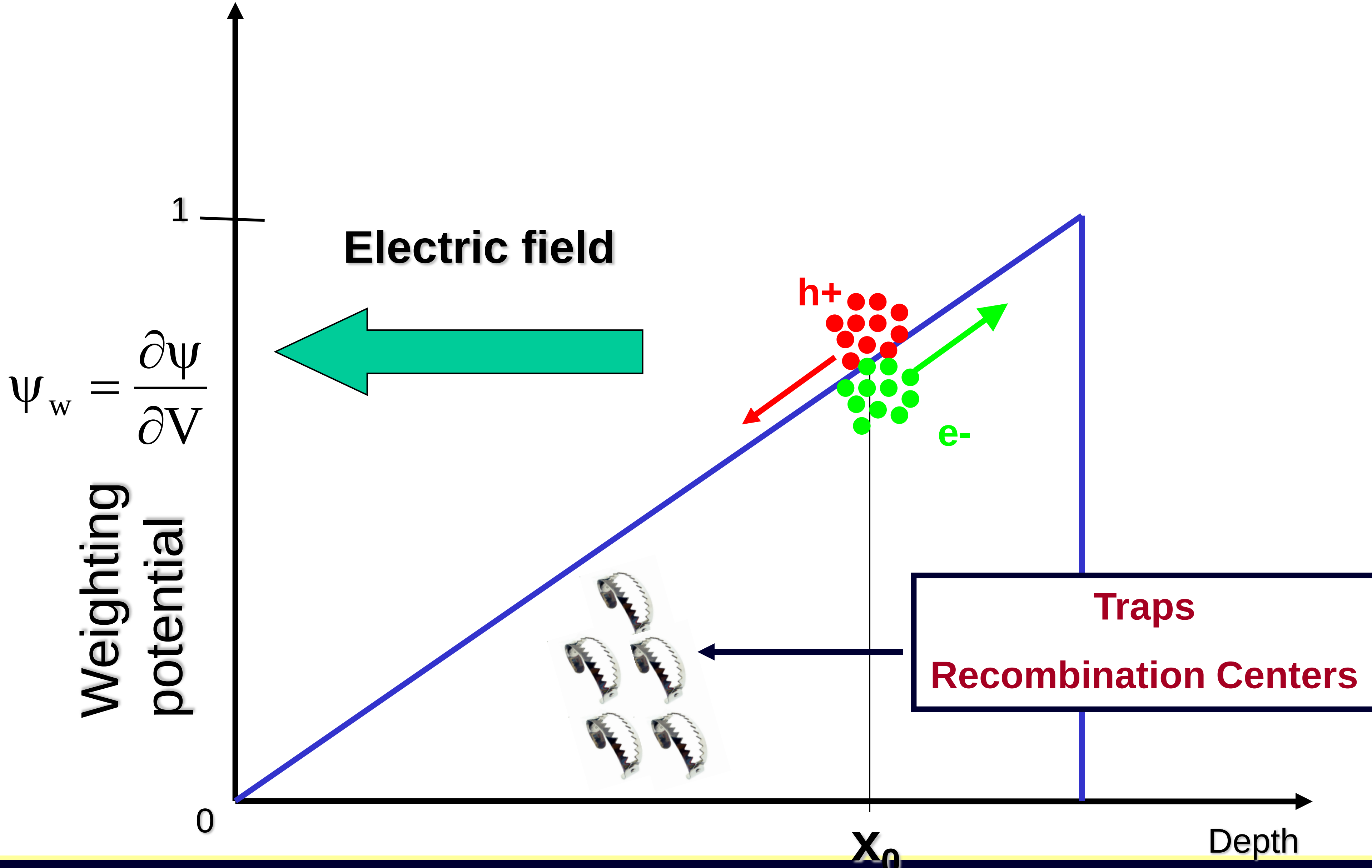

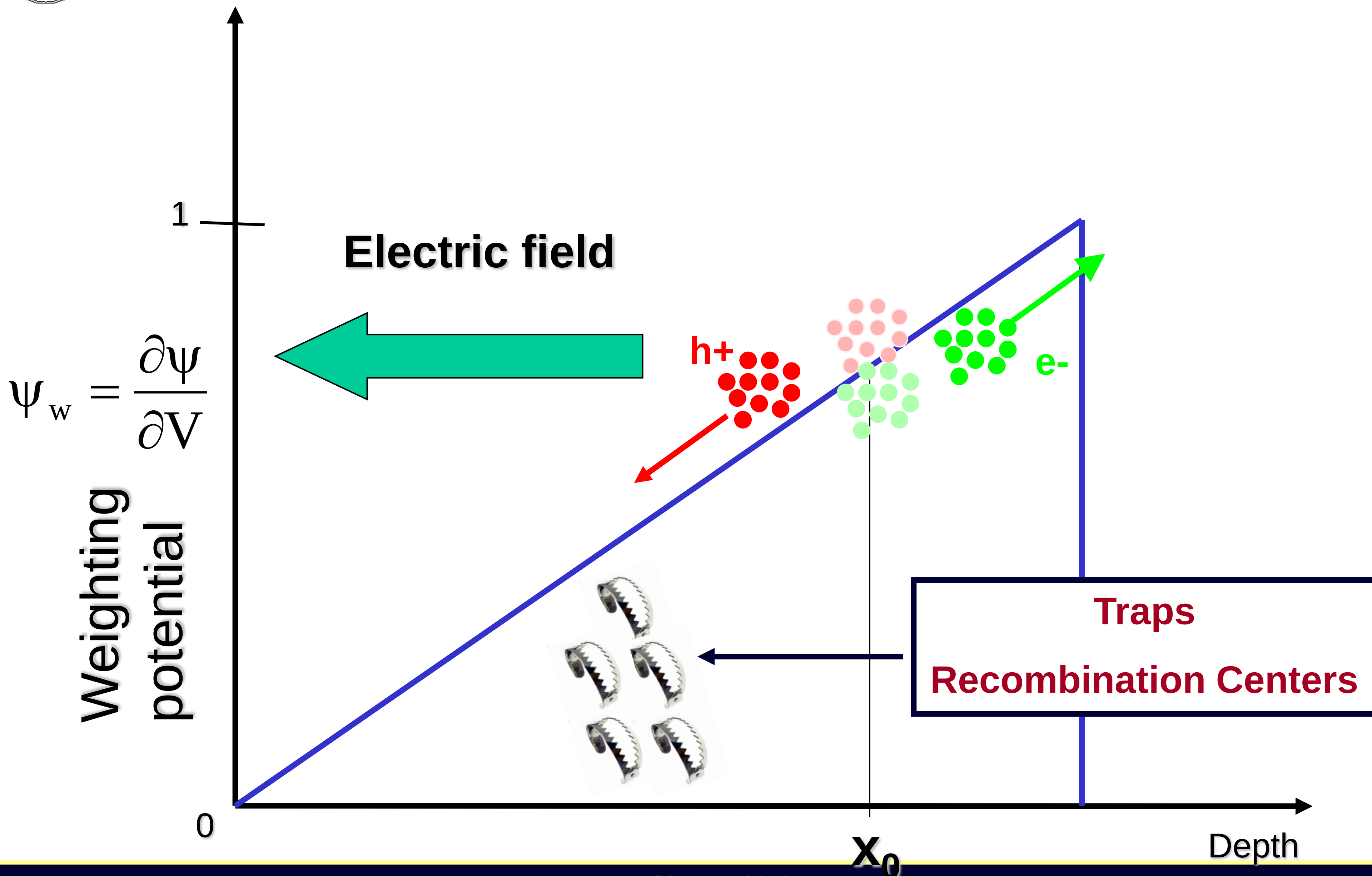

Electric field
h+
e-
1
0
$\psi_w = \frac{\partial \psi}{\partial V}$
Weighting potential
Traps
Recombination Centers
x_0
Depth

$$CCE = \frac{Q_{collected}}{Q_{Generated}} = \frac{q \cdot \sum_{electrons} \left[\left.\frac{\partial\psi}{\partial V}\right|_{\substack{final\\position}} - \left.\frac{\partial\psi}{\partial V}\right|_{\substack{initial\\position}} \right]}{q \cdot [\text{Total Number of electrons}]} = 1 - \frac{x_0}{w}$$

$$\psi_w = \frac{\partial\psi}{\partial V}$$

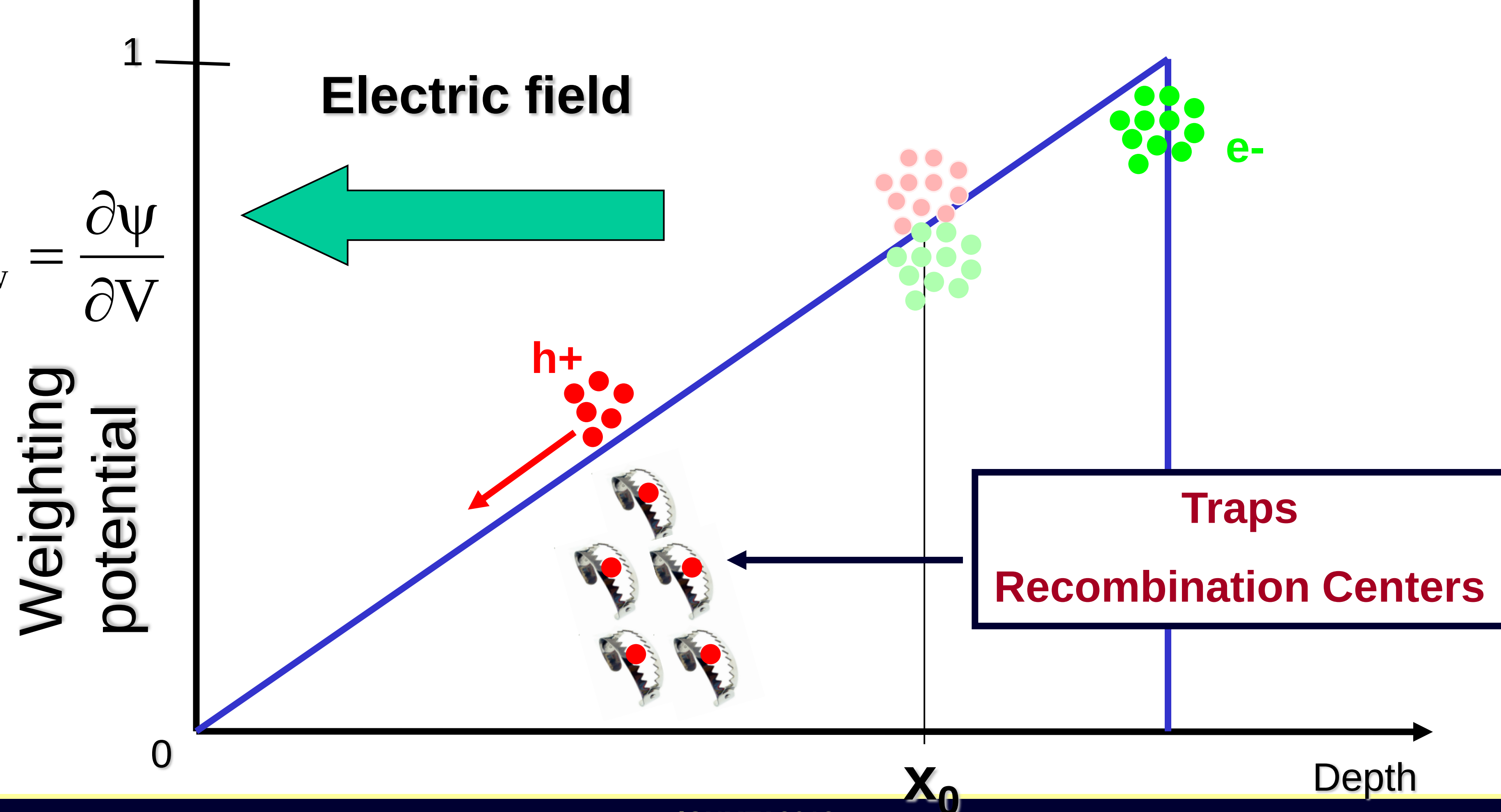

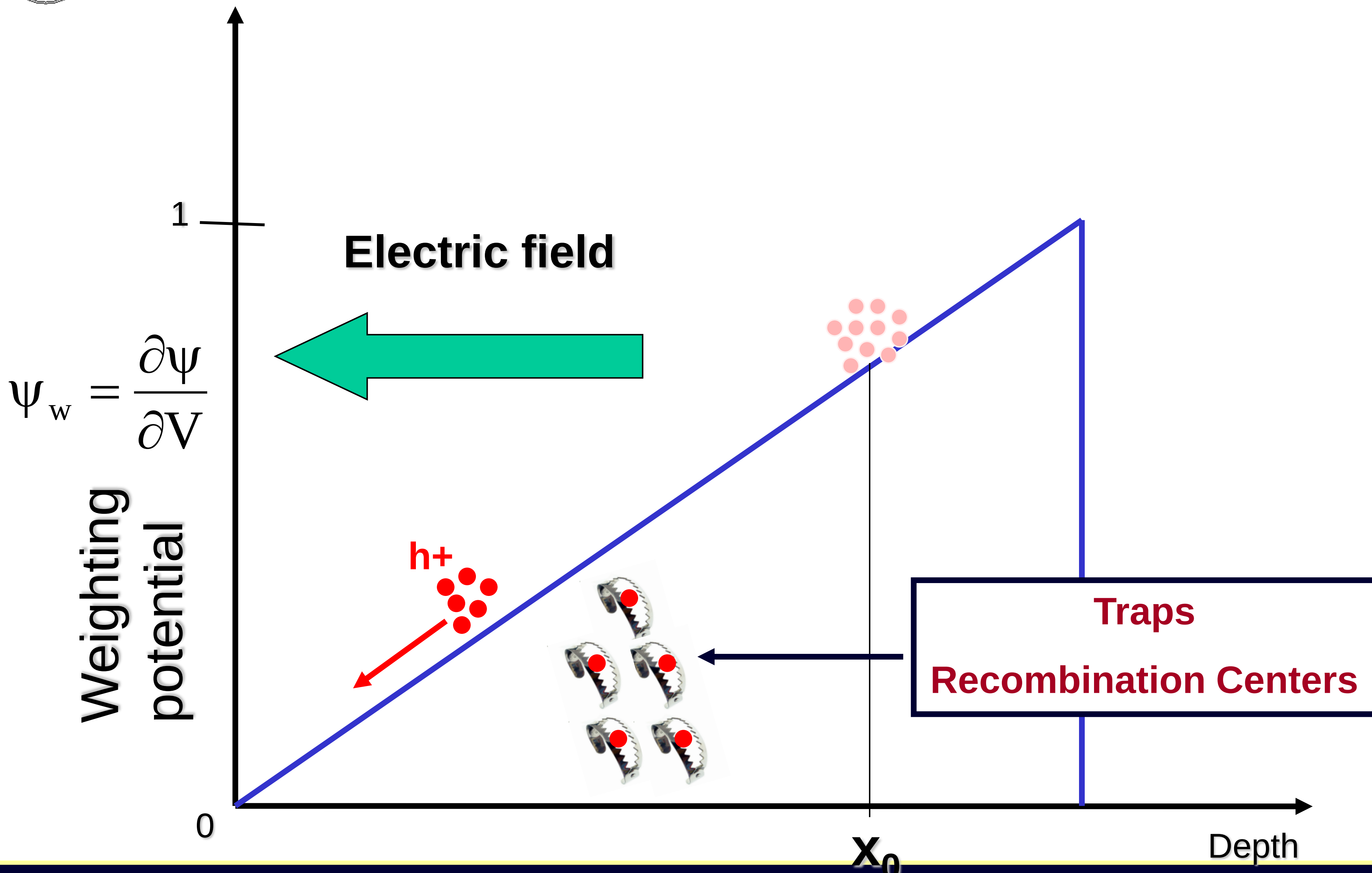

1
0
Electric field
$\psi_w = \frac{\partial \psi}{\partial V}$
Weighting potential
h+
Traps
Recombination Centers
x_0
Depth

$$CCE = \frac{Q_{collected}}{Q_{Generated}} = \frac{q \cdot \sum_{holes}\left[\left.\frac{\partial\psi}{\partial V}\right|_{\substack{final\\position}} - \left.\frac{\partial\psi}{\partial V}\right|_{\substack{initial\\position}} \right]}{q \cdot [\text{Total Number of holes}]} < \frac{x_0}{w}$$

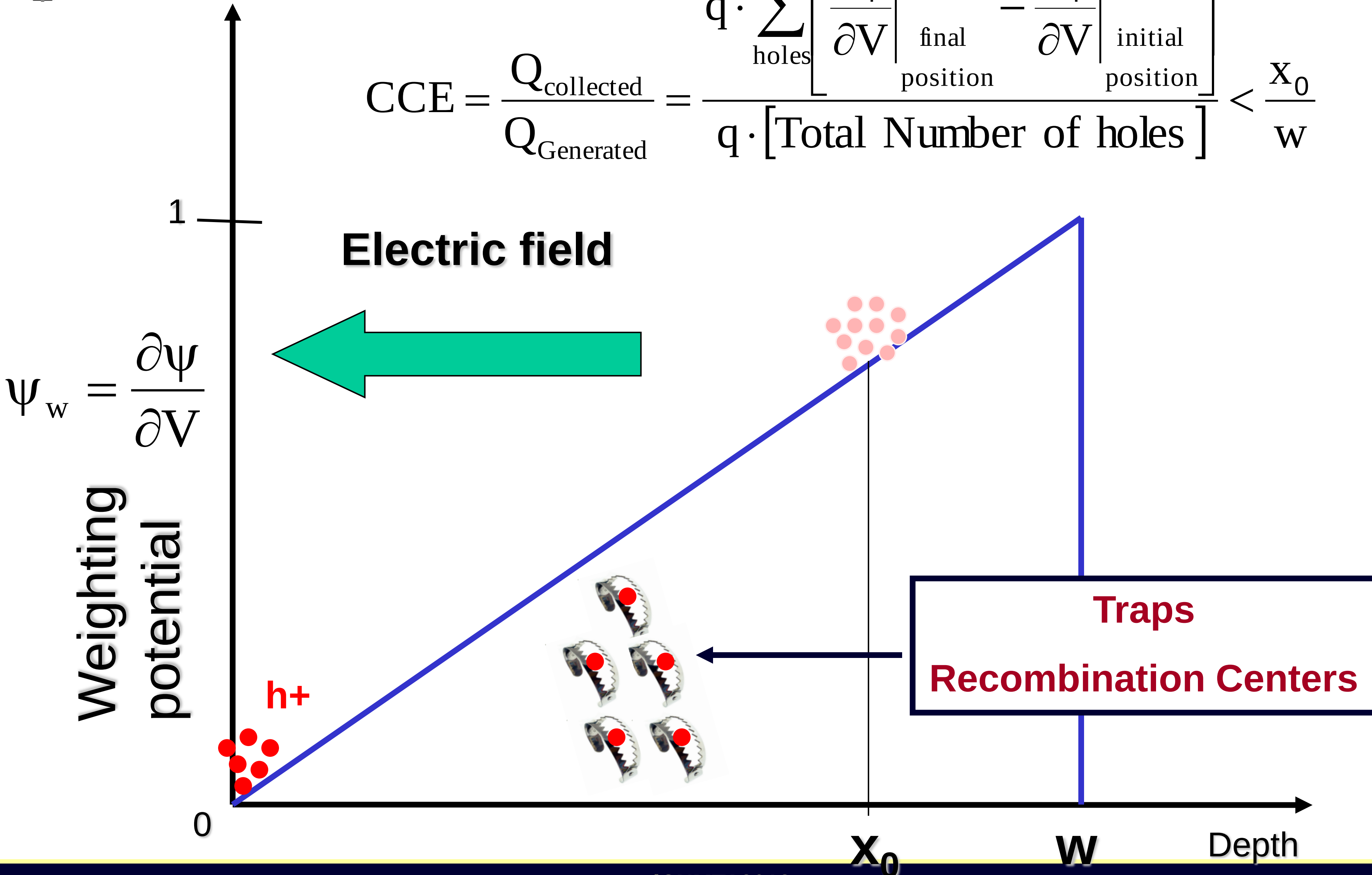

Radiation Damage in 4H-SiC

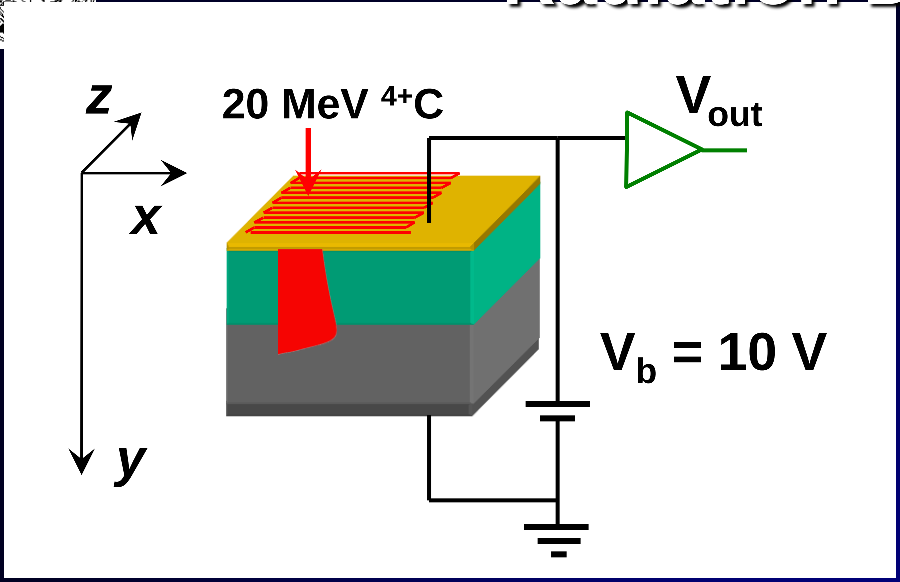

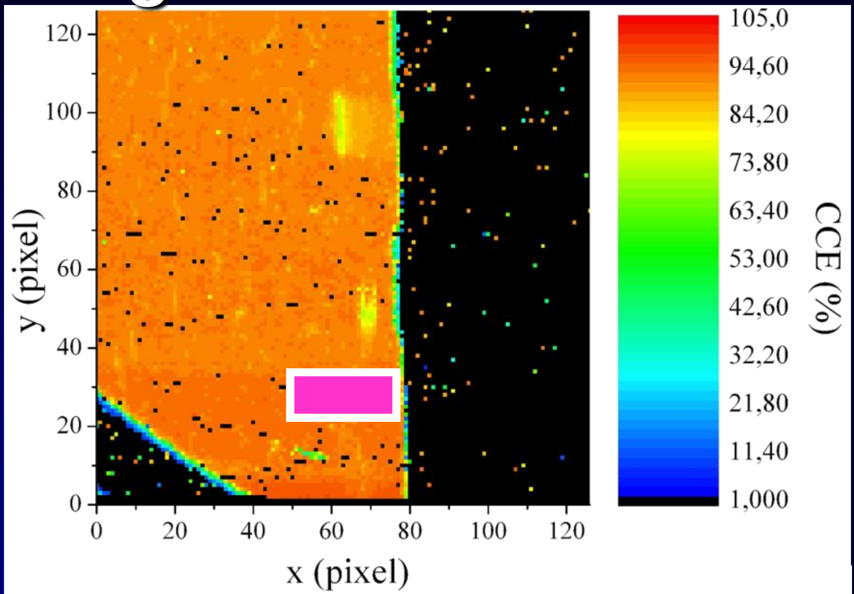

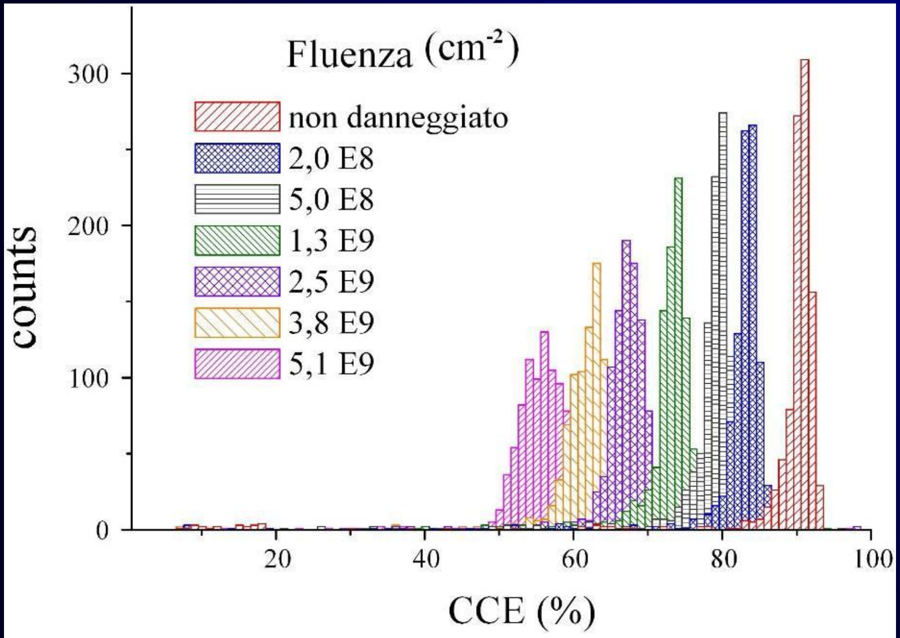

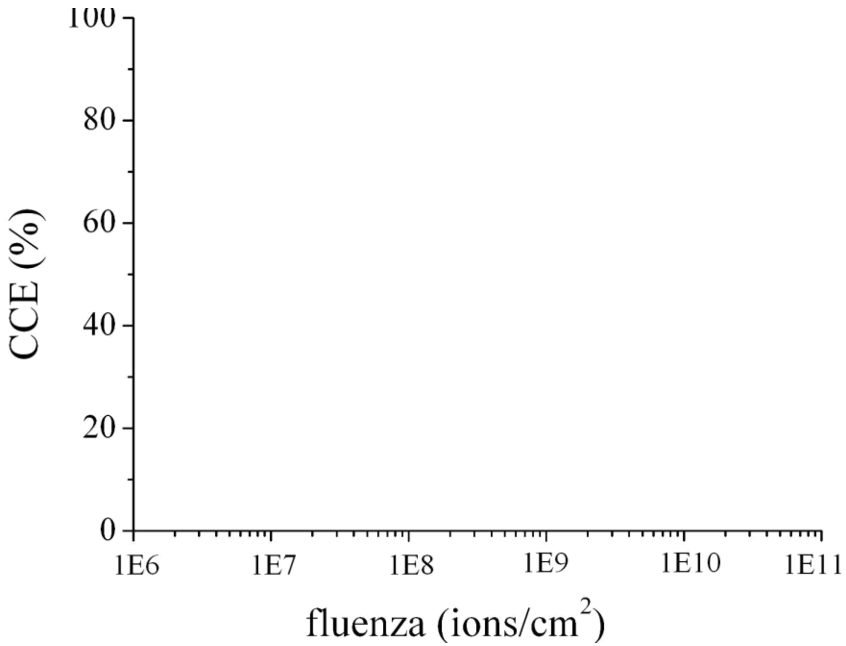

Transport equations

Electrostatics of the device (TCAD)

Vacancy profille (from SRIM; PAS)

Trap cross section (DLTS)

Shockley-Read-Hall Recombination/trapping model

Shockley-Ramo-Gunn Theorem

Low Level of damage

Trap/vacancy ratio
Radiation hardness

Oral Session 25/07/2012, h 9:00-10.30

#250: Milko Jaksic (invited) : Review of nuclear microprobe applications in material science

Oral Session 25/07/2012, h 11:00-12.30

#198: Gyorgy Vizkelethy: Investigation of ion beam induced radiation damage in Si and GaAs diodes

#92: Zeljko Pastuovic: Overview of radiation damage studies in silicon diodes exposed to focused ion beam irradiation-Proposed template for further research of radiation damage studies in semiconducting materials and devices by IBIC

Poster Session I (23/07/2012) h. 17.30-18.40

Poster #141: Veljko Grilj: Comparison of scCVD diamond and silicon SB detectors irradiated by low energy protons

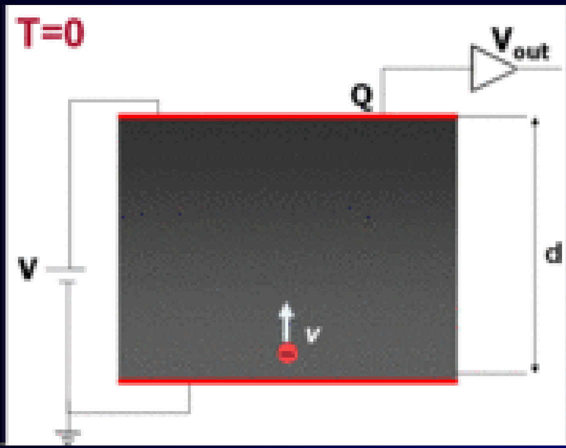

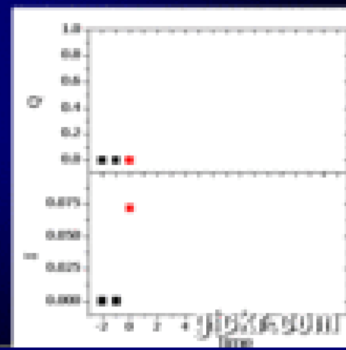

The induced charge Q into the sensing electrode is given by the difference in the weighting potentials between any two positions (r_A and r_B) of the moving charge

$$Q = q \cdot \left(\left.\frac{\partial \psi}{\partial V}\right|_{\substack{\text{final}\\ \text{position}}} - \left.\frac{\partial \psi}{\partial V}\right|_{\substack{\text{initial}\\ \text{position}}} \right)$$

CHARGE SHARING IN MULTIELECTRODE DEVICES

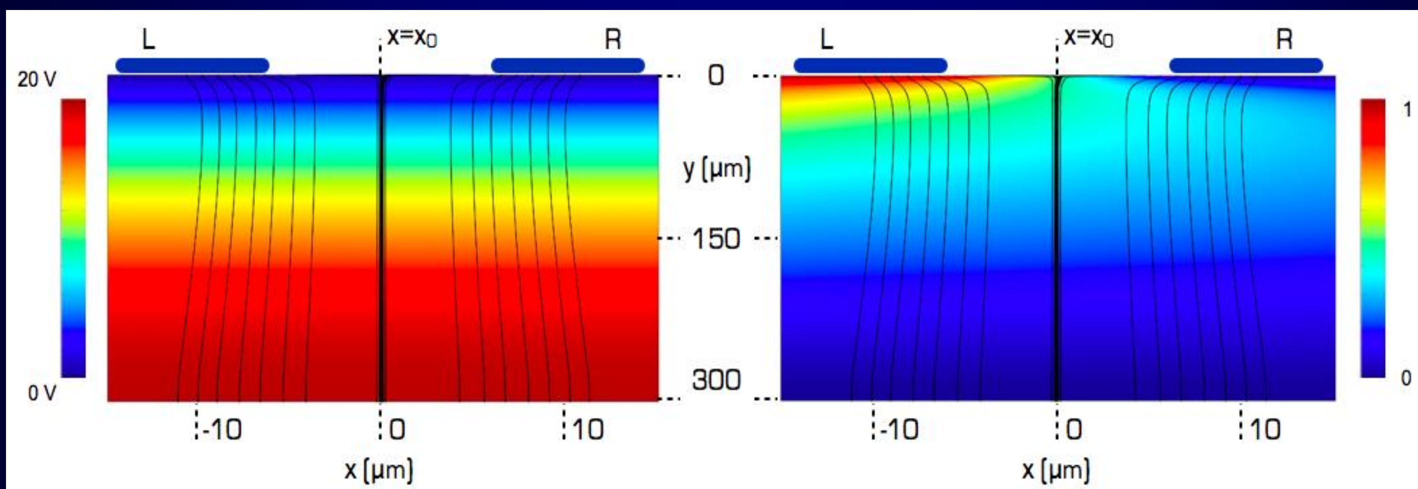

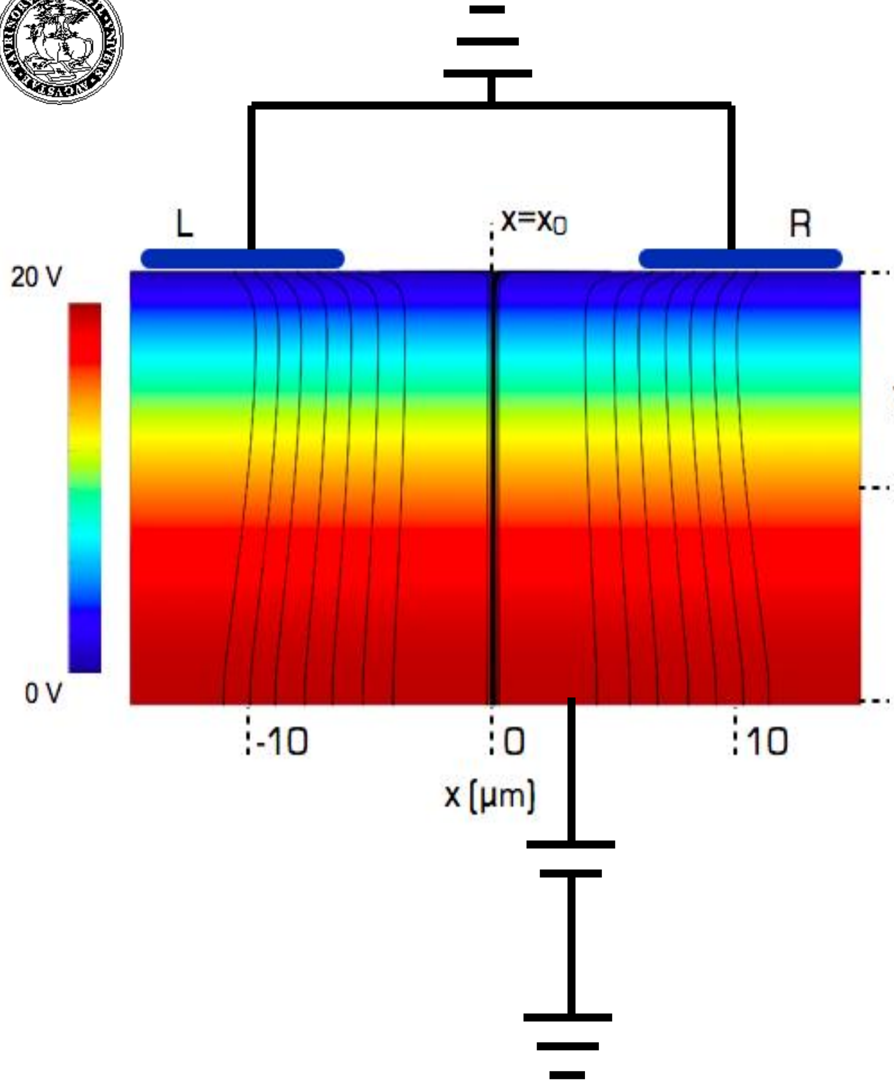

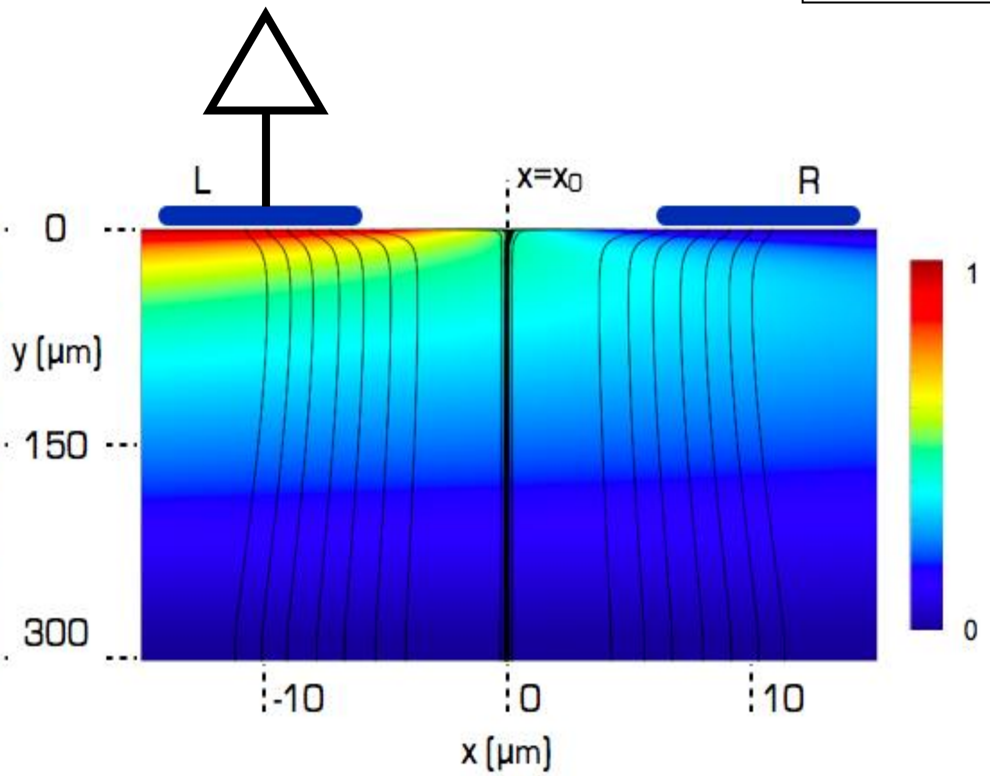

Actual potential

Weighting potential

Weighting potential

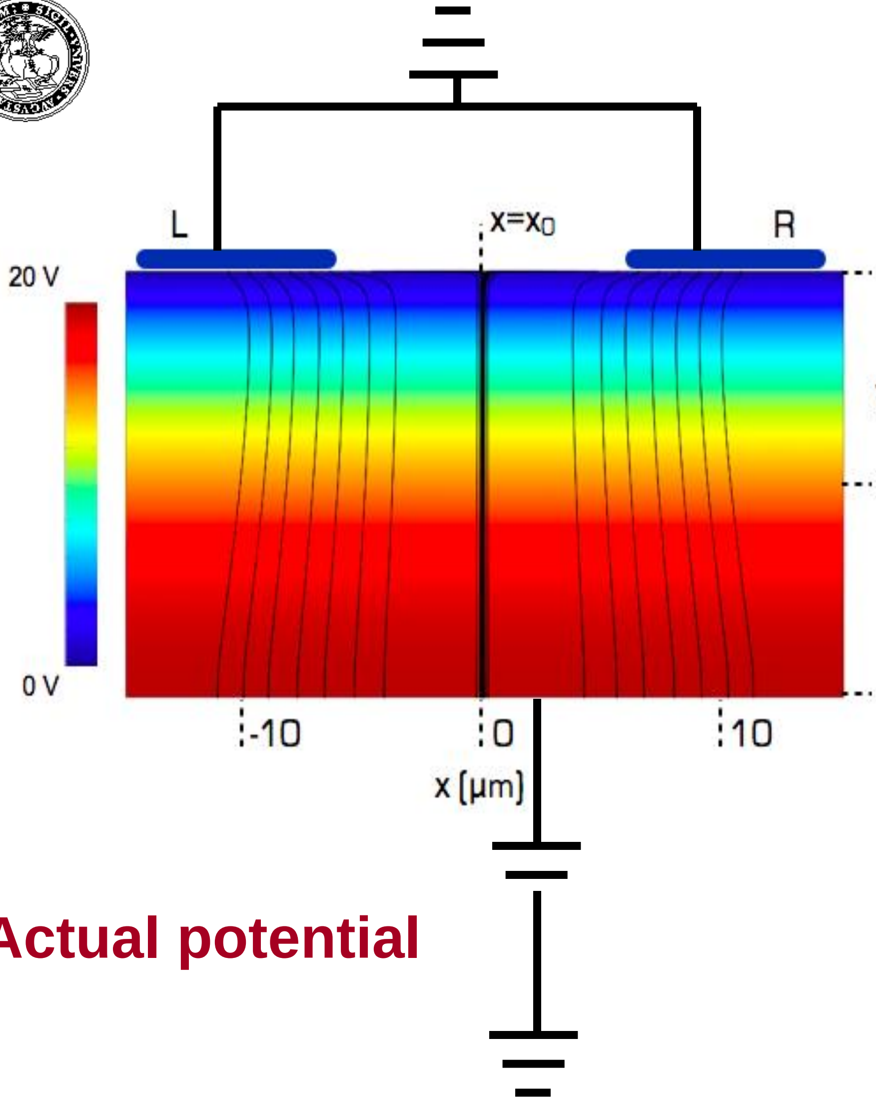

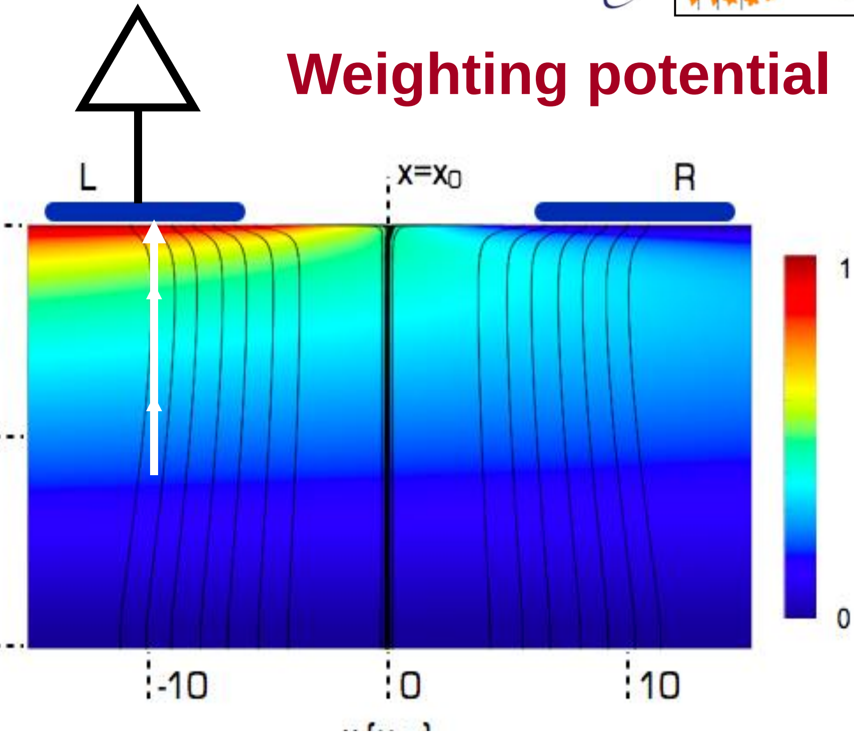

Actual potential

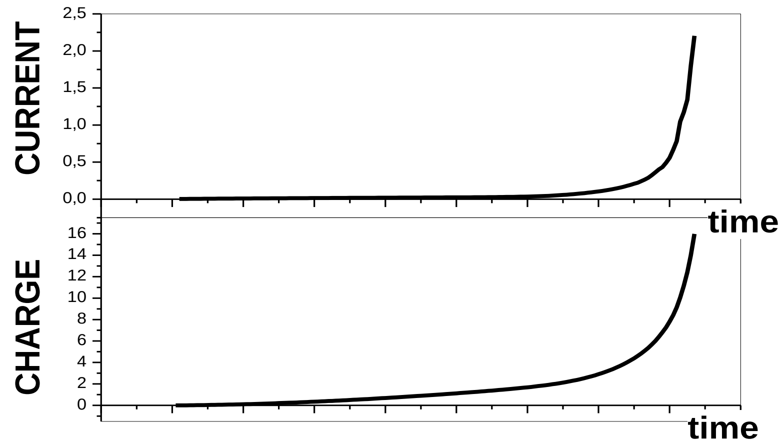

$$Q = q \cdot \left(\left. \frac{\partial \psi}{\partial V} \right|_{\substack{\text{final} \\ \text{position}}} - \left. \frac{\partial \psi}{\partial V} \right|_{\substack{\text{initial} \\ \text{position}}} \right)$$

Weighting potential

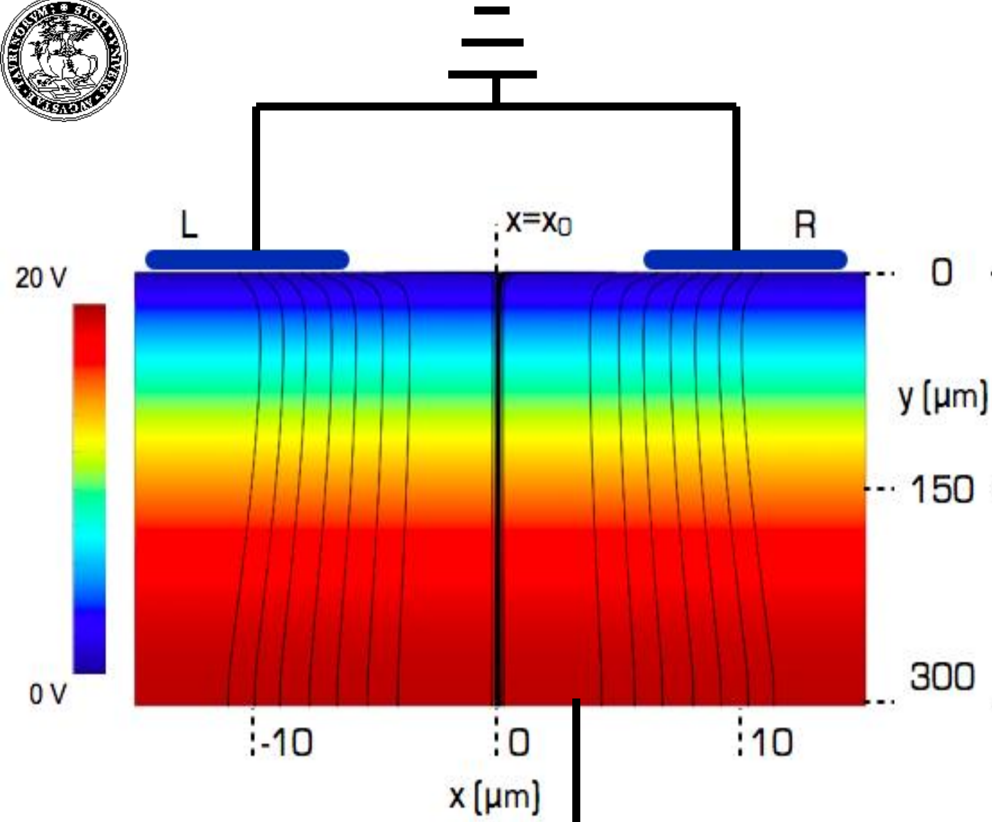

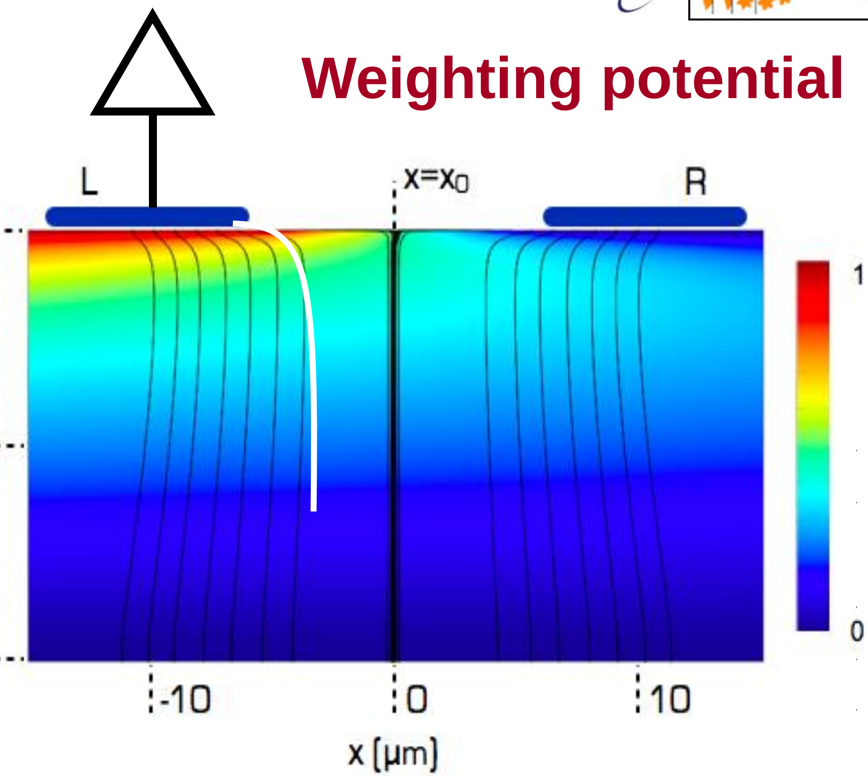

Actual potential

$$Q = q \cdot \left(\left.\frac{\partial \psi}{\partial V}\right|_{\substack{\text{final} \\ \text{position}}} - \left.\frac{\partial \psi}{\partial V}\right|_{\substack{\text{initial} \\ \text{position}}} \right)$$

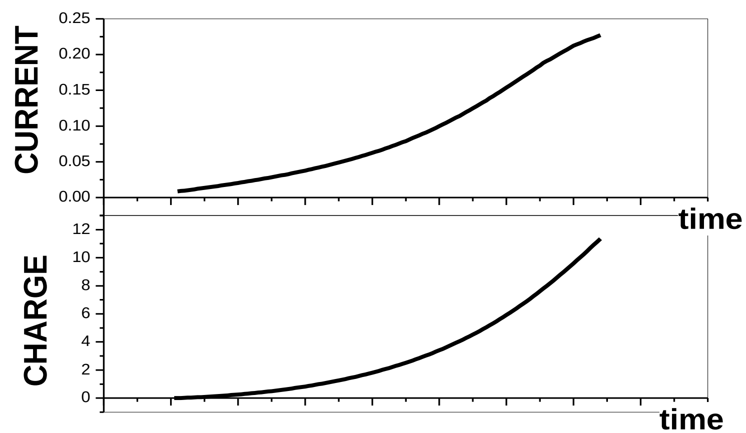

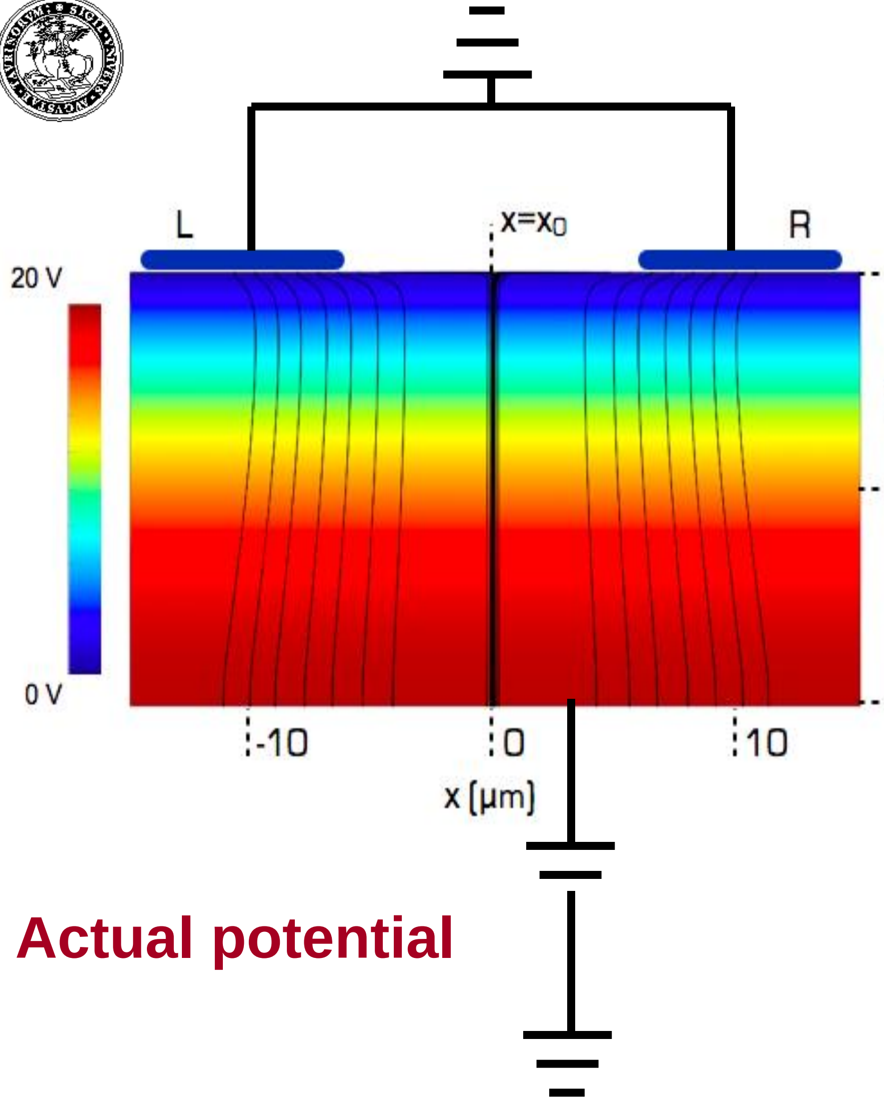

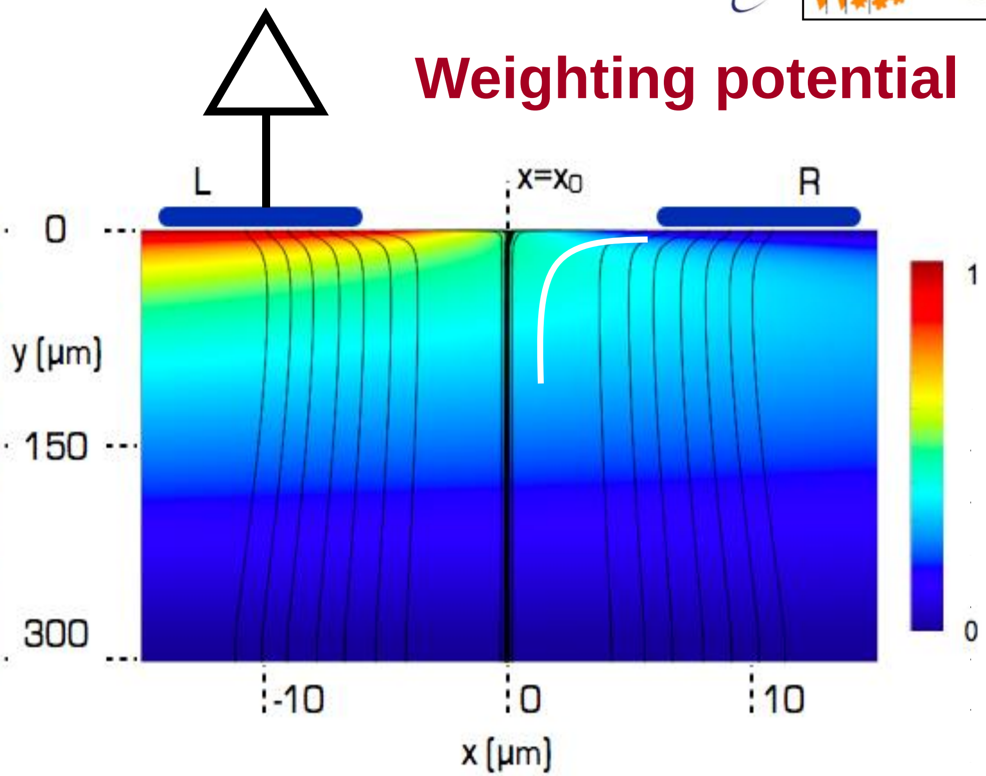

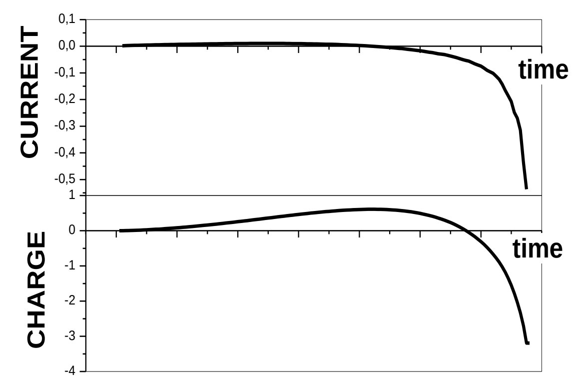

$$Q = q \cdot \left(\left.\frac{\partial \psi}{\partial V}\right|_{\substack{\text{final}\\ \text{position}}} - \left.\frac{\partial \psi}{\partial V}\right|_{\substack{\text{initial}\\ \text{position}}} \right)$$

Weighting potential

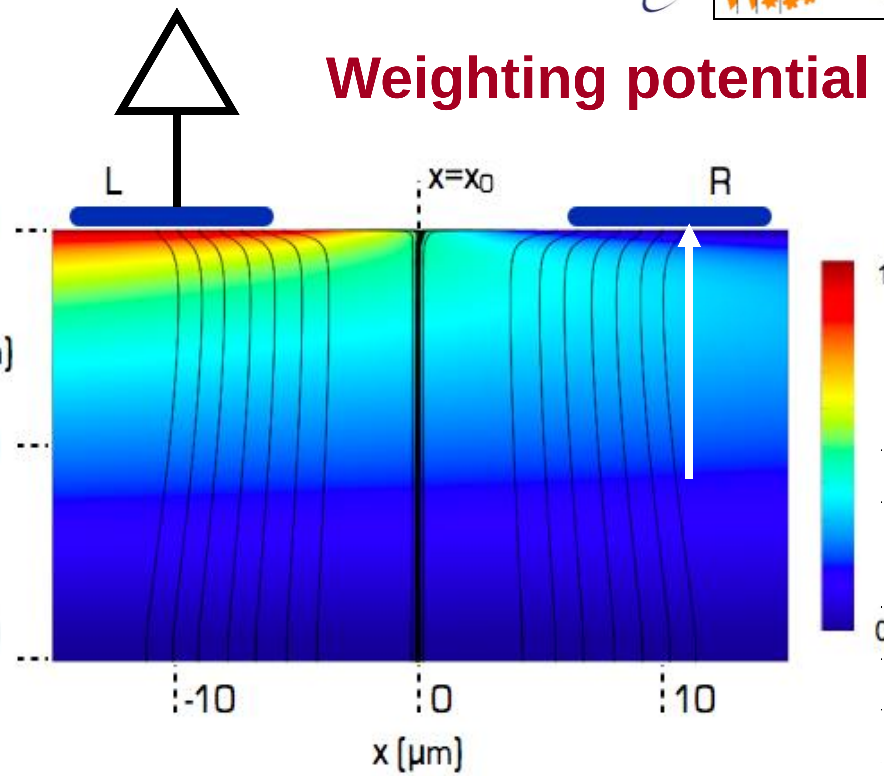

Actual potential

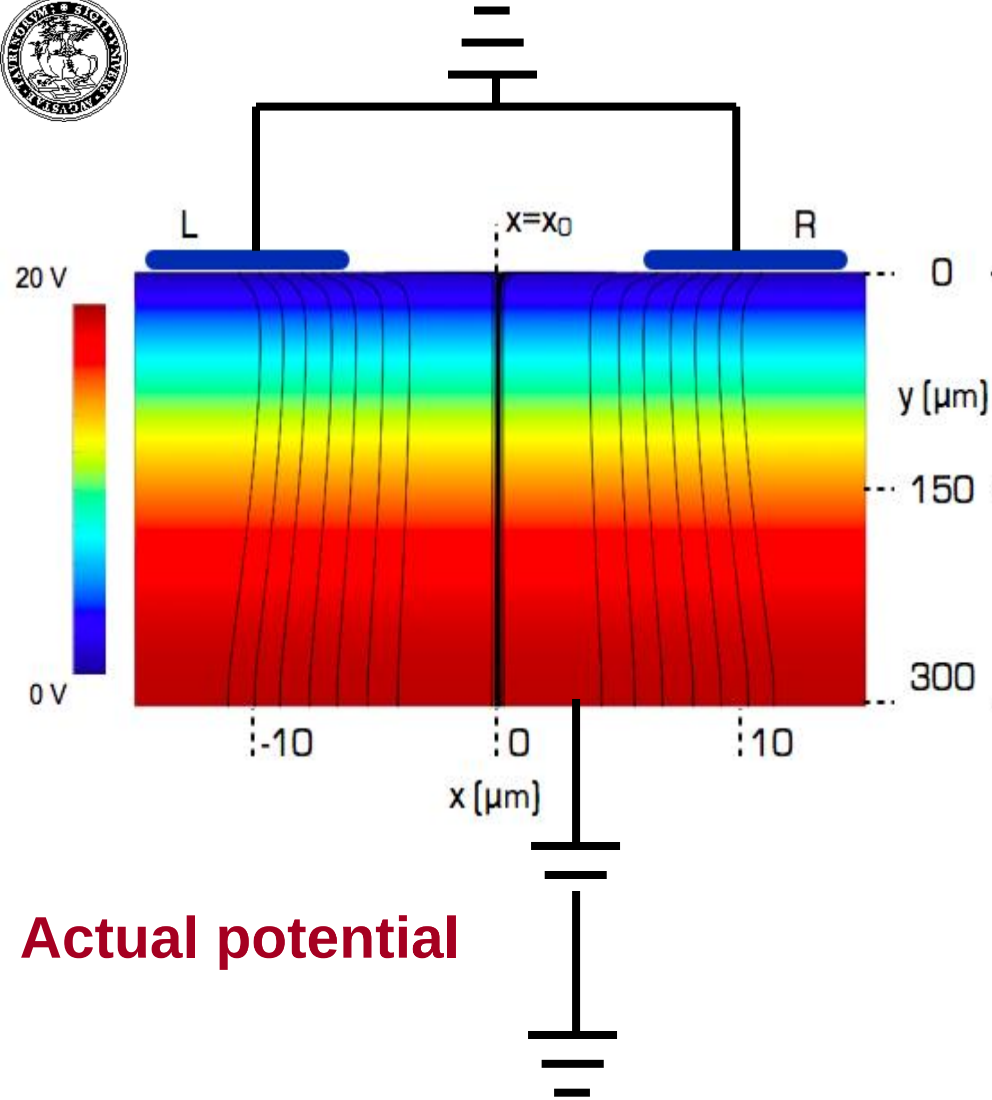

$$Q = q \cdot \left(\left.\frac{\partial \psi}{\partial V}\right|_{\substack{\text{final}\\ \text{position}}} - \left.\frac{\partial \psi}{\partial V}\right|_{\substack{\text{initial}\\ \text{position}}} \right)$$

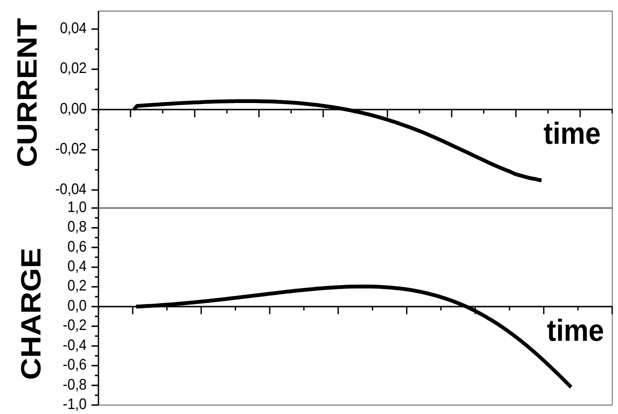

Poster Session I (23/07/2012) h. 17.30-18.40

Poster #123: Jacopo Forneris: IBIC characterization of an ion beam micromachined multi electrode diamond detector

Poster Session III (26/07/2012) h. 16.15-18.00

Poster #160: Laura Grassi: Charge collection study in the interstrip region of DSSSD using proton microbeam

Horizontal electric field

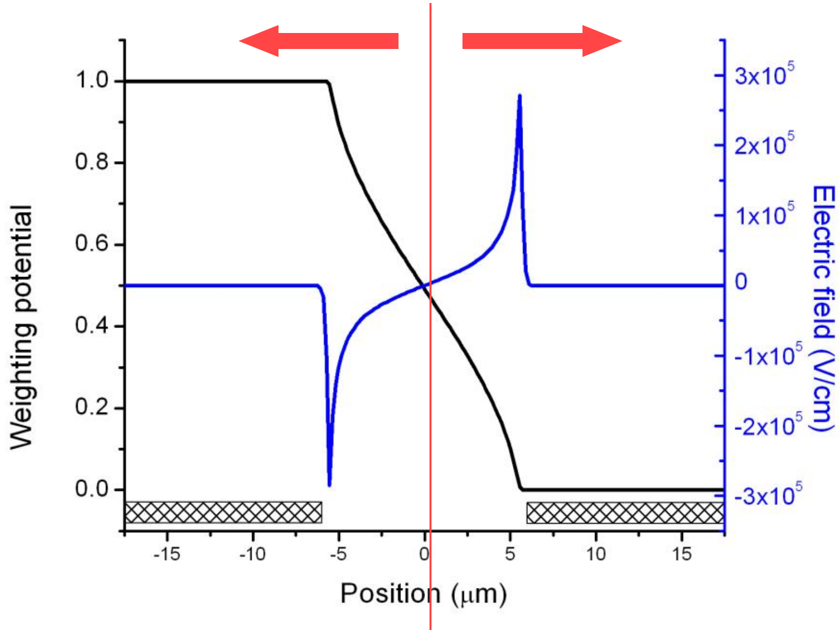

$$Q = q \cdot \left(\left. \frac{\partial \psi}{\partial V} \right|_{\substack{\text{final}\\ \text{position}}} - \left. \frac{\partial \psi}{\partial V} \right|_{\substack{\text{initial}\\ \text{position}}} \right)$$

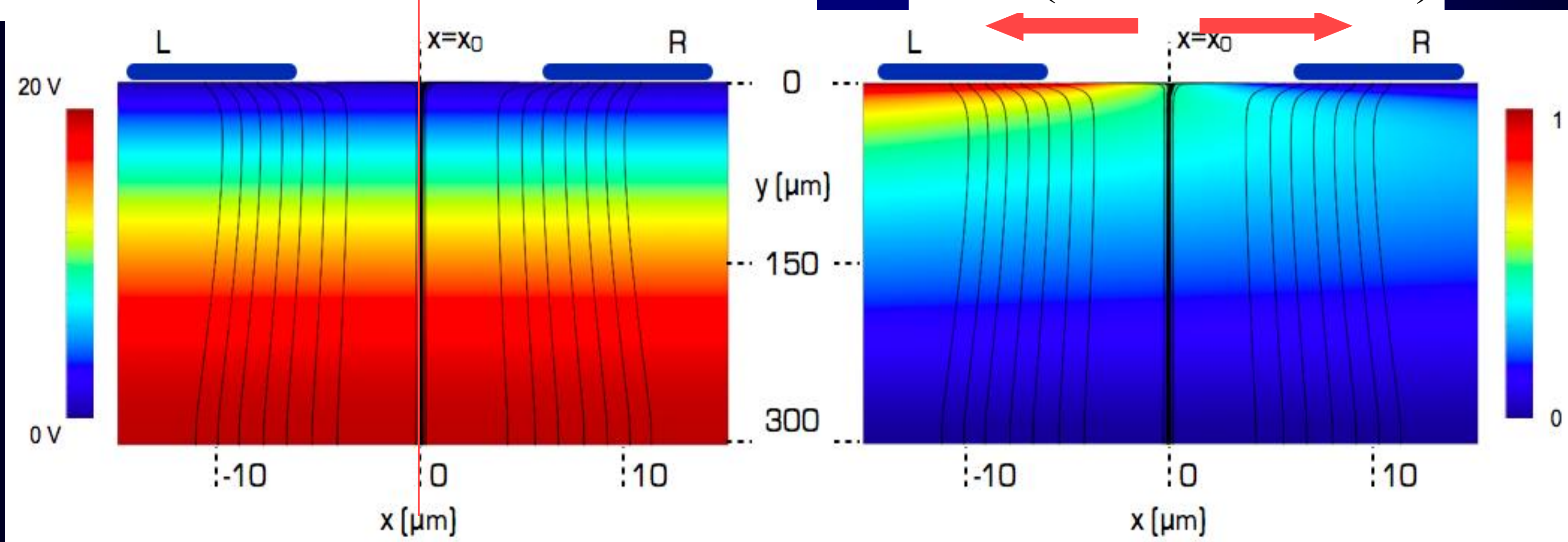

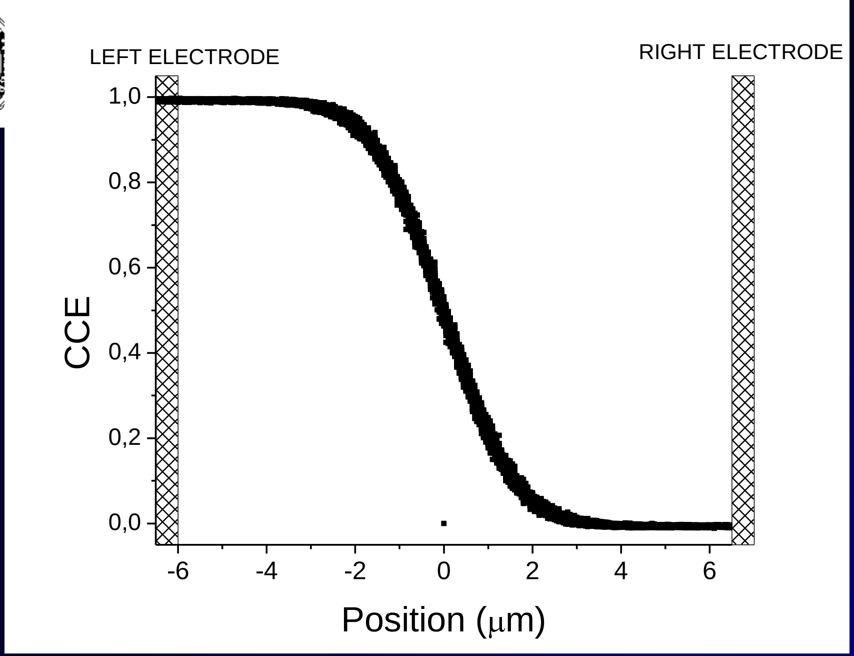

A SUB-MICROMETER POSITION SENSITIVE DETECTOR

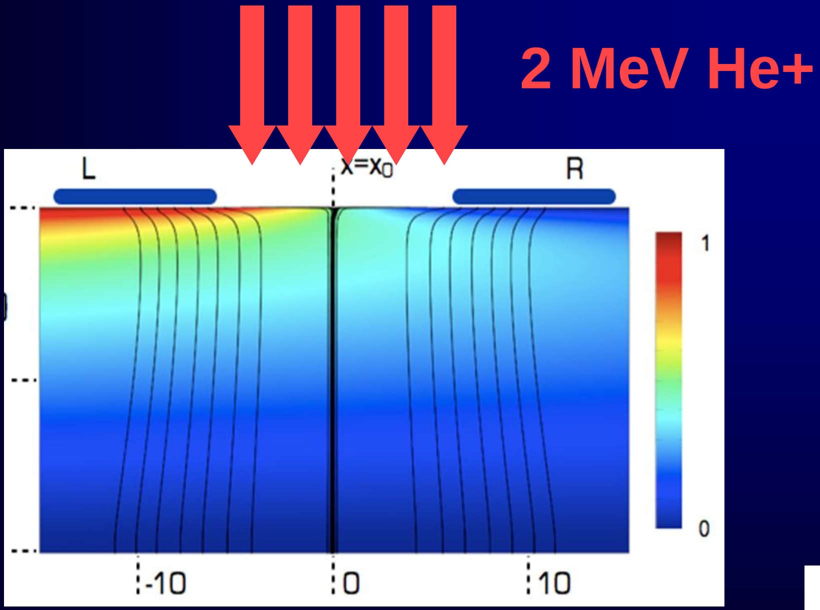

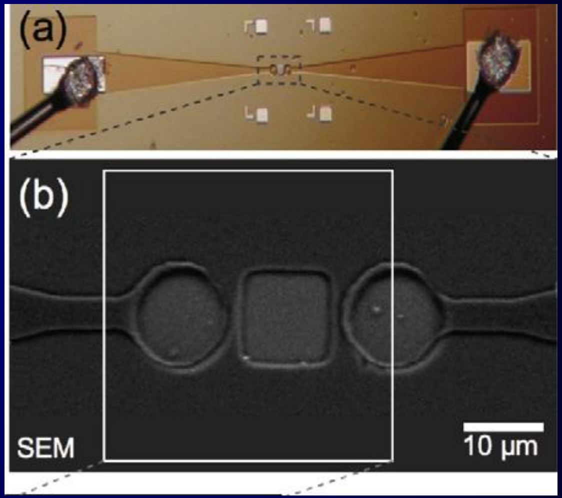

L.M. Jong et al. / Nuclear Instruments and Methods in Physics Research B 269 (2011) 2336–2339

Oral Session 25/07/2012, h 11:00-12.30

#133: David Jamieson (invited): Addressing roadmap challenges: adapting nuclear microprobe technology to build engineered atom devices

#124: Jacopo Forneris: Modeling of ion beam induced charge sharing experiments for design of high resolution position sensitive detectors.

I HOPE YOU

ENJOY YOUR TIME

AT THE ICNMTA2012

SOLUTION OF THE EQUATIONS OF MOTION

= TRAJECTORIES OF CHARGES

Initial point (r_A) ; final point (r_B)

$$I = -q \cdot \mathbf{v} \cdot \frac{\partial \mathbf{E}}{\partial V} = -q \cdot \mathbf{v} \cdot \mathbf{E}_w$$

$$Q = q \cdot \left(\psi_w(\mathbf{r}_B) - \psi_w(\mathbf{r}_A)\right)$$

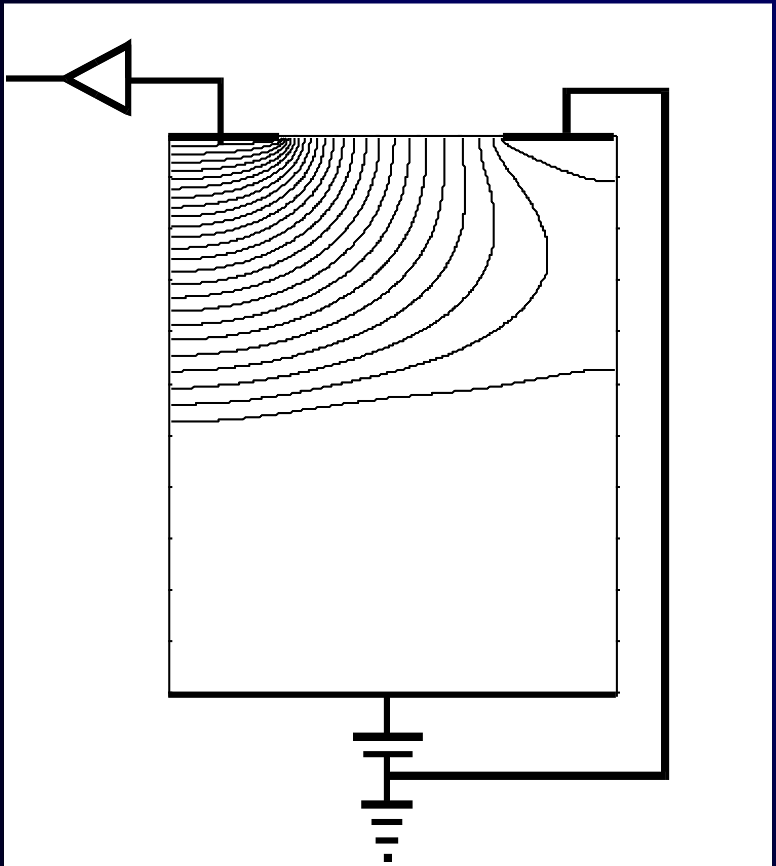

SOLUTION OF THE EQUATIONS OF MOTION

= TRAJECTORIES OF CHARGES

Initial point (r_A) ; final point (r_B)

$$I = -q \cdot \mathbf{v} \cdot \frac{\partial \mathbf{E}}{\partial V} = -q \cdot \mathbf{v} \cdot \mathbf{E}_w$$

$$Q = q \cdot \left(\psi_w(\mathbf{r}_B) - \psi_w(\mathbf{r}_A)\right)$$

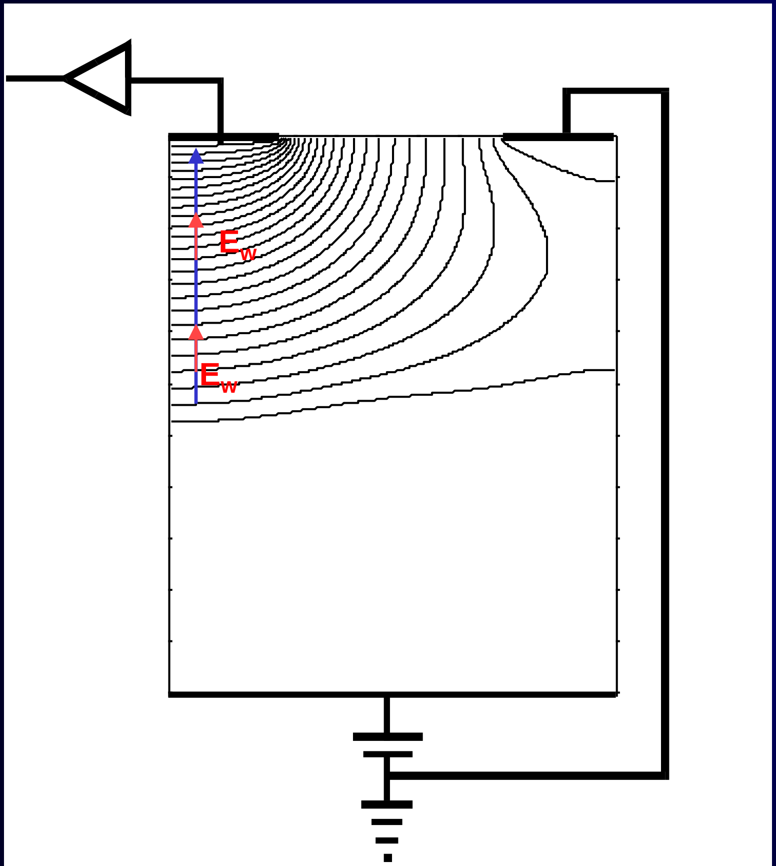

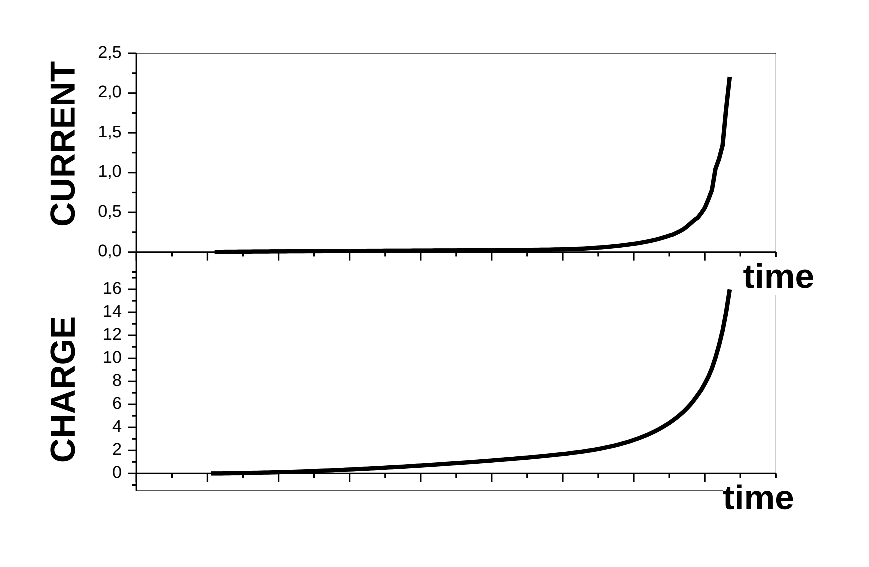

SOLUTION OF THE EQUATIONS OF MOTION

= TRAJECTORIES OF CHARGES

Initial point (r_A) ; final point (r_B)

$$I = -q \cdot \mathbf{v} \cdot \frac{\partial \mathbf{E}}{\partial V} = -q \cdot \mathbf{v} \cdot \mathbf{E}_w$$

$$Q = q \cdot \left(\psi_w(\mathbf{r}_B) - \psi_w(\mathbf{r}_A)\right)$$

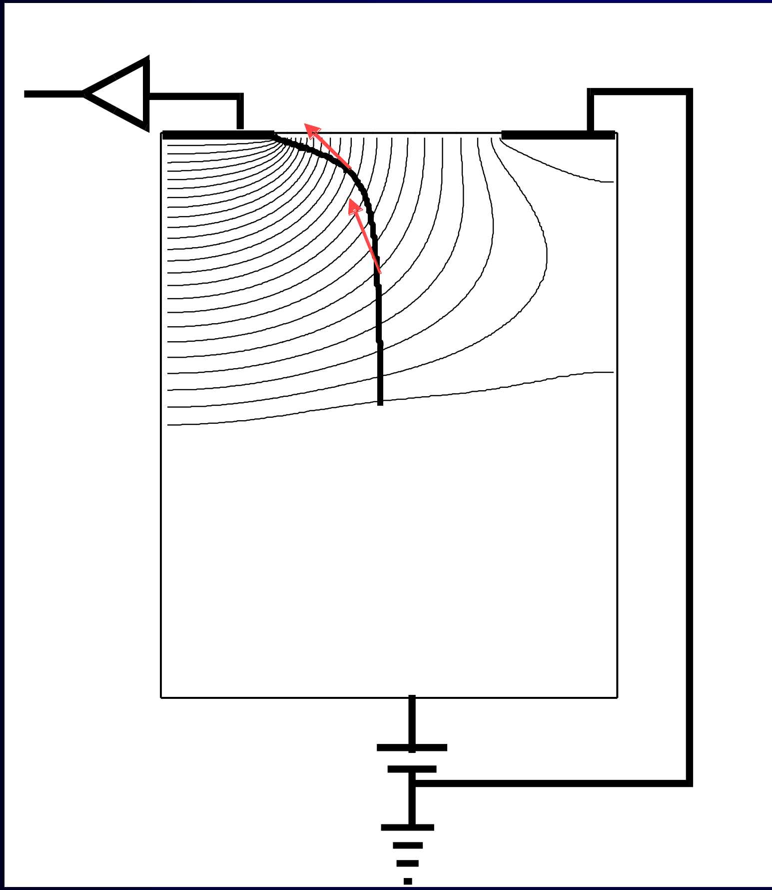

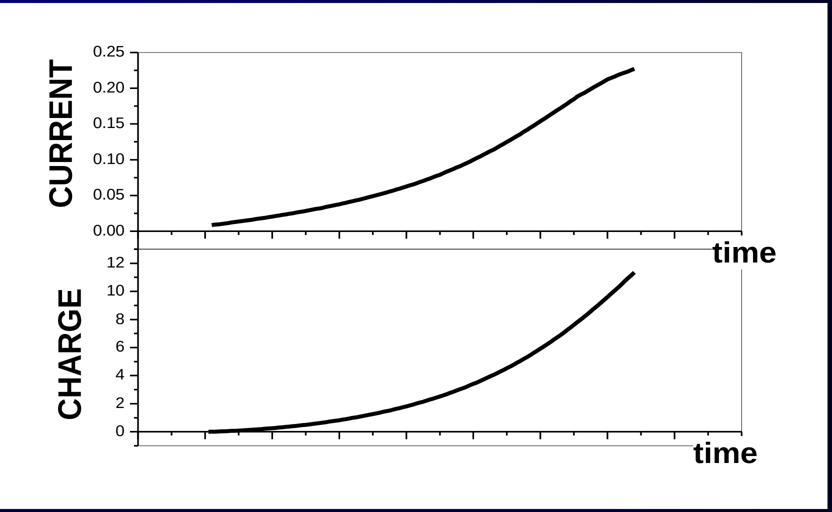

SOLUTION OF THE EQUATIONS OF MOTION

= TRAJECTORIES OF CHARGES

Initial point (r_A) ; final point (r_B)

$$I = -q \cdot \mathbf{v} \cdot \frac{\partial \mathbf{E}}{\partial V} = -q \cdot \mathbf{v} \cdot \mathbf{E}_w$$

$$Q = q \cdot \left(\psi_w(\mathbf{r}_B) - \psi_w(\mathbf{r}_A)\right)$$

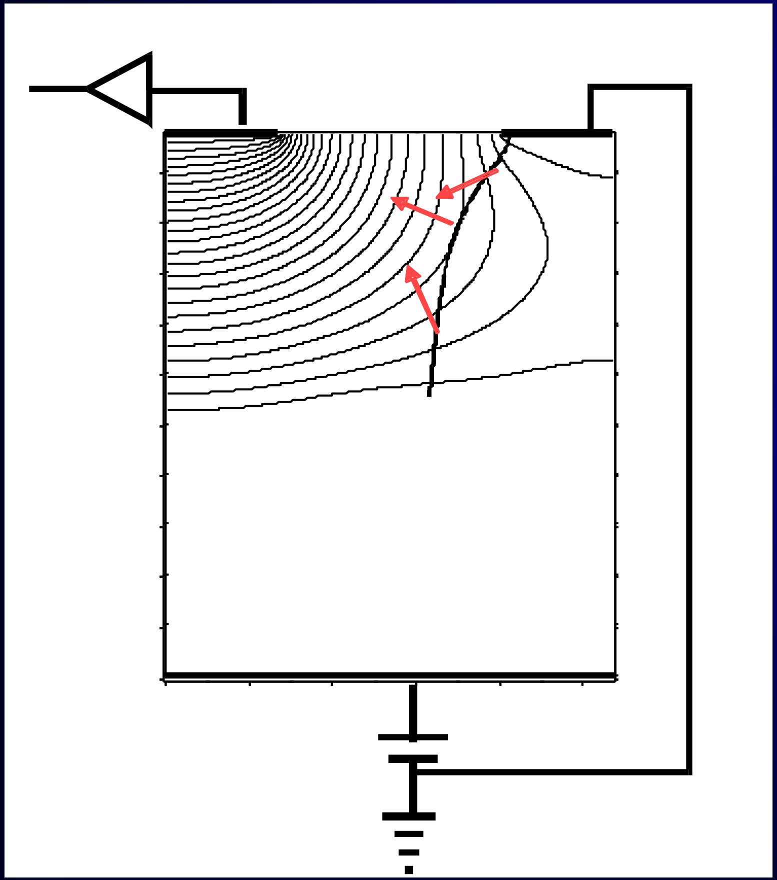

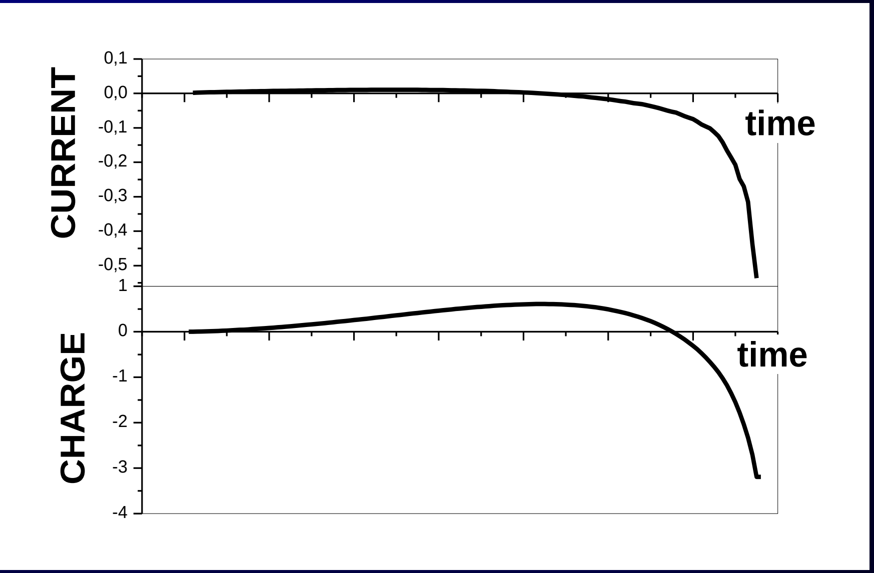

SOLUTION OF THE EQUATIONS OF MOTION

= TRAJECTORIES OF CHARGES

Initial point (r_A) ; final point (r_B)

$$I = -q \cdot \mathbf{v} \cdot \frac{\partial \mathbf{E}}{\partial V} = -q \cdot \mathbf{v} \cdot \mathbf{E}_w$$

$$Q = q \cdot \left(\psi_w(\mathbf{r}_B) - \psi_w(\mathbf{r}_A)\right)$$

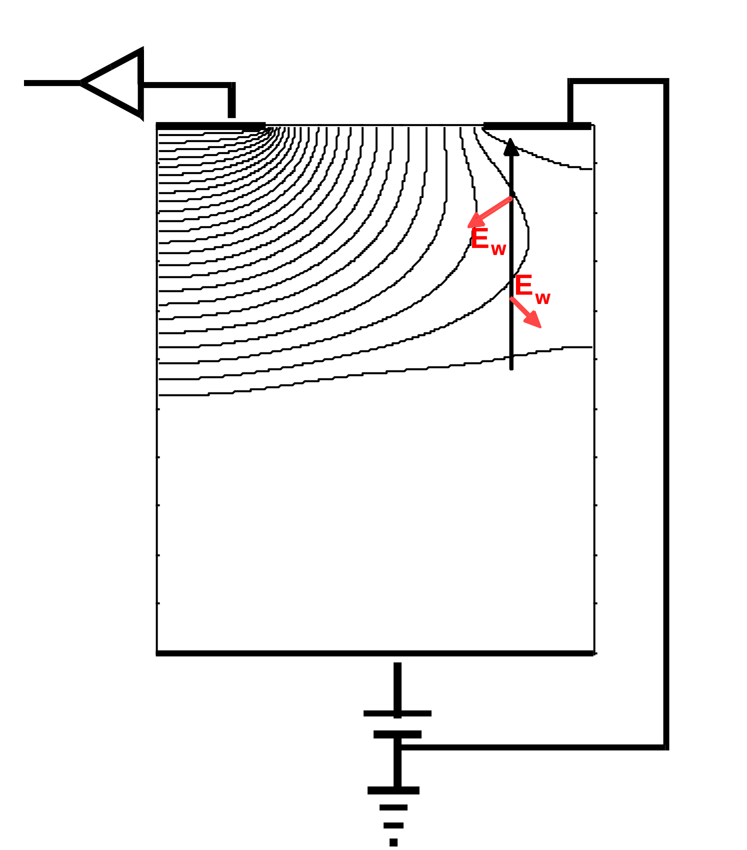

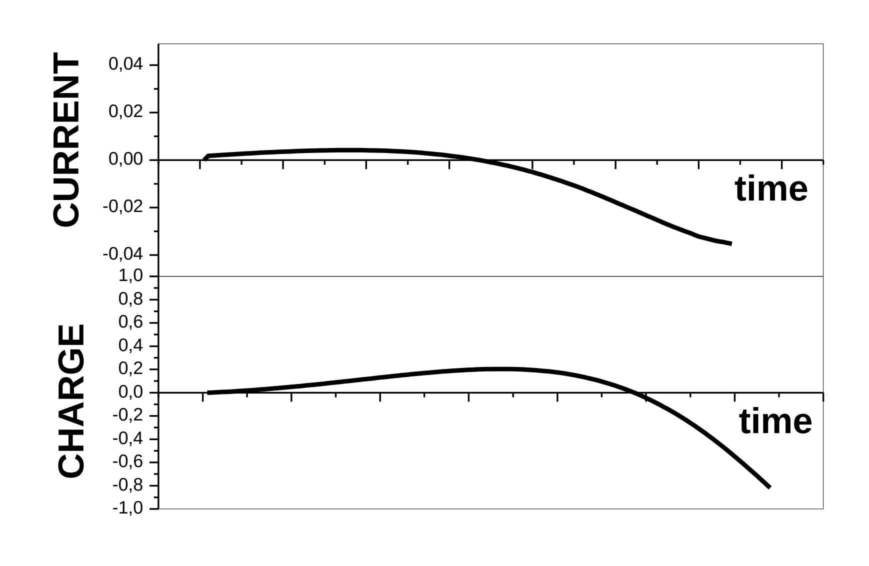

IBIC
(Ion Beam Induced Charge Collection)

Analytical technique suitable for the measurement of transport properties in semiconductor materials and devices

- **Control of in-depth generation profile**
- **Suitable for finished devices (bulk analysis).**
- **Micrometer resolution**
- **CCE profiles: Active layer extension; Diffusion length**
- **In-situ analysis of radiation damage**

Thanks for your kind attention

Temperature dependent IBIC (TIBIC)

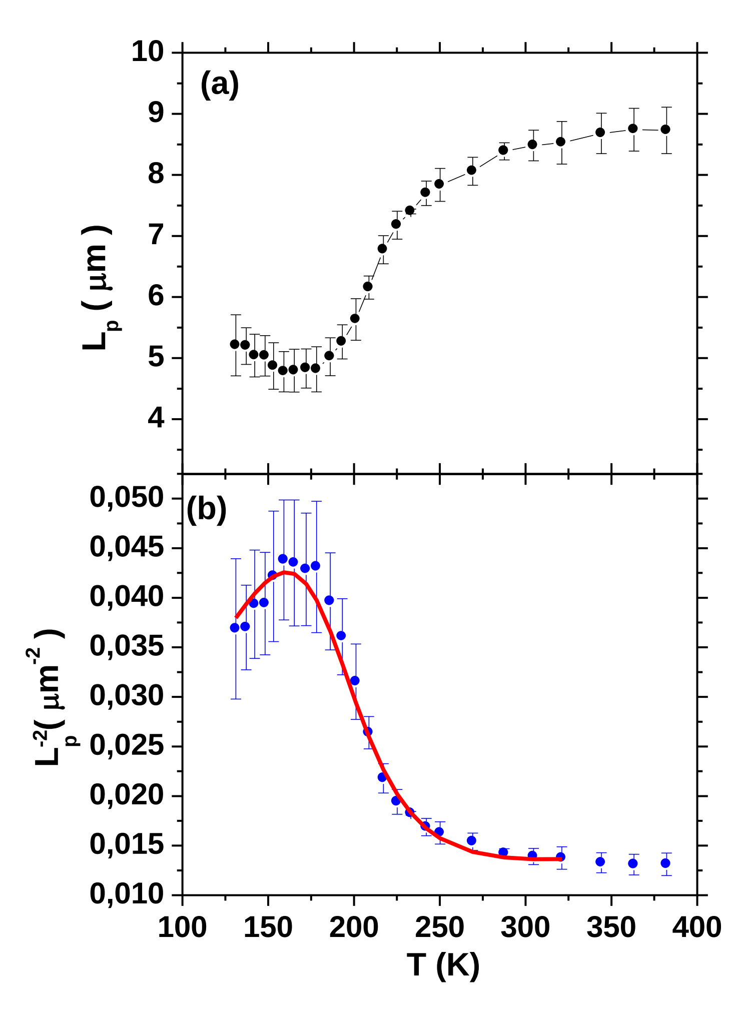

Two trapping levels

SRH recombination model

$$\frac{1}{L_p^2} = \frac{1}{D_p \cdot \tau} = \frac{1}{D_p} \cdot \left(\frac{1}{\tau(T)} + \frac{1}{\tau_B} \right) = A \cdot \frac{1}{T^{-0.5}} \cdot \left[\frac{1}{T^{-0.5} + \frac{B}{N_D} \cdot T \cdot \exp\left(-\frac{E_t}{k_B T} \right)} + \frac{1}{\tau_B} \right]$$

The fitting procedure provides a trapping level of about 0.163 eV which is close to the value found in similar 4H SiC Schottky diodes by DLTS technique (S1 level).

E. Vittone et al., NIM-B 231 (2005) 491.

Time resolved IBIC (TRIBIC) Silicon Power diode Mesa Rectifier

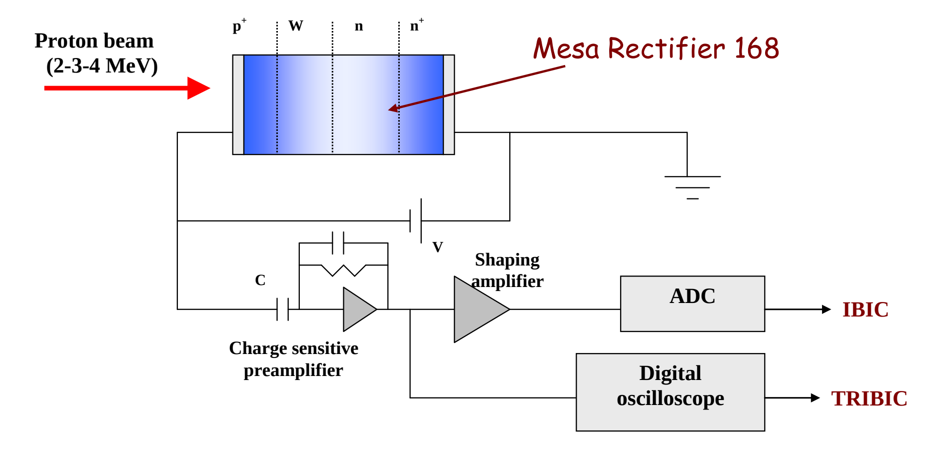

lifetime

τ_0 = (5 ± 1) μs

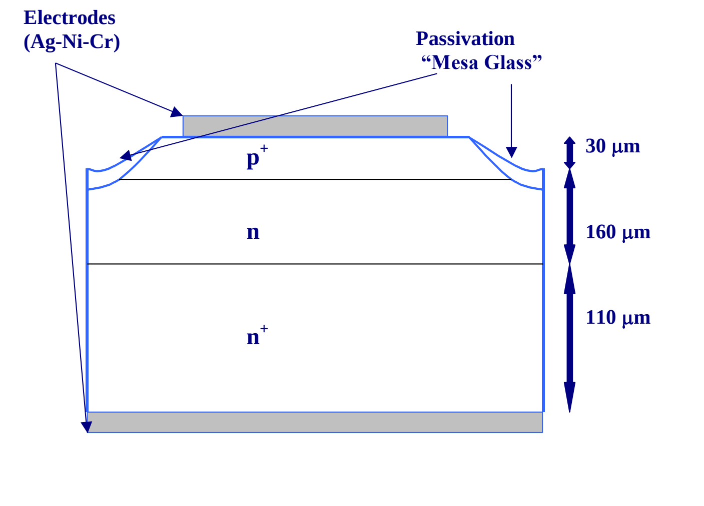

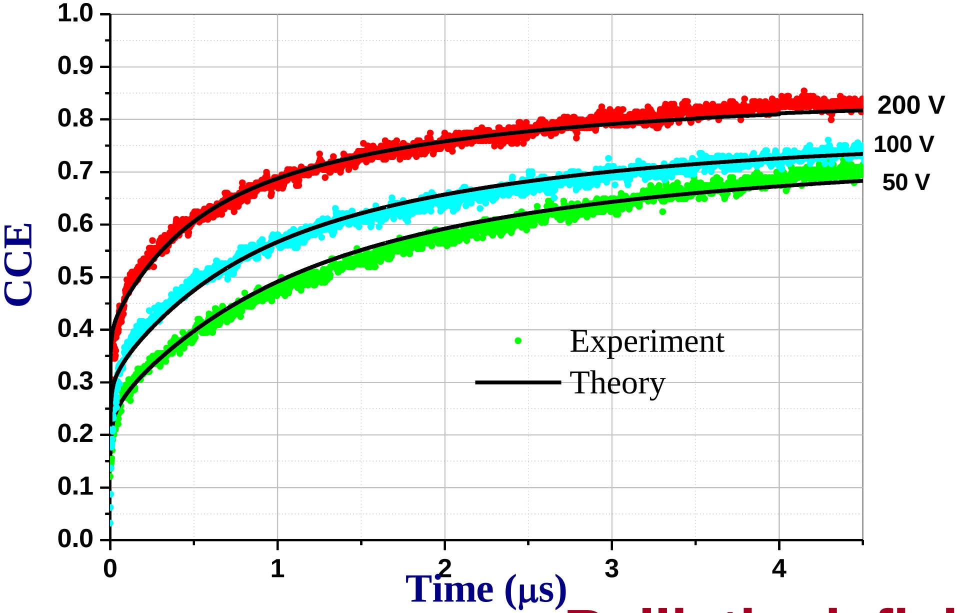

Ballistic deficit

Radiation Damage

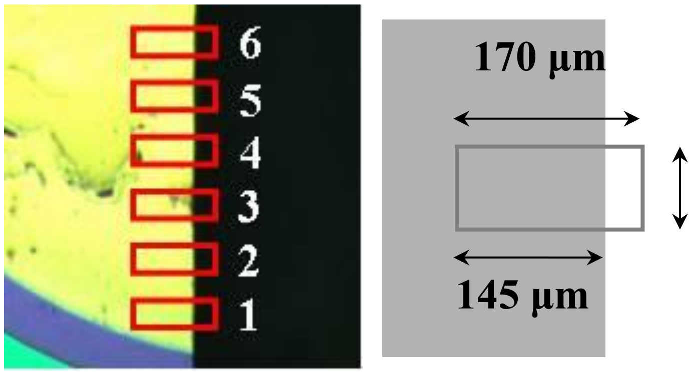

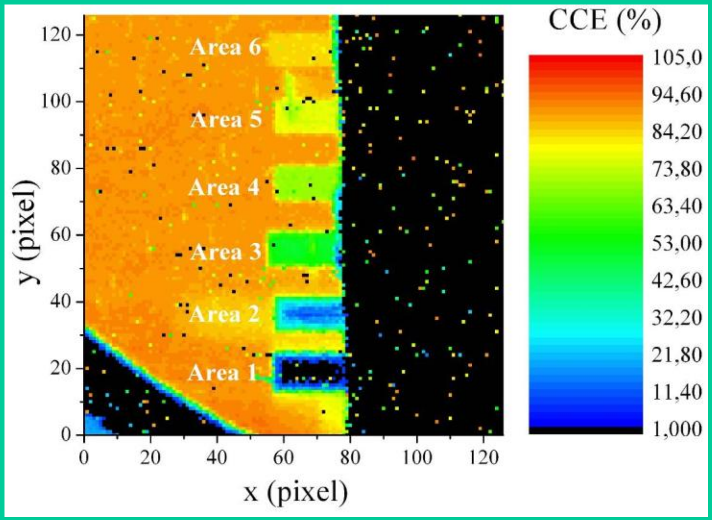

Fluences (cm^{-2})
Area 1:
Area 2: 1,8 E10
Area 3: 6,1 E9
Area 4: 2,0 E9
Area 5: 6,1 E8
Area 6: 2,0 E8

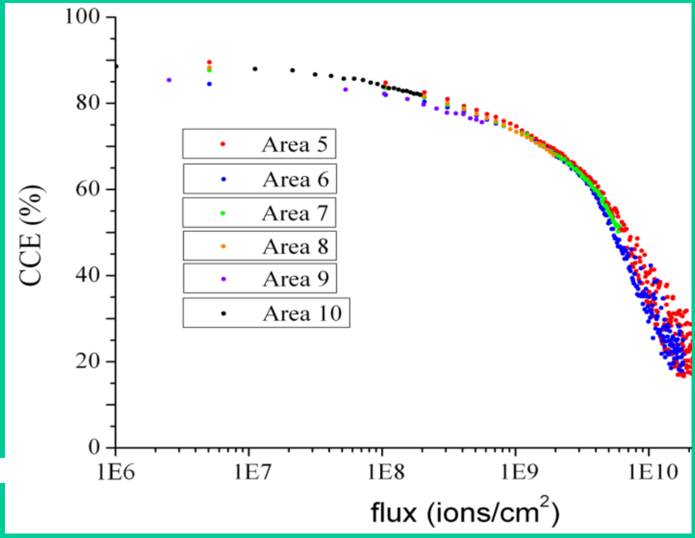

Good Reproducibility

Lateral IBIC

V_b = 50 V

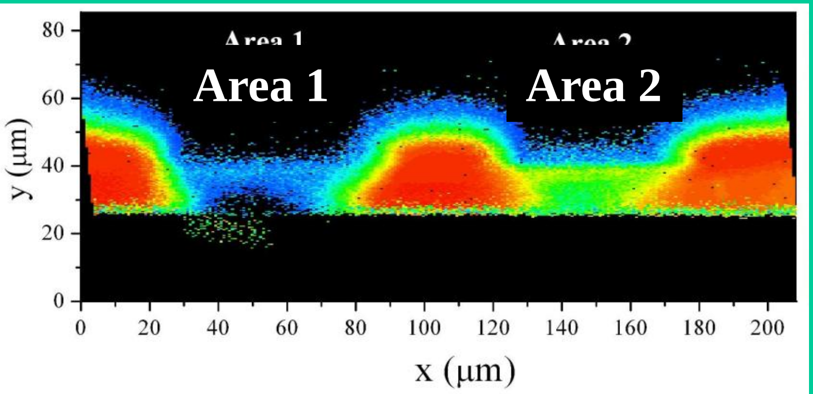

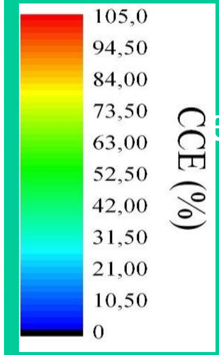

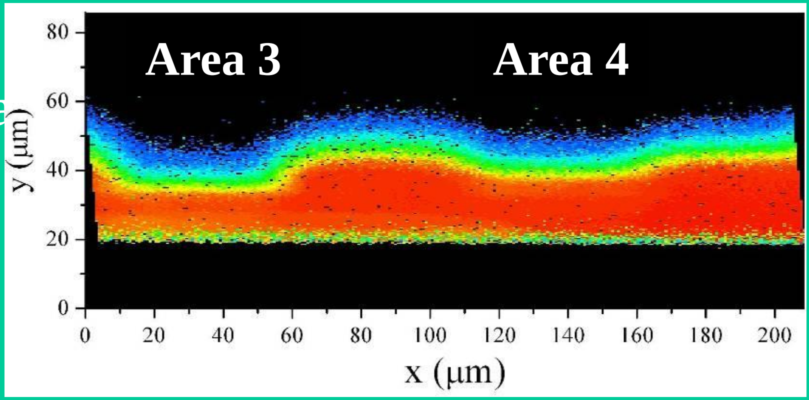

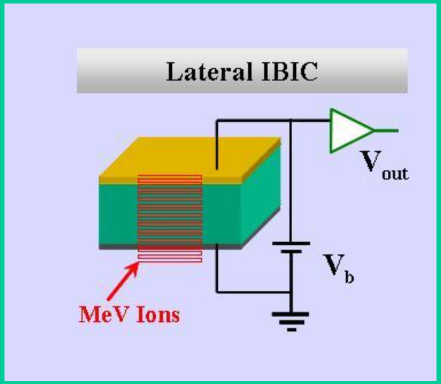

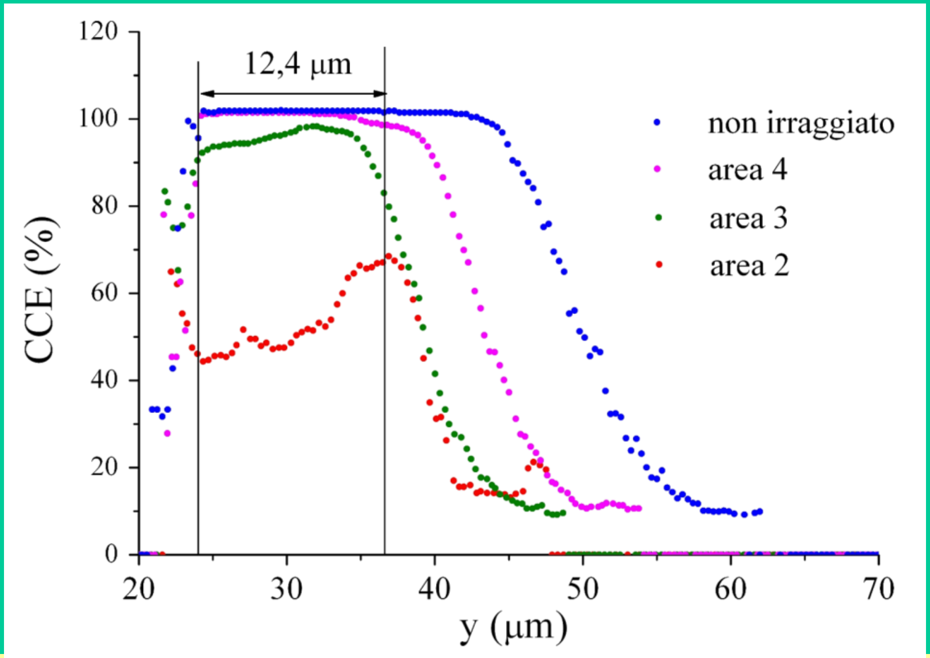

CCE profiles

- **Lifetime reduction**
- **Depletion region shrinking**

Frontal IBIC

Polycrystalline CVD diamond

APPLIED PHYSICS LETTERS VOLUME 84, NUMBER 22 31 MAY 2004

Temperature-dependent emptying of grain-boundary charge traps in chemical vapor deposited diamond

S. M. Hearne, D. N. Jamieson,[a)] E. Trajkov, and S. Prawer
School of Physics, University of Melbourne, Victoria, 3010, Australia

J. E. Butler
Naval Research Laboratory, Washington, DC 20375

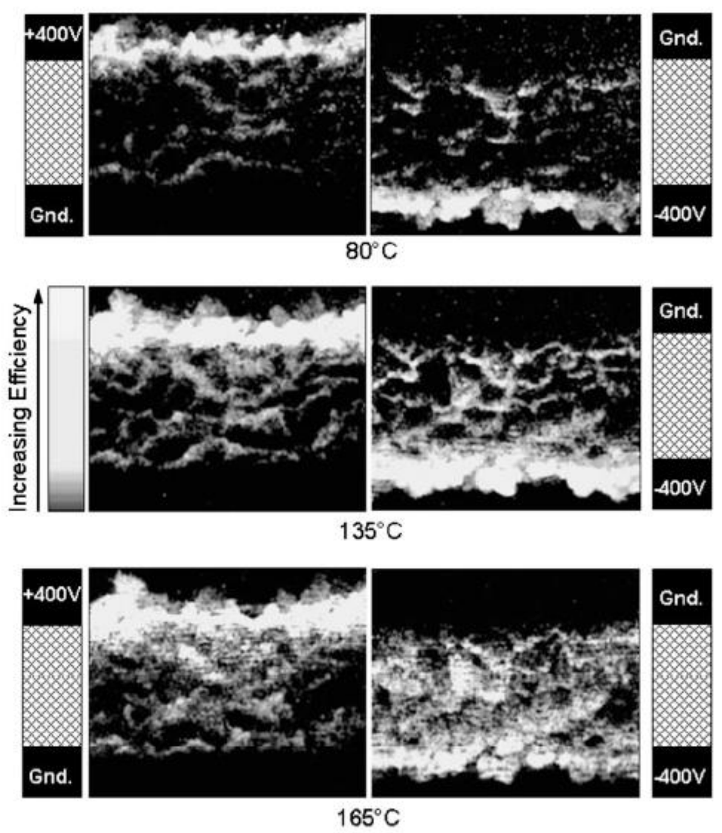

FIG. 1. Ion beam induced charge (IBIC) maps using a scanned 2 MeV He^+ microprobe of the charge collection in CVD diamond at various temperatures. The location of the electrodes is shown. Note that the charge collection efficiency is always highest near to the anode.

Diamond and Related Materials 11 (2002) 446–450

Effects of light on the 'primed' state of CVD diamond nuclear detectors

C. Manfredotti[a,b,*], E. Vittone[a,b], F. Fizzotti[a,b], A. Lo Giudice[a,b], C. Paolini[a,b]

Under illumination

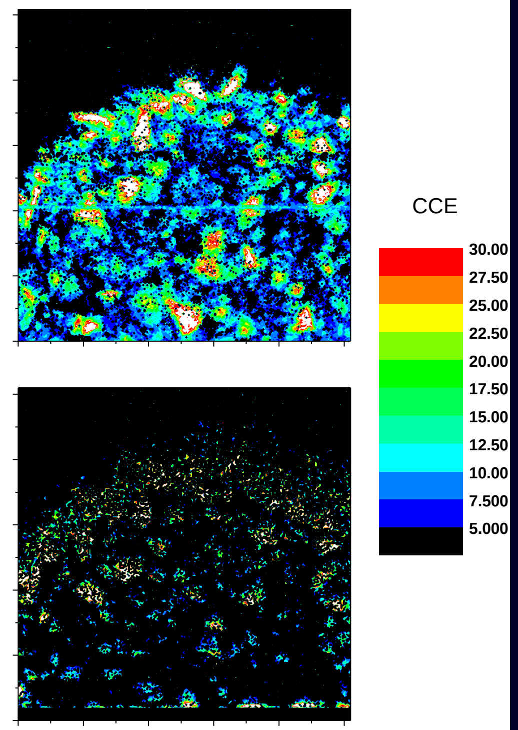

Dark conditions

Uniformity

(D.Meier, PhD thesis 1999, C.Manfredotti 2000)

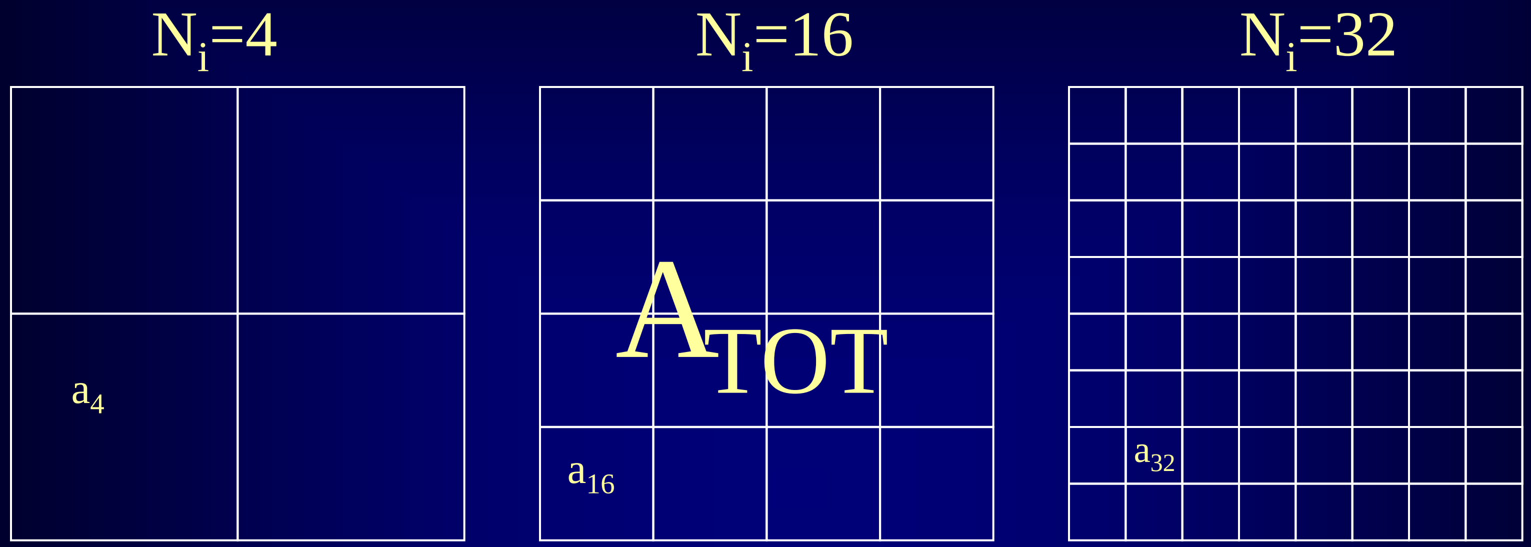

$$s_i = 1 - \frac{1}{\langle s \rangle} \cdot \sqrt{\frac{\sum_{j=1}^{N_i} \left(s_{i,j} - \langle s \rangle \right)^2}{N_i}}$$

$\langle s \rangle = \frac{1}{N_i} \cdot \sum_{j=1}^{N_i} s_{i,j}$ = overall average signal evaluated over the total scanned area A_{TOT}

N_i = Number of pixel of area a_i : $A_{TOT} = a_i \cdot N_i$

$s_{i,j}$ = signal from the j-th pixel of area a_i

IBIC maps with different pixel dimension

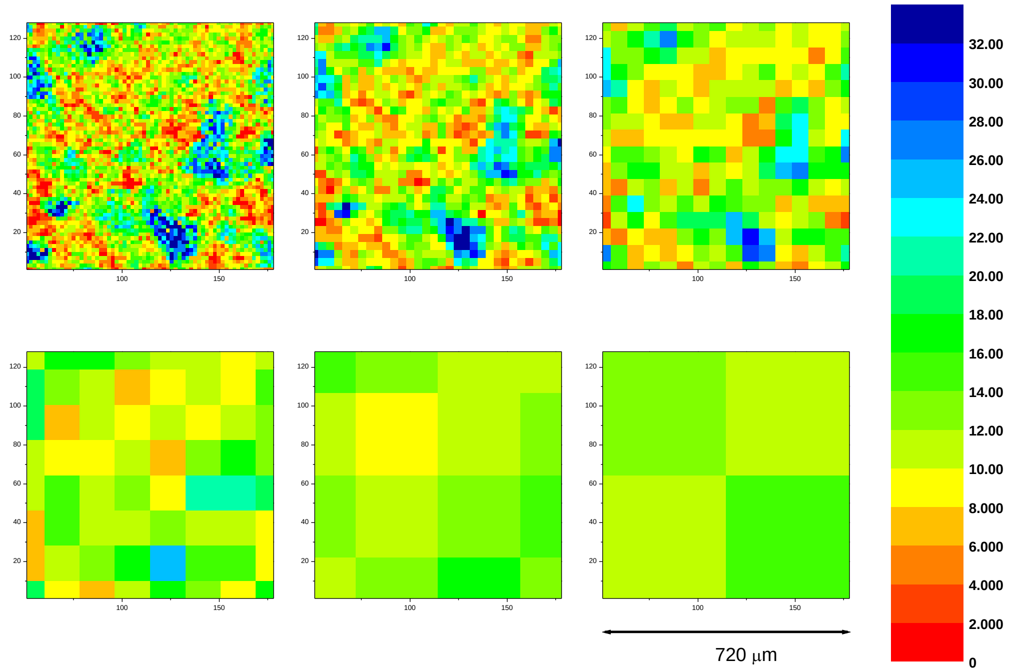

$$s_i = 1 - \frac{1}{\langle s \rangle} \cdot \sqrt{\frac{\sum_{j=1}^{N_i} \left(s_{i,j} - \langle s \rangle\right)^2}{N_i}}$$

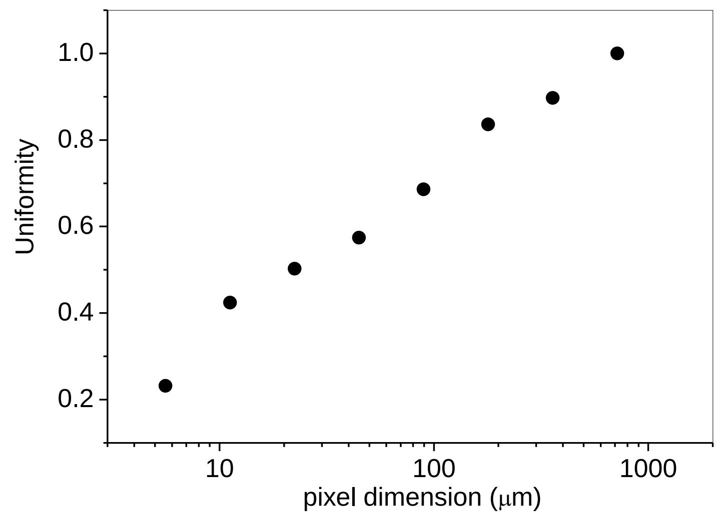

The uniformity is between 80% and 100% on the length scale above 200 µm; at 100 µm the uniformity is 69%

Schottky electrode

50 μm thick N-type epitaxial 4H-SiC layer

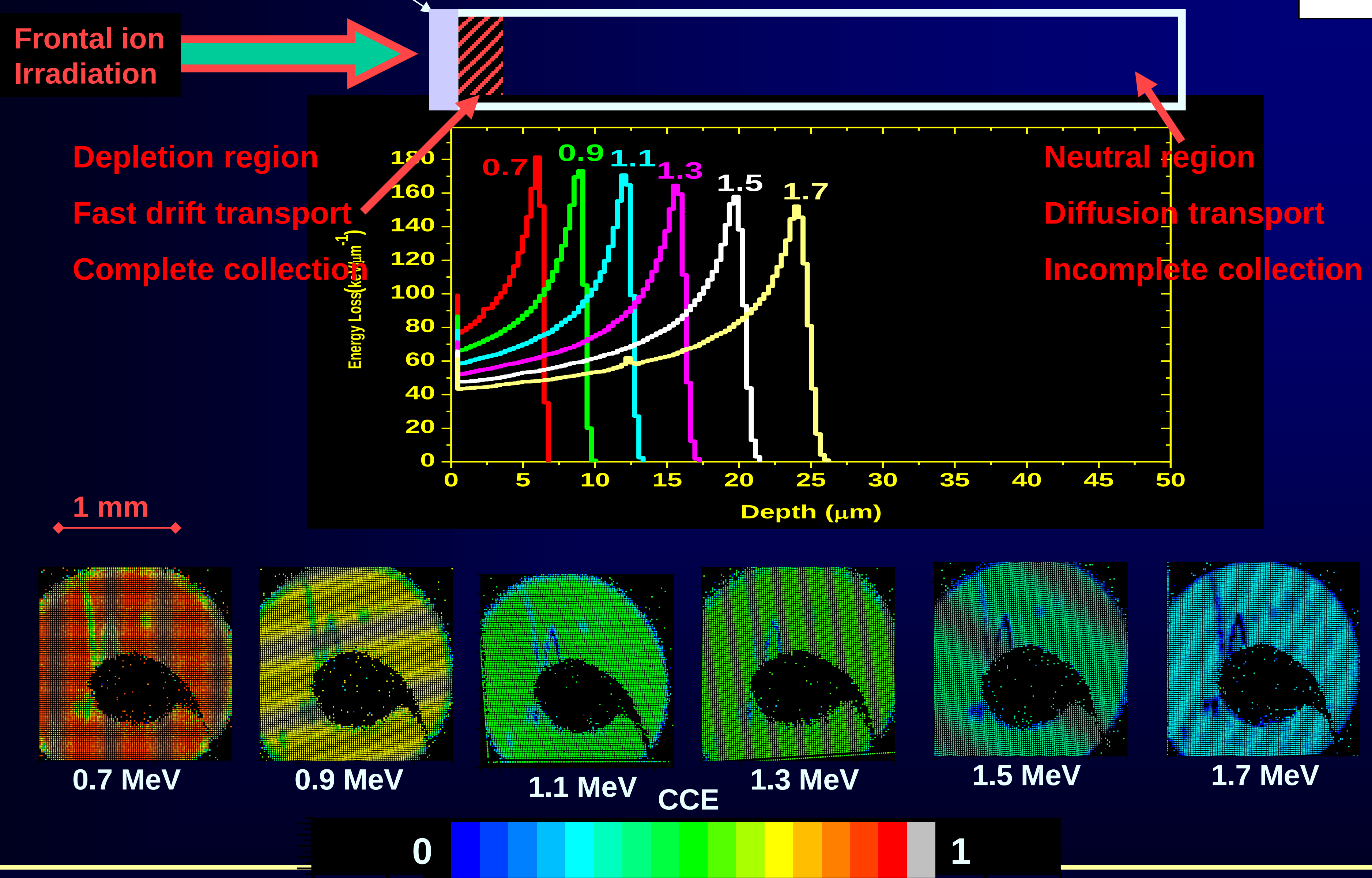

M. Jaksic et al.NIM-B, 188 (2002), 130-134

Numerical Simulations

$$L_p = (4{,}9 \pm 0{,}3)\,\mu m$$

$$\tau_p \approx 80\ ns$$

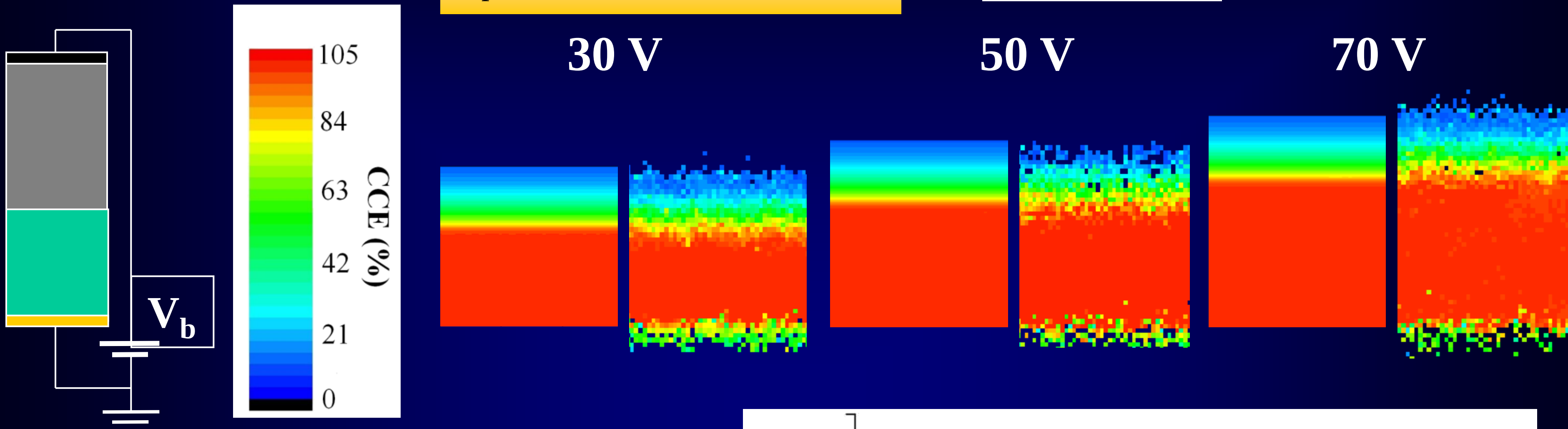

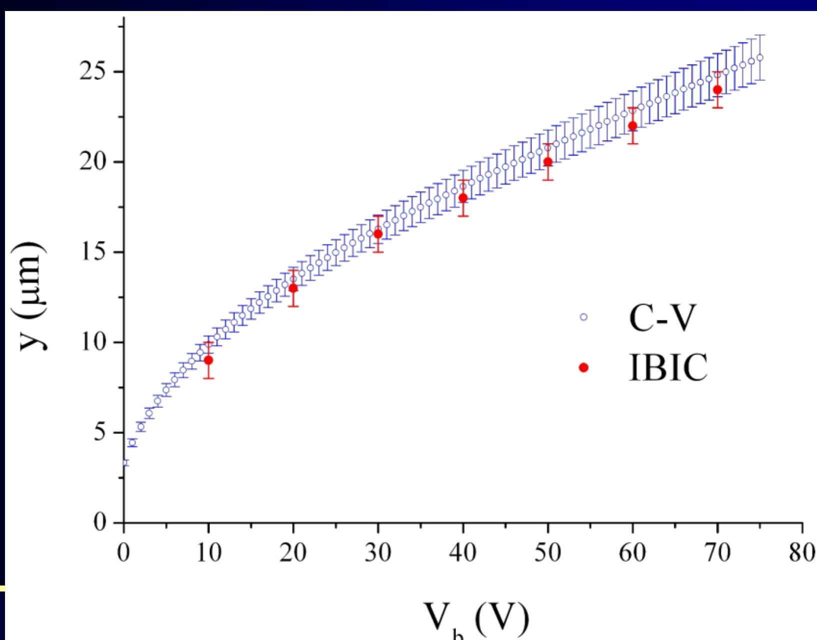

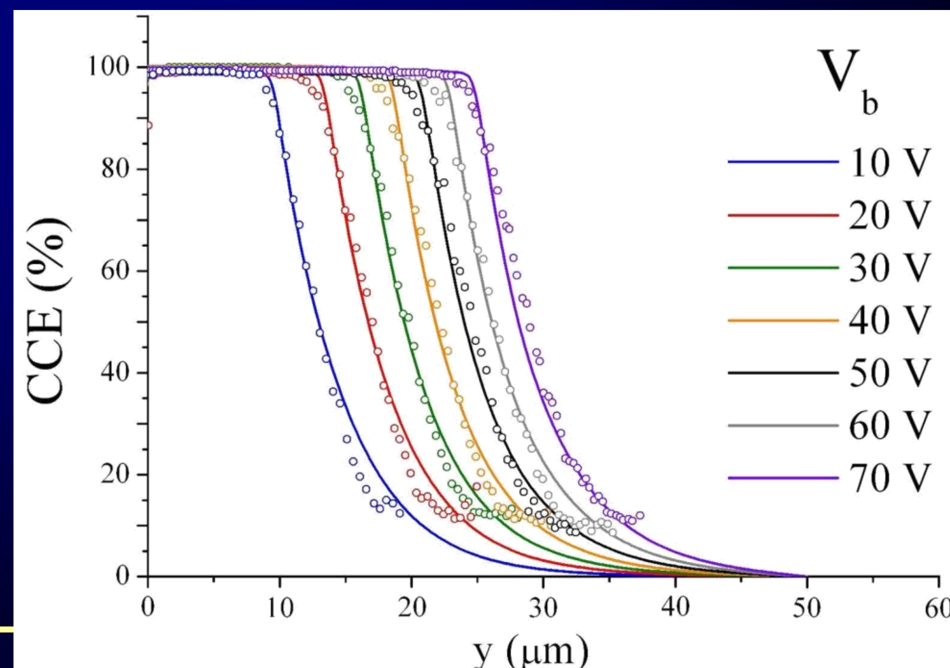

Lateral IBIC of a diamond Schottky diode

- ✓ Diamond Schottky diode structure:
  - ✓ homoepitaxial growth on HPHT substrates
  - ✓ (type Ib, 4×4×0.4 mm^3) slightly B doped (Acceptor concentration ≈ 10^{13}-10^{14} cm^{-3})
  - ✓ heavily B-doped buffer layer as back contact (Acceptor concentration ≈ 10^{18}-10^{19} cm^{-3})
  - ✓ 25 µm thick intrinsic layer as active volume
- ✓ Schottky contact: frontal Al circular contact (∅ = 2 mm, 200 nm thick) on intrinsic layer
- ✓ back contact on B-doped layer → ohmic contact
- ✓ sample cleaved in order to expose its cross section for IBIC characterization

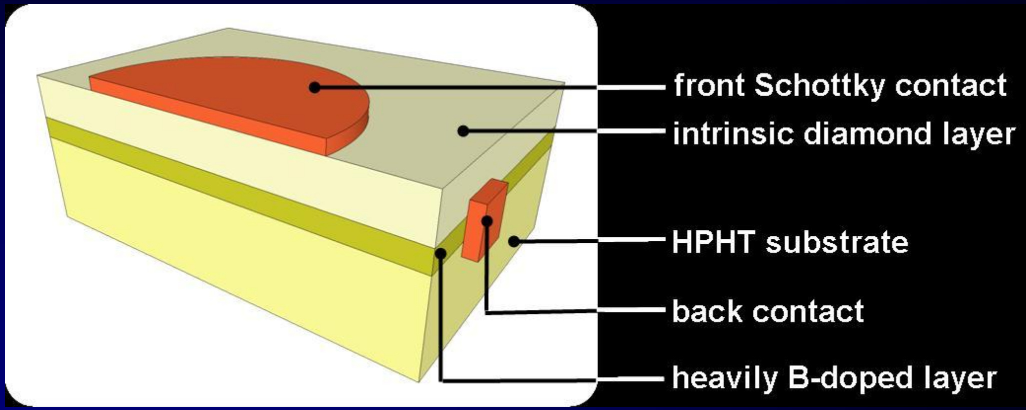

ideality factor: n = (1.51 ± 0.04)

series resistance: R_s = (5.1 ± 1.6) kΩ

→ back B-doped contact

shunt resistance: R_{sh} = (900 ± 6) GΩ

@ 50 V -> I<50 pA

S. Almaviva et al. "*Synthetic single crystal diamond dosimeters for conformal radiation therapy application*"
Diamond & Related Materials 19 (2010) 217–220

4H-SiC Schottky diode

Starting Material: 360 μm n-type 4H-SiC by CREE (USA)
Epitaxial layer from Institute of Crystal Growth (IKZ), Berlin, Germany
Devices from Alenia Marconi System

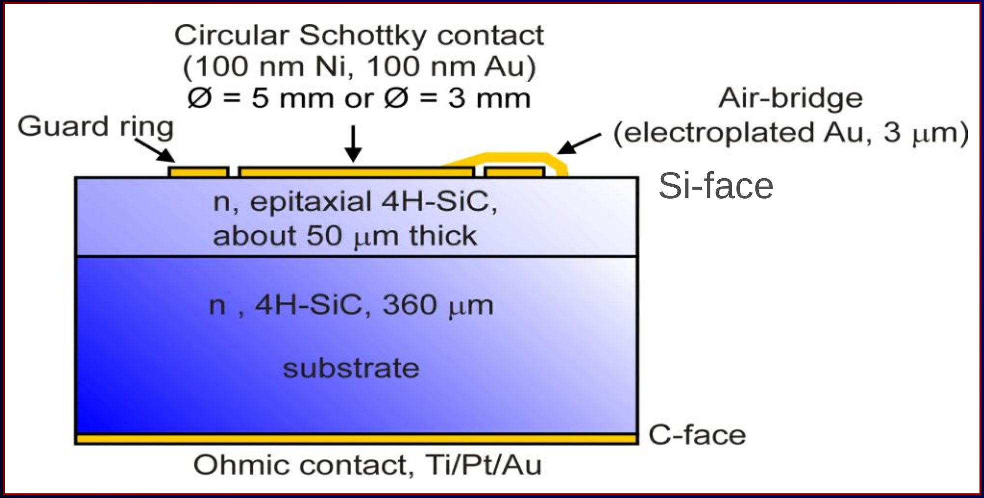

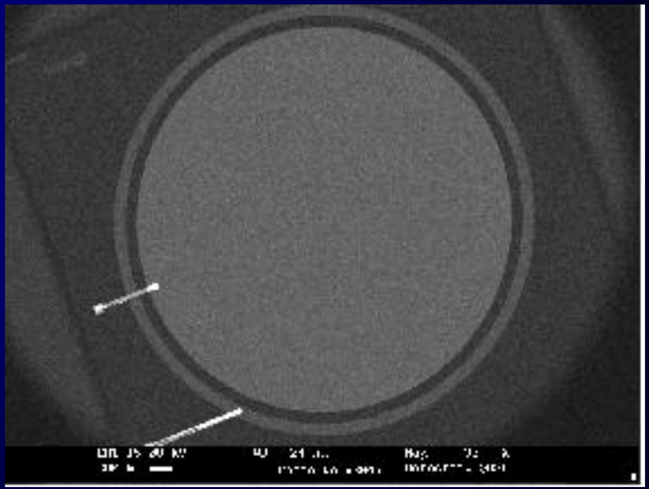

Lateral IBIC measurements performed at the ion microbeam line of the AN2000 accelerator of the National Laboratories of Legnaro (LNL-INFN)

charge sensitive electronic chain and synchronous signal acquistition with microbeam scanning

- ✓ ion species and energy: H^+ @ 2 MeV
- ✓ ion current: $\leq 10^3$ ions s^{-1} → no pile up or charging effects
- ✓ ion beam spot on the sample: FWHM = 3 μm
- ✓ raster-scanned area: S = 62×62 μm²

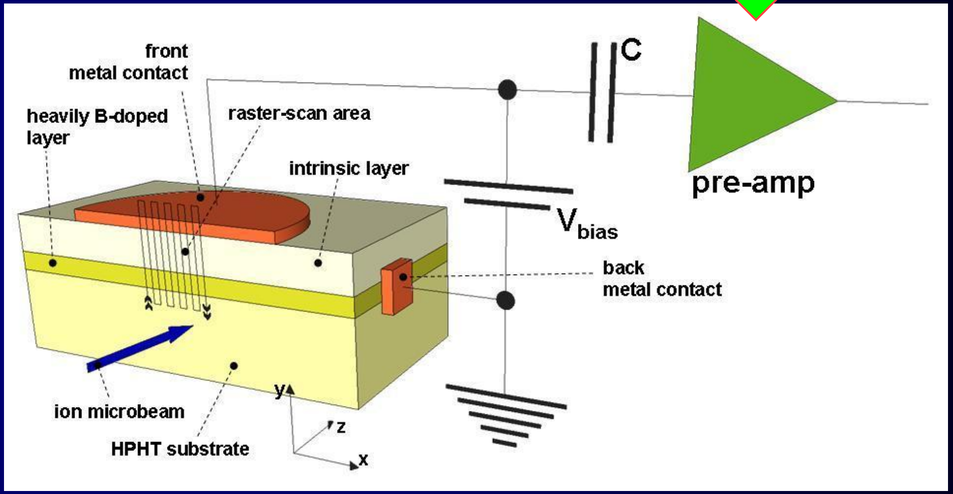

4 MeV Protons (100 μm range)
4H SiC Schottky barrier